QATAR UNIVERSITY

COLLEGE OF PHARMACY

THE ROLE OF P90 RIBOSOMAL S6 KINASE AND AUTOPHAGY IN SUNITINIB AND PONATINIB-INDUCED CARDIOTOXICITY

BY

MUNA SULEIMAN

A Thesis Submitted to

the Faculty of the College of Pharmacy

in Partial Fulfillment of the Requirements for the Degree of

Masters of Science in Pharmacy

June 2019

COMMITTEE PAGE

The members of the Committee approve the Thesis of

Muna Suleiman defended on 22/05/2019.

Dr. Fatima Mraiche
Thesis/Dissertation Supervisor

Dr. Huseyin Yalcin
Thesis co-Supervisor

Dr. Hesham Korashy
Committee Member

Dr. Shahab Uddin
Committee Member

Dr. Hazem Elewa
Committee Member

Dr. Mohamed Izham
Committee Member

Approved:

Mohammad Diab, Dean, College of Pharmacy

ABSTRACT

SULEIMAN, MUNA, M., Masters : June : 2019, PHARMACY

Title: The Role of p90 Ribosomal S6 Kinase and Autophagy in Sunitinib and Ponatinib-Induced Cardiotoxicity

Supervisor of Thesis: Fatima, Mraiche.

In recent years, the paradigm cancer management has shifted towards a targeted approach. Among the newly targeted anticancer therapies are ponatinib and sunitinib, small molecules tyrosine kinase inhibitors (TKIs), used for various types of cancer. Despite their superb anticancer effects, their use has been associated with cardiovascular toxicities. Therefore, the present study aimed to investigate the cardiotoxic effects associated with ponatinib and sunitinib and to define the underlying cardiotoxic signaling pathways.

In the current study, an in vitro rat cardiomyoblast (H9c2) model was used to assess the cardiotoxic effects of sunitinib and ponatinib following 6 and 24 hours. Cardiomyoblast loss was characterized by MTT assay and flow cytometer analyses. Cardiomyoblast hypertrophy was assessed by measuring H9c2 cell surface area and atrial natriuretic peptide (ANP) mRNA expression. The potential molecular mechanisms of cardiotoxicity was examined by measuring p90RSK phosphorylation and autophagic flux. Both ponatinib and sunitinib induced the highest cardiotoxic effects among the screened TKIs. Sunitinib and ponatinib treatment reduced H9c2 cardiomyoblast cell viability and induced apoptotic cell death. Sunitinib treatment induced cardiomyoblast hypertrophy, while ponatinib treatment caused cellular detachment and cellular shrinkage. In terms of molecular pathways, ponatinib

treatment induced p90RSK phosphorylation and autophagy, while sunitinib treatment inhibited p90RSK activity and induced autophagy. Inhibition of p90RSK or autophagy using BID or CQ, respectively, was associated with further cellular death.

Our study compared the cardiotoxicity of different clinically-approved TKIs and identified the potential mechanisms of cardiotoxicity. This study demonstrated for the first time the different cardiotoxic effects associated with ponatinib treatment in H9c2 cell line.

DEDICATION

To my beloved mother

ACKNOWLEDGMENTS

I thank Almighty Allah as without His mercy, blessings, and guidance, I would never have completed this work.

I would like to thank my supervisor and mentor Dr. Fatima Mraiche for everything she taught me throughout the MSc thesis journey and for helping me to become the junior scientist I am today. Thank you very much for your invaluable support, guidance, patience, care, and all the great advice you have given me. Words will never be enough to express how grateful I am for all the opportunities you provided me with!

My appreciation goes to my co-supervisor Dr. Huseyin Yalcin for his continuous support and encouragement. I would also like to thank my Graduate Student Supervisory Committee members; Dr. Shahab Uddin, Dr. Hesham Korashy, Dr. Hazem Elewa, and Dr. Mohamed Izham for their support, insightful comments and guidance.

I would like to acknowledge Dr. Fatima Mraiche's lab members; Mr. Nabeel Abdulrahman and Ms. Jensa Joseph for their technical assistance, support, and continues encouragement. Also, I would like to thank Dr. Siveen kodappully from the interim translational research institute (iTRI) for training me and providing support during flow cytometer experiments.

I thank Qatar University and the College of Pharmacy for funding me to disseminate this work at an international conference.

Finally, I would like to extend my sincere gratitude to my loving family; my parents and my brothers, for their tremendous support and encouragement throughout my academic endeavors.

TABLE OF CONTENTS

LIST OF TABLES

LIST OF FIGURES

ABBREVIATIONS

ABL, Abselon murine leukemia

ALL, Acute lymphoblastic leukemia

AMPK, AMP-activated protein kinase

AT1R, ANG II type I receptor

AT2R, ANG II type II receptor

BAD, BCL-2-associated death promoter

BAP-1, BRCA-associated protein-1

BAX, BCL2-associated X protein

BCR, breakpoint cluster region

BID, BI-D1870

BNIP3, Bcl-2/E1B-interacting protein 3

BNP, brain natriuretic peptide

ccRCC, Clear cell RCC

CHF, Congestive heart failure

chRCC, Chromophobe RCC

CMA, Chaperone-mediated

CML, Chronic myeloid leukemia

CQ, Chloroquine

CREB, cAMP response element-binding protein

CTRCD, Cancer therapy-related cardiac dysfunction

DAPK, death-associated protein kinase

eNOS, Endothelial nitric oxide synthase

ERK, Extracellular signal-regulated kinase

FDA, Food and Drug Administration

FGFR, Fibroblast growth factor receptor

FLT1/3, FMS-like tyrosine kinase-1 and 3

GIST, Gastrointestinal stromal tumor

GRB2, Growth factor receptor-bound protein 2

GSK3, Glycogen synthase kinase 3

HF, Heart failure

HER2, Human epidermal growth factor receptor 2

hiPSC-CMs, Human induced pluripotent stem cell–derived cardiomyocytes

hiPSC-ECs, Human induced pluripotent stem cell–derived endothelial cells

hiPSC-FCs, Human induced pluripotent stem cell–derived cardiac fibroblasts

HIF, hypoxia-inducible factor

IE, immediate-early

IRIS, International Randomized study of Interferon-α and low-dose cytarabine versus STI571

I/R, Ischemia/reperfusion

K_d, Dissociation constant

LAMP2, lysosome-associated membrane protein-2

LC3, Microtubule-associated protein 1 light chain 3

LV, Left ventricular

LVEF, Left ventricular ejection fraction

MAPK, Mitogen-activated protein kinase

MEK1/2, MAPK-extracellular signal-regulated kinase 1/2

mTOR, Mammalian target of rapamycin

NCI, National Cancer Institute

NFATc4, Nuclear factor of activated T-cells 4

NF-kB, Nuclear factor-kB

NHE1, Na^+/H^+ exchanger 1

NO, Nitric oxide

NRVMs, Neonatal rat ventricular cardiomyocytes

PACE, Ponatinib Ph^+ ALL and CML Evaluation

PBRM-1, Polybromo-1

PDGFR, Platelet-derived growth factor receptor

PI3K, Phosphatidylinositol 3 kinase

pRCC, Papillary RCC

PTEN, Phosphatase and tensin homolog

RCC, Renal cell carcinoma

RET, Rearranged during transfection

ROS, Reactive-oxygen species

RSK, Ribosomal S6 kinase

RTK, Receptor tyrosine kinase

SDS-PAGE, Sodium dodecyl sulfate polyacrylamide gel electrophoresis

Ser/Thr, Serine-threonine

SENP2, Small ubiquitin-like modifier-specific protease-2

SETD-2, SET domain containing-2

SOS, Son of sevenless

SRF, Serum response factor

STAT5, Signal transducer and activator of transcription-5

TKIs, Tyrosine kinase inhibitors

TSC2, Tuberous sclerosis complex 2

US, United States

VEGFR 1-3, Vascular endothelial growth factor receptor 1-3

VHL, Von Hippel-Lindau

CHAPTER 1: INTRODUCTION

1.1. Cardio-oncology: An Emerging Multi-Disciplinary Field

Cancer and heart diseases remain the top leading cause of morbidity and mortality in developed society (1). Cancer survival rate and prognosis have improved substantially over the past 30 years due to advancement in early detection and treatment modalities (2). Despite the clinical success in cancer management, traditional and novel anticancer approaches have increased the prevalence of cardiovascular morbidities and mortalities among cancer patients and survivors (2-4). To satisfy the need for specialized discipline to provide cardiovascular care for cancer patients and survivors, a new medical field, cardio-oncology or onco-cardiology, was introduced (5, 6).

Cardio-oncology is an emerging multi-disciplinary field that focuses on understanding the pathophysiology of cancer therapy-induced cardiotoxicity and providing early detection and treatment for cancer patients and survivors (7). Multiple societies, such as The Canadian Cardiovascular Society, have developed guidelines and position statements to help clinicians to better deal with the arising issue of cardiotoxicity (8, 9). The Canadian Cardiovascular Society guidelines addresses four main areas to guide the cardiovascular care in cancer patients. These areas include: i) the identification of the population at high risk to develop cardiotoxicity; ii) detection and prevention strategies of cardiotoxicity; iii) cardiotoxicity treatment; and iv) the establishment of a multi-disciplinary approach for the management of cancer therapy-induced cardiovascular toxicity (9).

1.2. Cardiotoxicity

Although anticancer therapy-induced cardiotoxicity or cancer therapy-related cardiac dysfunction (CTRCD) is well-known, there is no agreed upon definition for cardiotoxicity (10, 11). Several cardiovascular and cancer organizations have defined cardiotoxicity according to clinical or subclinical manifestations (11, 12). The National Cancer Institute (NCI) describes cardiotoxicity as "toxicity that affects the heart" (13, 14). Whereas, the cardiac review and evaluation committee for trastuzumab (Human epidermal growth factor receptor 2; HER2 monoclonal antibody) clinical trials, defines cardiotoxicity as i) cardiac disease with a decreased left ventricular ejection fraction (LVEF); ii) symptoms of congestive heart failure (CHF); iii) signs of heart failure (HF); and iv) a symptomatic reduction of > 5% to ≤ 55% in LVEF baseline or a reduction of > 10% to ≤ 55% in LVEF without accompanying signs and symptoms of HF (12, 15). An expert consensus published by the American Society of Echocardiography and European Association of Cardiovascular Imaging defines CTRCD as > 10% to < 53% decline in LVEF that requires subsequent imaging, within 2-3 weeks, for confirmation (14, 16).

CTRCD involves functional, structural or a combination of both injuries induced by anticancer treatments (17). These injurious events include, but are not limited to, cardiomyocyte death, endothelial alteration and ion channel damage; which leads to cardiac dysfunction, cardiomyopathies and congestive heart failure (6, 17-19).

Based on the severity and the degree of reversibility, CTRCD is classified as type I or type II (14). Type I causes irreversible cardiac toxicity and damage, resulting in ultrastructural changes, myofibrillar disarray, myocyte necrosis and permeant cardiac dysfunction (20-23). Anthracyclines are an example of type I

CTRCD (14, 20, 24). Anthracyclines are a group of anticancer antibiotic (such as, daunorubicin, doxorubicin, idarubicin, epirubicin, and mitoxantrone) and are effective against various hematological cancers including leukemia and lymphoma, as well as solid cancers such as, breast cancer and sarcoma (10, 14, 18). Although anthracyclines are effective against cancer, their use is restricted due to the associated cardiotoxicity. Left ventricular (LV) dysfunction and HF are some of anthracycline-induced complications affecting patients (10). The incidence of doxorubicin-induced CHF is dose-dependent. Patients treated with doxorubicin at a cumulative dose of 400 mg/m^2 are at 3-5% risk of developing CHF, 7-26% risk with a dose of 550 mg/m^2, 48% risk when receiving a dose of 700 mg/m^2 (2, 18, 25, 26). Multiple molecular mechanisms have been implicated in anthracycline-induced cardiotoxicity, including iron-based oxygen free radical generation, topoisomerase II inhibition, mitochondrial dysfunction, and cardiomyocyte apoptosis (6, 10, 11, 14, 21).

Contrary to type I, type II CTRCD cardiotoxicity is dose-independent, reversible, and is not associated with ultrastructural myocardial abnormalities (20, 21). This type of toxicity is commonly experienced with trastuzumab, an anti-HER-2 agent which targets HER-2/neu-positive receptors (known as ErbB2) in breast cancer. The mechanism of cardiotoxicity is mediated through inhibiting ErbB2 signaling cascade required for cardiomyocyte homeostasis, survival, growth, and repair (6, 10, 18, 21, 27). Besides trastuzumab, several novel targeted therapies have been associated with type II CTRCD, including small molecule tyrosine kinase inhibitors (TKIs) (such as, imatinib, sunitinib, sorafenib, and lapatinib) (24, 28, 29).

Current cancer therapeutics include chemotherapy, radiation, surgical resection, immunotherapy and molecular targeted therapy (17). In the last decade,

the focus has been shifted towards employing targeted cancer therapies in cancer management (30). Targeted therapy with TKIs demonstrates an ability to inhibit multiple tyrosine kinases in cancerous cells. However, TKIs also inhibit protein kinases present in noncancerous cells, including cardiomyocytes. The nonspecific targeting of molecular pathways, which are necessary for cardiac function, could result in undesirable cardiovascular adverse effects (31, 32).

TKIs exhibit two types of toxic effects on cardiomyocytes: on-target and off-target cardiotoxicity. In "on-target" toxicity, TKIs inhibit signaling pathways that are essential to cancer and non-cancerous cell survival and homeostasis. Trastuzumab is a classic example of on-target cardiotoxic agent, which exhibits its cardiotoxicity by ErbB2 inhibition. "Off-target" toxicity occurs when TKIs inhibit a kinase (or a signaling mechanism) not intended to serve as a pharmacological target. Sunitinib-induced cardiotoxicity is an example of the off-target cardiotoxic effect, which inhibits cytoprotective kinase, ribosomal S6 kinase (RSK), and cellular homeostasis regulator, AMP-activated protein kinase (AMPK) (33-37). Although the cardiotoxicity induced by radiotherapy and conventional chemotherapy is well-established (17), the molecular mechanisms governing the cardiotoxicity induced by TKIs is not fully understood. An understanding of on-target and off-target cardiotoxicity is required for more efficient use of TKIs therapy (38).

The present research highlights the mechanism of cardiotoxicity associated with ponatinib and sunitinib. Ponatinib is a 3rd generation TKI, which is used to treat chronic myeloid leukemia (CML) patients, including those harboring T315I mutation, and Philadelphia chromosome-positive (Ph^{+}) acute lymphoblastic leukemia (ALL) (39). Whereas, sunitinib is a multi-tyrosine kinase inhibitor, which was first approved for advanced renal cell carcinoma (RCC) and currently is used

additional indications, including gastrointestinal stromal tumor (GIST) and pancreatic cancer (40). This chapter seeks to address ponatinib and sunitinib and their main indications, CML and RCC, respectively, and focuses on delineating the mechanism of cardiotoxicity associated with ponatinib and sunitinib.

1.3. Chronic Myeloid Leukemia (CML): Epidemiology, Pathophysiology, and Management

CML is a myeloproliferative neoplasm characterized by a unique molecular pathophysiology and clinical manifestation (41, 42). According to global cancer statistics, in 2013, there were 414,000 incident leukemia cases worldwide and 265,000 incident deaths among leukemic patients (43). In 2000, the prevalence of CML, in the United States (US), was estimated at 30,000 cases, then increased, in 2017, to 100,000 cases and is predicted to reach a plateau at 180,000 CML cases by 2030 (41).

CML affects the hematopoietic stem cells. Central to its pathogenesis is the reciprocal translocation between the ABL (Abselon murine leukemia) gene, a non-receptor tyrosine kinase expressed in several tissues, on chromosome 9, and the BCR gene (breakpoint cluster region) on chromosome 22, t(9;22) (q34;q11), known as Philadelphia chromosome. The resulting chimeric fusion gene, known as BCR-ABL, encodes a constitutively active protein tyrosine kinase and is a key to disease development, detection, and monitoring and also serves as a target for newly developed therapeutics (44-49).

At a molecular level, BCR-ABL oncoprotein promotes cellular proliferation, survival, growth and maintenance of CML leukemogenesis through interaction with numerous intracellular signaling molecules such as, RAS/mitogen-activated protein kinase (MAPK), phosphatidylinositol 3 kinase (PI3K)/AKT, signal transducer and

activator of transcription-5 (STAT5), mammalian target of rapamycin (mTOR), Src kinases, Jun, and Myc (41, 42, 50-54). Clinically CML exists in three phases, starting with a chronic phase, progressing into an unstable stage known as accelerated phase, and transitioning to a terminal phase known as blast phase or blast crisis (42, 47, 49).

The advent of TKIs has dramatically changed CML management with a 10-year survival rate exceeding 80%. Prior to the development of TKIs, CML management relied on either palliative therapy, including spleen irradiation and cytoreductive agents (such as, arsenic, busulfan and hydroxyurea) or curative therapy, including interferon-α and allogeneic stem-cell transplantation (45, 54). However, these modalities were associated with few drawbacks; cytoreductive agents possess palliative but not curative effect, while interferon-α is poorly tolerable and allogenic stem-cell transplantation is associated with high morbidity and mortality (54). In 2003, IRIS study (International Randomized Study of Interferon-α and low-dose cytarabine versus STI571) proved the superiority of STI571 (now known as imatinib) in comparison with combination therapy in newly diagnosed chronic phase CML patients (55).

Despite the breakthrough results of IRIS study, follow-up studies have shown high rates of discontinuation due to intolerance and/or primary and acquired resistance to imatinib treatment (47, 56). This resistance is due to the amplification of BCR-ABL oncogene, upregulation of multidrug resistant p-glycoprotein, down regulation of OCT-1 influx transporter, and/or single amino acid mutation (point mutation) on BCR-ABL kinase domain, which limits TKIs binding (44, 47). Shortly after imatinib introduction, second-generation TKIs, dasatinib, nilotinib, and bosutinib, were developed to manage imatinib-resistant CML (54, 56). However,

second-generation TKIs lack sensitivity against BCR-ABL T315I point mutation (57). T315I gatekeeper mutation is among the frequent point mutations in CML, accounting to 2-20% cases. This mutation is resistant to a broad-spectrum of TKIs and is only inhibited by a third-generation agent, ponatinib (44, 58).

1.3.1. Ponatinib

Ponatinib is a small molecule, orally active, and potent BCR-ABL inhibitor against numerous domain mutations, including T315I gatekeeper mutation (54, 56, 58) (Figure 1.1). In CML, ponatinib induces its anti-proliferative and anti-survival effects by inhibiting BCR-ABL oncoprotein and its downstream signaling molecules (Figure 1.2) (53, 54). Besides BCR-ABL, ponatinib effectively inhibits up to 40 kinases, including, SRC, PDGFR (platelet-derived growth factor receptor), FGFR (fibroblast growth factor receptor), VEGFR 1-3 (vascular endothelial growth factor receptor 1-3), RET (rearranged during transfection), KIT, AKT, ERK (extracellular signal-regulated kinase), and FLT1/3 (FMS-like tyrosine kinase-1 and 3) and other kinases (59-61).

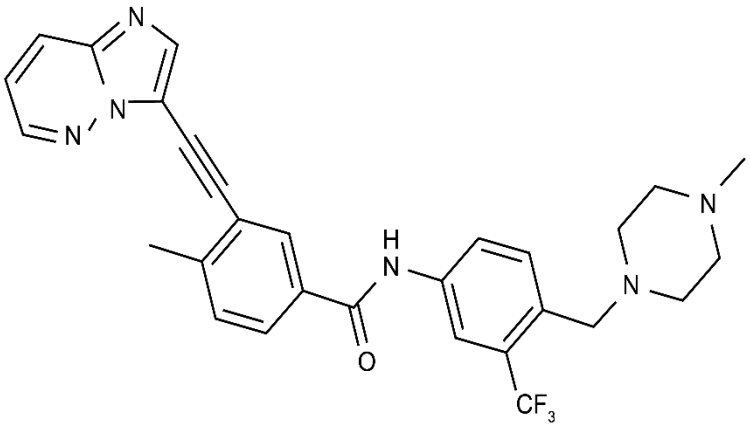

Figure 1.1 Chemical structure of ponatinib, free base. Ponatinib is 3-(2-imidazo[1,2b]pyridazin-3-ylethynyl)-4-methyl-N-[4-[(4-methyl-1-piperazinyl)methyl]-3-(trifluoromethyl)phenyl]-benzamide (59, 62).

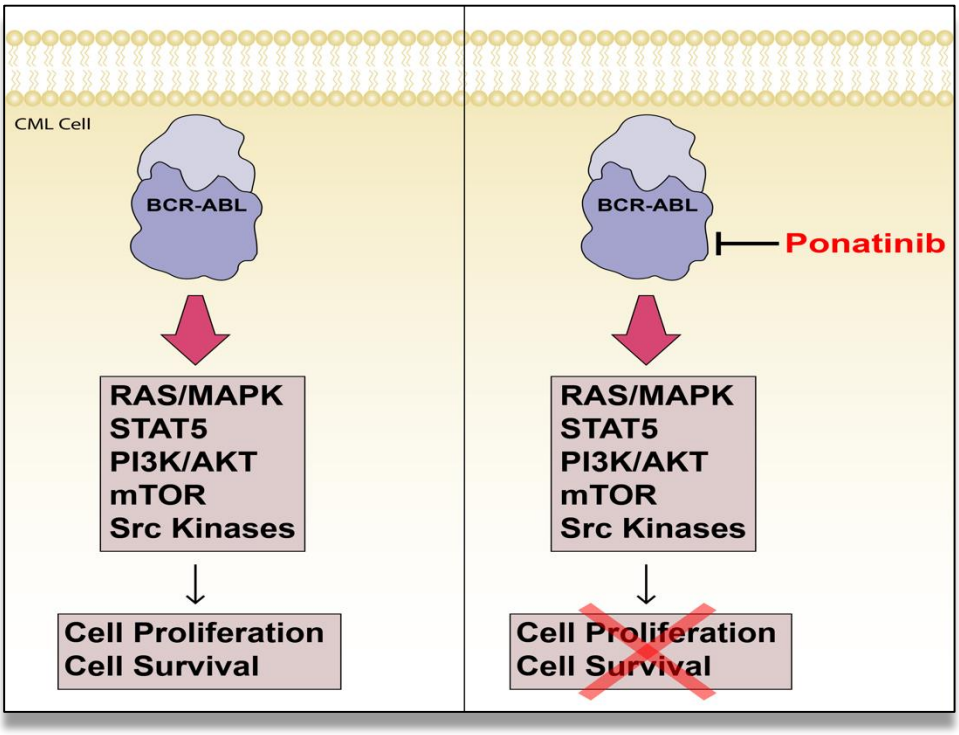

Figure 1.2 Mechanism of action of ponatinib. The novel tyrosine kinase inhibitor, ponatinib, exerts its activity by inhibiting BCR-ABL oncoprotein and its downstream effectors, thereby decreasing leukemic cell proliferation and survival. This figure was adapted from Dao et al. (2013) and Pophali et al. (2016) (53, 54).

1.3.1.1. Ponatinib-Induced Cardiotoxicity

In 2012, due to promising results from a phase II PACE study (Ponatinib Ph^+ ALL and CML Evaluation), ponatinib was granted an accelerated approval as a treatment for CML patients with resistance or intolerance to previous TKI therapies (54, 63, 64). However, ponatinib was associated with increased incidence of cardiovascular issues. At a median follow-up of 28 months, PACE trial reported 10% cardiovascular, 7% cerebrovascular, 7% peripheral arterial, 19% arterial thrombotic, and 5% venous thromboembolic events (65). In addition, it was reported that 26% of patients developed systemic hypertension, which is probably attributed to VEGFR inhibition by ponatinib (61, 65). Due to concerns of heart failure and vascular occlusive events, ponatinib was temporarily withdrawn from the US market by the Food and Drug Administration (FDA) and was reintroduced to the market in 2014 (60, 64, 66).

Cardiovascular toxicity is an alarming concern with the new BCR-ABL TKIs, including ponatinib; however, it is uncommon with imatinib. In fact, imatinib demonstrates beneficial cardiovascular effects, improved cardiac function and enhanced exercise capacity in patients with pulmonary arterial hypertension (67, 68). In addition, a retrospective cohort analysis showed lower incidence of peripheral arterial occlusive disease events in CML patients receiving imatinib than those receiving nilotinib or not treated with TKIs (69). Given the fact of lower cardiovascular toxicity of imatinib, it is probable, therefore, that ponatinib-induced cardiovascular toxicity is an off-target effect and not necessarily an on-target effect (61).

Although ponatinib-induced cardiovascular toxicity and dysfunction is well-recognized, the molecular mechanism behind cardiotoxicity remains unclear (70).

One known mechanism of cardiotoxicity is through inhibition of VEGFR1-3, which is associated with increased incidences of hypertension (similar to vascular signaling pathway inhibitor, sunitinib) via increased endothelin-1, as well as reduced nitric oxide (NO), or reduced density of capillaries (66, 71, 72).

Several studies have investigated ponatinib-induced cardiotoxicity on different in vitro and in vivo models. In a study that used a cell-based model, human induced pluripotent stem cell–derived cardiomyocytes, endothelial cells and cardiac fibroblasts (hiPSC-CMs, hiPSC-ECs, hiPSC-FCs, respectively) for high-throughput cardiotoxicity screen of 21 TKIs, it was found that ponatinib led to remarkable cell death in hiPSC-derived cell models (73). In agreement, another study found that treatment with 5μM and 10μM ponatinib lead to significant reduction in hiPSC-CMs cell viability (74). Moreover, a previous study demonstrated a significant neonatal rat ventricular cardiomyocytes (NRVMs) damage following treatment with 2μM ponatinib. Authors found that ponatinib-treated NRVMs exhibits morphological disruption of sarcomeres, myofibril loss, and reduction of myocyte cellular density. In this study, authors found that ponatinib-induced cardiotoxicity may be an on-target effect (ABL inhibition) and/or an off-target effect (other protein kinases) (75). Furthermore, recently, Singh et al. studied the cardiotoxicity of CML-approved TKIs, including dasatinib, imatinib, ponatinib, nilotinib, and bosutinib using zebrafish and NRVMs. Investigators indicated ponatinib as the most toxic agent, among all screened TKIs, to zebrafish in vivo model. In addition, they found that treatment with 50nM ponatinib induced AKT and ERK prosurvival inhibition which is central to NRVMs apoptosis. Authors observed that other CML-TKIs could not suppress AKT-ERK pathway; indicating that it is a distinctive effect induced by ponatinib. Moreover, authors found that pretreatment of NRVMs with Neuregulin-

1β (a PI3K/AKT and ERK pathways inducer) is able to significantly reduce ponatinib-induced cardiomyocyte death. (76). Figure 1.3 is a summary of a proposed model of known mechanisms governing ponatinib-induced cardiotoxicity, which may predispose to cardiac dysfunction. **Taken together, it is evident that ponatinib treatment is associated with cardiotoxicity. Hence, it is critical to identify the potential mechanisms of cardiotoxicity induced by ponatinib, in order to develop preventative strategies and to optimize patients care.** Herein, we focused on investigating two potential mechanisms of cardiotoxicity, ribosomal S6 Kinase and autophagy alteration, which will be discussed in the upcoming sections.

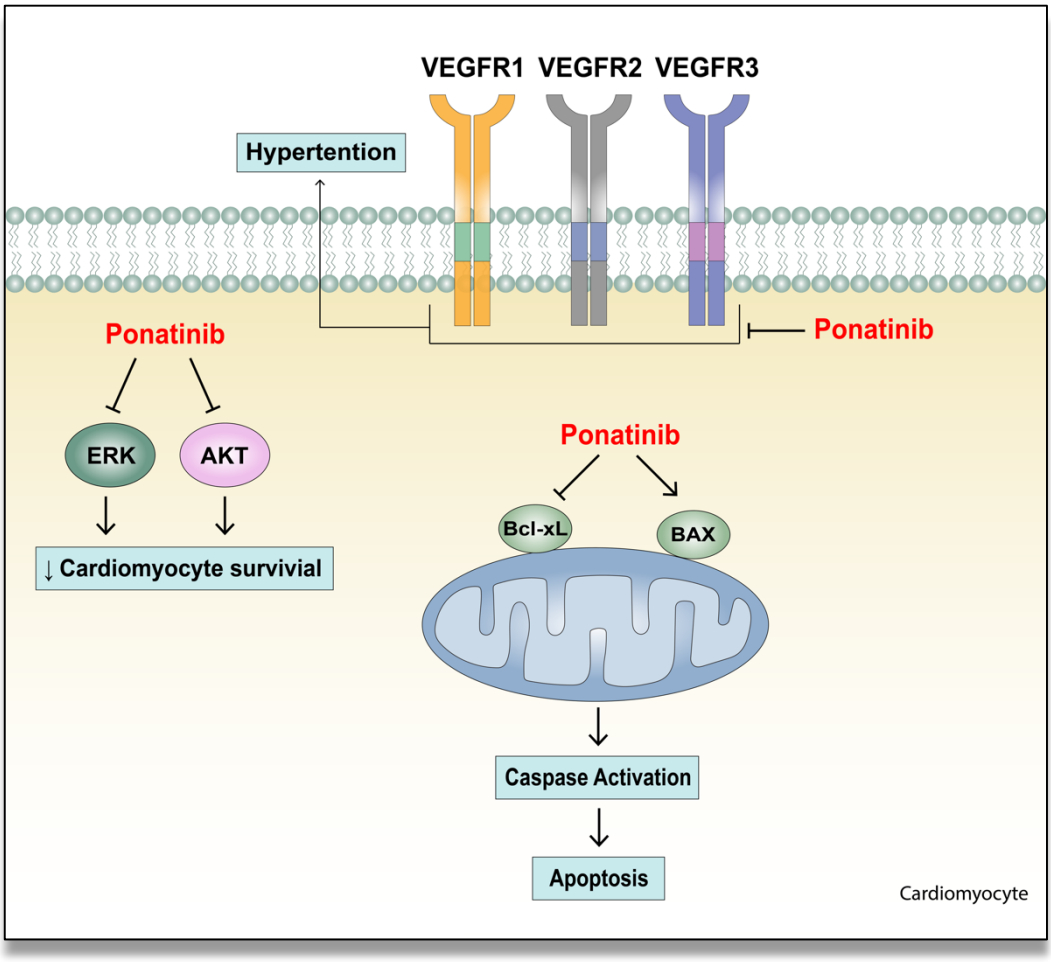

Figure 1.3 Summary of a proposed model of molecular mechanisms of ponatinib-induced cardiotoxicity. Treatment with ponatinib is associated with cardiotoxic effects that may be mediated through an on-target and off-target mechanism. Ponatinib inhibits VEGFR1-3, which induces systemic hypertension. Another cardiotoxic mechanism of ponatinib involves the inhibition of AKT/ERK prosurvival pathway and caspase-dependent apoptotic cell death. These cardiotoxic effects induced by treatment with ponatinib may predispose to cardiac dysfunction (66, 71, 76).

1.4. Renal Cell Carcinoma (RCC): Epidemiology, Pathophysiology, and Management

Renal cell carcinoma (RCC) or kidney cancer comprises of a heterogeneous group of chemotherapy-resistant cancers that can be distinguished by distinct histopathological features, molecular characteristics, and genetic abnormalities (77, 78). In 2013, RCC was ranked the 16th most common cause of cancer worldwide and the 10th common cancer in developed countries (43). Globally, in the same year, a total of 295,000 incident cases and 134,000 incident deaths from kidney cancer were reported. In the US, in 2016, the kidney cancer incidence and death were estimated to be 62,700 and 14,240 cases, respectively. The median age at diagnosis was estimated to be 64 years with an estimated 5-year relative survival rate that stands at 73% (79, 80).

Histologically, RCC can be classified into clear cell RCC (ccRCC), papillary RCC (pRCC) and chromophobe RCC (chRCC). ccRCC is the most common subtype, originating in the proximal tubule and accounting for 80% of all RCC cases (81-84). Central to ccRCC carcinogenesis is the biallelic loss of function of von Hippel-Lindau (VHL) tumor suppressor gene, which leads to stabilization of hypoxia-inducible factors (HIF-1α and HIF-2α) and activates downstream genes, including VEGF and PDGF; leading to increased cellular growth, survival, and angiogenesis. Moreover, mutations of epigenetic regulators (like, Polybromo-1 (PBRM-1), along with BRCA-associated protein-1 (BAP-1)), abnormalities of chromatin remodeling genes (SET domain containing-2 (SETD-2)), and mutations involving mTOR signaling pathway (PTEN, PI3K, AKT, and mTOR) is a characteristic feature of ccRCC (77, 78, 82, 84, 85).

In the past, RCC was considered as a chemotherapy-resistant condition. Interferon-α and interleukin-2 were used as standard therapy for metastatic RCC. Due to low response and survival rate and high adverse effects, their use was limited. Nonetheless, the basic understanding of disease etiology and development of antiangiogenic agents targeting VEGF and VEGFR, immune checkpoint inhibitors and mTOR inhibitors have led to a substantial improvement in RCC treatment and clinical outcomes. Sunitinib is a multitargeted TKI, which inhibits multiple factors and receptors, including, but not limited to, VEGFR and PDGFR and is commonly used as a first-line agent (40, 77, 78, 82, 85).

1.4.1. Sunitinib

Sunitinib is an orally active small molecule multi-tyrosine kinase inhibitor (Figure 1.4). It potently inhibits VEGFR 1-3, PDGFR-α and β, FLT-3, and stem cell factor receptor (c-KIT), and RET. Inhibition of these tyrosine kinases blocks multiple signaling pathways, including PI3K/AKT, MAPK, and protein kinase C, thereby triggering anticancer effects by inhibiting tumor progression, proliferation, and angiogenic effects, and promoting vascular disruption (Figure 1.5) (32, 71, 86-89).

Sunitinib has been approved as a first-line treatment for advanced RCC and as a second-line treatment for GIST (32, 87). Motzer et al. compared between sunitinib and Interferon-α in patients with untreated RCC and found that sunitinib was superior to Interferon-α. In this trial, the progression-free survival was longer (11 months vs 5 months, respectively, $P < 0.001$) and the response rate was higher in sunitinib arm (86, 90). Sunitinib treatment was associated with adverse events including, fatigue, hand-foot syndrome, nausea, diarrhea, cardiovascular events (86, 90). Whilst sunitinib has improved the clinical outcomes of RCC cancer patients, its

therapeutic use is limited due to its associated cardiotoxicity (91). Therefore, understanding the mechanisms of sunitinib-induced cardiotoxicity is critical to identifying preventative strategies.

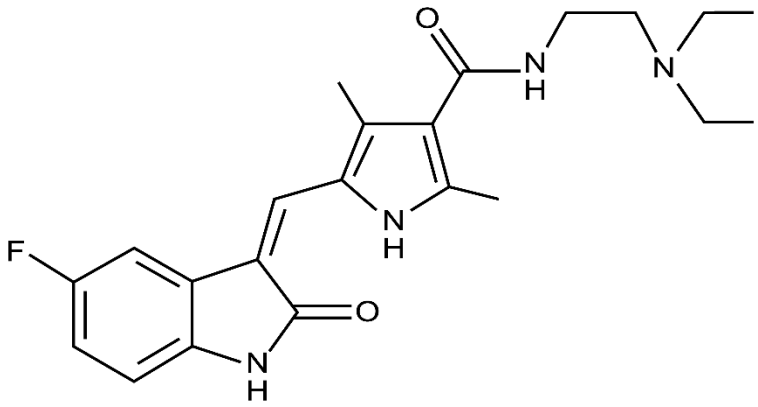

Figure 1.4. Chemical structure of sunitinib, free base. Sunitinib is N-[2(Diethylamino)ethyl]-5-[(Z)-(5-fluoro-1,2-dihydro-2-oxo-3H-indol-3-ylidene)methyl]-2,4-dimethyl-1H-pyrrole-3-carboxamide (92).

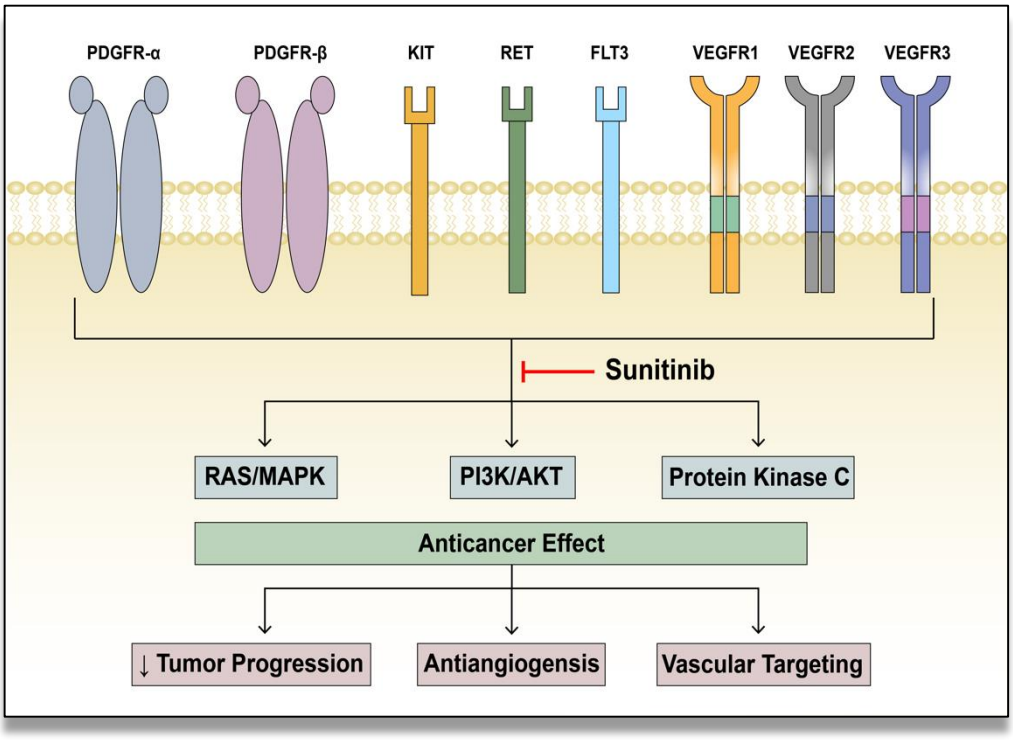

Figure 1.5. Mechanism of action of sunitinib. Sunitinib inhibits multiple tyrosine kinases such as, PDGFR-α and β, KIT, RET, FLT3, and VEGFR1-3. As a result, sunitinib inhibits several signaling pathways, including RAS/mitogen-activated protein kinase (MAPK), phosphoinositide 3-kinase (PI3K)/AKT, and Protein Kinase C, thereby triggering antitumor effects by blocking tumor progression and angiogenic effects and promoting vascular disruption. This figure was adapted from Faivre et al. (2007) and Aparicio-Gallego et al. (2011) (88, 89).

1.4.2. Sunitinib-Induced Cardiotoxicity

Cardiovascular safety profile of sunitinib has received a growing attention following multiple clinical studies (93). Sunitinib use has been associated with multiple cardiovascular adverse effects including, hypertension, decline in LVEF, LV systolic dysfunction, myocardial infarction and heart failure (71, 87, 90, 94). A phase III randomized, double blinded, trial patients with GIST showed incidence of

reduction in LVEF by 11% in sunitinib arm versus 3% in placebo arm (93, 95). Another study, involving patients treated with sunitinib for metastatic ccRCC, showed that 4.7% of patients experienced declines in LVEF (96). In a meta-analysis consisting of 13 clinical trials and a total of 4999 patients, it was reported that the incidence of all-grade hypertension among patients treated with sunitinib were 21.6% (71). Although sunitinib-induced cardiovascular toxicity is well-recognized, the underlying mechanisms of cardiotoxicity are not fully understood.

At a cellular level, Chu et al. have shown that sunitinib-induced cardiac dysfunction is characterized by cardiomyocyte abnormalities, mitochondrial swelling and activation of apoptosis (94). This observation could be attributed, in part, to the inhibition of PDGFR-β, which is involved in angiogenic regulation of cardiomyocyte response to pressure overload. Chintalgattu et al. have found that absence of PDGFR-β in cardiomyocytes led to impaired angiogenesis, myocardial dysfunction and heart failure (87, 97). In addition, sunitinib inhibits VEGFR1-3, which leads to systemic hypertension and heart failure. This is due to reduction of NO production (32, 98).

Another mechanism of sunitinib-induced cardiotoxicity involves the inhibition of AMPK signaling, which leads to mitochondrial dysfunction, ATP depletion and apoptosis. AMPK plays an indispensable role during energy depleted conditions; it regulates energy utilization and activates energy generation pathways. Through inhibition of AMPK by sunitinib, cells lose energy by blocking energy-generating mechanisms and activating energy-consuming mechanisms. Also, inhibition of AMPK by sunitinib along with inhibition of VEGFR and PDGFR decrease adaptation to cardiac stress (31, 32, 87, 99, 100). Other suggested mechanisms of sunitinib-mediated cardiotoxicity involve RSK inhibition and activation of autophagy, (31, 38, 100, 101), which will be highlighted in the following sections of this chapter. Figure

1.6 is a summary of a proposed model of some mechanisms governing sunitinib-induced cardiotoxicity, which may predispose to cardiac dysfunction.

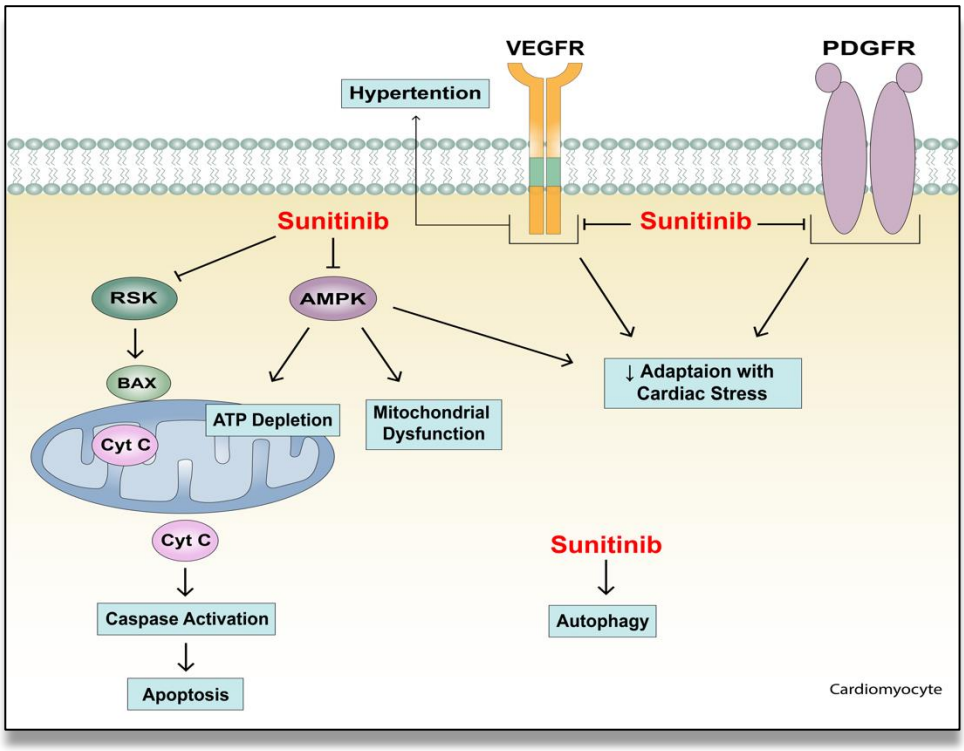

Figure 1.6. Summary of a proposed model of molecular mechanisms of sunitinib-induced cardiotoxicity. Treatment with sunitinib is associated with cardiotoxic effects that may be mediated through an on-target and off-target mechanism. A postulated mechanism of sunitinib-induced involves the inhibition of VEGFR1-3 and PDGFR, which causes systemic hypertension and decreases adaptation to cardiac stress. Also, sunitinib treatment induces cardiomyocyte caspase-dependent apoptotic cell death through inhibiting prosurvival RSK pathway. Another mechanism of sunitinib-induced cardiotoxicity involves the inhibition of AMPK, which decreases adaptation to cardiac stress, causes ATP depletion, and leads to mitochondrial dysfunction. Sunitinib has also shown to induce autophagic flux in cardiomyocyte. This figure was adopted from Gorini et al. (2018) (31).

1.5. Speculated Molecular Mechanisms of Sunitinib and Ponatinib-Mediated Cardiotoxicity

1.5.1. Ribosomal S6 Kinase (RSK)

The Ras-MAPK pathway plays an indispensable role in regulating different cellular processes (102-104). Various extracellular stimuli, including neurotransmitters, hormones, growth factors, and chemokines stimulates receptor tyrosine kinase (RTK) autophosphorylation. This leads to activation of adaptor proteins, such as growth factor receptor-bound protein 2 (GRB2), son of sevenless (SOS), and activation of Ras and Raf protein kinases. Raf then phosphorylates MEK1/2 (MAPK-extracellular signal-regulated kinase 1/2) and ERK1/2. Downstream to this pathway is a 90 kDa family of highly conserved serine-threonine (Ser/Thr) proteins, ribosomal S6 kinases 1-4 (RSK1-4), which are directly and exclusively phosphorylated by ERK1/2 (Figure 1.7). RSK isoforms are ubiquitously expressed in many cell lines and tissues; RSK1 is expressed in the brain, lung, kidney, and pancreas. RSK2 and 3 are expressed in the brain, heart, and pancreas (102, 105, 106). Various pan-RSK inhibitors exist, including competitive inhibitors (SL0101 and BI-D1870), which target the ATP-binding site of the amino terminal kinase domain (NTKD), and irreversible inhibitor (fluoromethyl ketone (FMK)), which targets the cysteine residue-ATP-binding site of the carboxyl-terminal kinase domain (CTKD) (105, 107).

1.5.1.1. Role of RSK in Cellular Processes

Based on the nature of RSK substrates, several roles can be deduced; RSK regulates multiple processes, including cellular growth, survival, proliferation, and cell cycle progression (104-106, 108). Activated RSK has been shown to phosphorylate numerous transcription factors that induce immediate-early (IE) gene expression, including cAMP response element-binding protein (CREB), serum response factor (SRF), nuclear factor-kB (NF-kB), transcription initiation factor TIF1A, ETS translocation variant-1, and cytoplasmic nuclear factor of activated T-cells 4 (NFATc4), and estrogen receptor-a. In addition, RSK can phosphorylate IE gene products, including c-Fos, c-Jun, and nuclear receptor subfamily (Nur77) (102-105, 109). In addition, RSK has been implicated in protein synthesis and cell growth through the phosphorylation of tuberous sclerosis complex 2 (TSC2) and Raptor, which stimulate mTOR signaling (110, 111). Moreover, RSK phosphorylates and inhibits GSK3 (Glycogen synthase kinase 3), which causes stabilization of Myc-c and cyclin D1 and mediates cell cycle progression and survival (112, 113). Further, RSK regulates protein synthesis through stimulating the translation initiation protein, eIF4B (114). Also, RSK regulates cell survival through 1) the inactivation of death-associated protein kinase (DAPK), a pro-apoptotic and tumor suppressor protein (115) and 2) reduction of pro-apoptotic activity of BCL-2-associated death promoter (BAD) (116). Another role of RSK involves regulating cell cycle through participating in G1-phase progression by phosphorylating cyclin-dependent kinase inhibitor $p27^{kip1}$ (117), and in G1-S phase progression by activating c-Fos (102, 118).

Taken together, RSK, as a downstream effector of Ras-MAPK pathway, is implicated in various critical cellular processes. Aberration or mutation in genes encoding Ras-MAPK pathway constitutes have been implicated in several

pathologies, including cancer, cardiovascular diseases, diabetes, inflammatory and neurodegenerative disorders (102, 104, 108, 119). Herein, we focused on the role of RSK in cancer and cardiac pathophysiology.

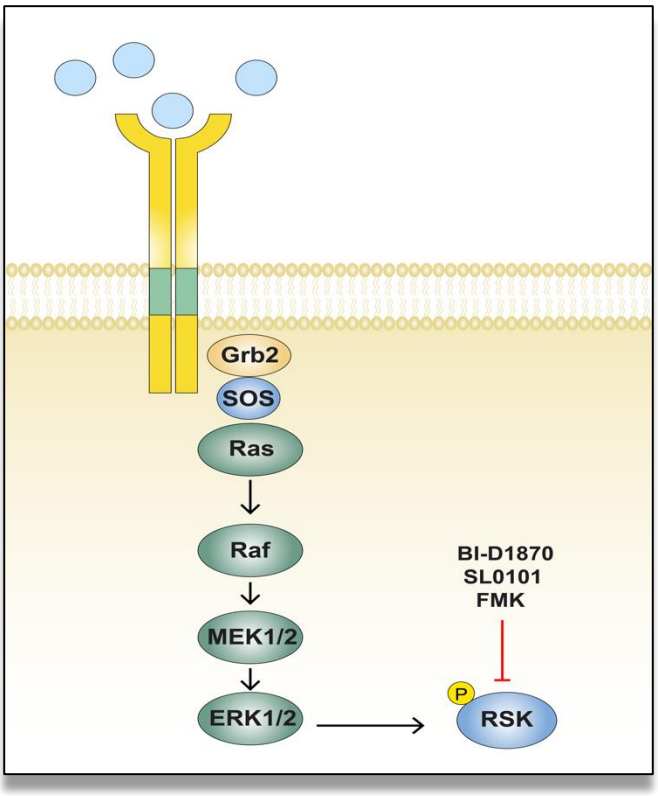

Figure 1.7. Illustration of ribosomal S6 kinase (RSK) activation.

1.5.1.2. RSK and Cancer

RSK is an important Ras-MAPK effector and attracted considerable interest as a potential target for multiple cancer therapies. Dysregulated RSK activity has been implicated in various forms of cancer. RSK1 and RSK2 have been implicated in cancer progression through mediating tumor cell survival and growth (105, 108). They promote pro-survival and reduce pro-apoptotic genes through phosphorylation of CREB, BAD, DAPK, and BimEL (115, 116, 120, 121). In addition, they

phosphorylate TSC2 and raptor, stimulating mTOR pathway and promoting cell growth (110, 111). Moreover, RSK1 and RSK2 were shown to inhibit GSK3 and phosphorylate c-Fos and $p27^{kip1}$, promoting cell proliferation (102, 107, 117). Furthermore, they reduce cell adhesion and promote tumor invasion and metastasis through phosphorylating SH3 domain-containing protein (SH3P2) (122), FRA1 (123, 124), c-Jun (123, 124), and filamin A (125), as well as inactivating the integrin activation (126). Contrary to RSK1 and RSK2, both RSK3 and RSK4 were shown to act as tumor suppressors (102). Overall, it is notable that RSK is involved in cancer pathophysiology through direct and indirect molecular mechanisms.

1.5.1.3. RSK and Cardiovascular Diseases

In the heart, RSK has an imperative role in cardiac physiology, where its aberrant activity is correlated with cardiac hypertrophy and heart failure. Increased RSK activity was previously detected following hypertrophic stimulation of cardiac myocytes and fibroblasts and in failing hearts of patients with end-stage dilated cardiomyopathy (127, 128). Takeishi et al. found that p90RSK is activated under ischemia/reperfusion (I/R) condition in guinea pigs (129). In addition, it was shown that Na^+/H^+ exchanger 1 (NHE1)-p90RSK activation promotes cardiomyocyte hypertrophy (130). Moreover, Yamaguchi et al. found that activated p90RSK decreases GSK3 and promotes cardiac hypertrophy in mice expressing aberrant type 2 ryanodine receptor ion channel (131). Further, stimulation of p90RSK via prostaglandin E2 in neonatal ventricular myocytes was shown to induce c-Fos, brain natriuretic peptide (BNP), and early growth response 1, promoting myocyte growth and possibly cardiomyocyte hypertrophy (132).

In addition to cardiac hypertrophy, activated p90RSK was shown to inhibit voltage-gated K^+ channel activity, prolonging the cardiac QT intervals, and

predisposing the heart to arrhythmias (133).

Furthermore, during atherosclerosis, p90RSK is activated, resulting in phosphorylation of small ubiquitin-like modifier-specific protease-2 (SENP2) and promotes SENP2 nuclear export. P90RSK-mediated SENP2 nuclear export induces endothelial cell apoptosis, inflammation, endothelial NO synthase (eNOS) reduction, and formation of atherosclerosis plague (134, 135). Le et al. found that p90RSK inhibitor induced anti-atherosclerosis effects by decreasing the expression of adhesion molecule and increasing expression of eNOS (136). Overall, these findings confirm the complex role of RSK in the pathophysiology of cardiovascular diseases.

1.5.1.4. RSK in TKIs-Induced Cardiotoxicity

Role of RSK in cardiovascular toxicity is paradoxical. Recently, it was shown that ponatinib upregulates p90RSK protein expression in human endothelial cell lines (137). This activation plays a role in endothelial cell death and formation of atherosclerotic lesions. However, whether ponatinib induces p90RSK in cardiomyocyte model is not yet known. In a previous study, the biochemical inhibitory activity of 313 kinases was screened using 1µM of 25 kinase inhibitors. Treatment with 1µM ponatinib has weakly inhibited RSK1, 2, 3, and 4 by 32%, 30%, 62%, and 13%, respectively (138).

Conversely, inhibition of RSK activity has been a postulated mechanism of cardiotoxicity induced by sunitinib. It was previously demonstrated that treatment with 1µM sunitinib is able to potent inhibition RSK1-4 by 95-97% (138). In addition, Karaman et al. screened 38 kinase inhibitors, including 21 TKIs, against a panel of 317 protein kinases and determined the binding dissociation constant (K_d) for each interaction. Based on kinase map interaction, they found that the K_d for RSK1 following 10µM treatment with sunitinib was 0.14µM, K_d for RSK2 was

0.017μM, and K_d for RSK3 was 0.58μM (35). As a result, Force et al. hypothesized that sunitinib-induced cardiotoxicity is via the inhibition of RSK signaling pathway, which would lead to release of the pro-apoptotic factor BAD, subsequent activation of BCL2-associated X protein (BAX), and release of cytochrome c, resulting in the activation of apoptosis and ATP depletion. Activated apoptosis would promote cardiomyocyte loss, which along with ATP depletion would cause LV dysfunction and mediate cardiac hypertrophy (Figure 1.6) (38). As a proof of concept, Hasinoff et al. studied whether sunitinib inhibits RSK, promotes myocyte damage, and induces cellular death. Authors found that treatment of NRVMs with sunitinib inhibited RSK1 with a half maximal inhibitory concentration (IC_{50}) of 0.36μM. In addition, it was shown that sunitinib treatment increased caspase-3/7 activity without change in BAX activity (100). These findings demonstrate that ponatinib is an inducer of p90RSK activity whereas sunitinib is a potent inhibitor. Therefore, it is important to delineate the exact role of RSK in ponatinib-mediated cardiotoxicity.

1.5.2. Autophagy

Autophagy, from the Greek word “self-eating”, is described as a highly conserved cellular pathway in eukaryotes. It involves degrading and recycling of intracellular components to maintain cellular homeostasis and to eliminate misfolded proteins and damaged organelles. During autophagy, cytoplasmic components are delivered to lysosome and then degraded or recycled to active monomers (139, 140).

Autophagy is classified into three types: chaperone-mediated (CMA), microautophagy and macroautophgy. Macroautophagy is the most prevalent autophagic pathway, hereafter termed autophagy, involves the formation of a double membrane structure, termed autophagosome, that engulfs the intracellular components, and then fuses with the lysosomes for degradation (141). Autophagy is

regulated by a number of highly conserved Atg (Autophagy) genes and serves as regulator for several physiological and pathological processes (142). Although autophagy occurs at basal conditions, it can be triggered by various stimuli including, nutrient-depletion conditions, oxygen insufficiency, and hormones (143, 144).

1.5.2.1. Monitoring Autophagy

There are several methods to monitor autophagy, including measurement of autophagosome abundance by immunoblotting, measurement of long-lived protein degradation by electron microscopy, quantification of autophagic flux in the presence and absence of autophagy inhibitors, and utilization of microtubule-associated protein 1 light chain 3 (LC3) fluorescent probe to quantify autophagic flux (145, 146).

Under physiological conditions, the microtubule-associated protein 1 light chain 3 (LC3) exists as LC3-I (cytosolic form). Once autophagy is activated, LC3 is conjugated to phosphatidylethanolamine and lipidated to form LC3-II, which is recruited to the inner and outer autophagosomal membrane (147, 148). Measuring the amount of LC3-II expression by immunoblotting is a commonly-used indicator of the number of autophagosome and autophagic structure. However, LC3-II is not an appropriate marker of autophagic activity, as LC3-II accumulation could reflect induction of autophagosome formation and/or aberrant autophagosome degradation. Therefore, to evaluate the autophagic activity, it is critical to monitor the autophagic flux using autophagy inhibitors (such as, chloroquine, bafilomycin, and pepstatinA) (145, 146, 148, 149).

Another widely used method to monitor autophagic flux involves assessing p62 degradation (148). Degradation of p62 is directly dependent on autophagy; it accumulates when autophagy is blocked and decreases when autophagy is induced (150).

1.5.2.2. Role of autophagy in Cellular Processes

Although autophagy is robustly activated upon starvation, under normal conditions, autophagy occurs at basal rate to maintain the cellular homeostasis and the integrity of macromolecules and organelles. This is through eliminating unneeded, damaged, or misfolded proteins and organelles and preventing protein aggregates and pathogens (145, 151, 152).

Activated autophagic processes, in times of metabolic stress including, nutrient deprivation, hypoxia, and growth factor reduction, is thought to play an adaptive role. In nutrient deprivation condition, autophagic degradation generates amino acids and free fatty acids that are used for the de novo synthesis of proteins and ATP production (152, 153). In case of oxygen deficiency, autophagy is induced by HIF-1α through increasing Bcl-2/E1B-interacting protein 3 (BNIP3), protecting against cell damage. BNIP3 activates autophagy through releasing BCL-2 and BCL-XL-bound Beclin1 (154).

Autophagy exhibits cytoprotective effects; its inhibition promotes type I cell death (apoptotic cell death). Boya et al. have shown that inhibition of autophagy by interfering RNA or using pharmacological inhibitors induces apoptotic type of cell death (155). Since autophagy plays a critical role in homeostasis, its dysregulation has been implicated in several pathologies, including neurodegenerative disorders, cancer, and cardiac dysfunction (139, 152, 156).

1.5.2.3. Autophagy and Cancer

The role of autophagy in cancer is paradoxical. Based on a number of factors, for example, tumor type, autophagy could have prosurvival or pro-death roles. Such contrasting dual roles of autophagy has been reported with Ras and p53 proteins,

frequently mutated in human cancer (157, 158).

Since aberrant autophagy was implicated in tumorigenesis, it was initially thought to have a tumor-suppressive role (159, 160). Beclin1, an autophagy gene, can suppress tumor formation; lower expression level of Beclin1 was observed in human breast cancer cells compared with higher expression level in normal breast epithelia (142, 161). Moreover, tumor suppressor phosphatase and tensin homolog (PTEN), frequently mutated in variety of cancers, was shown to promote autophagy (162, 163). These findings demonstrate that autophagy is not only implicated in tumor-suppression, but it could also promote tumor formation.

Autophagy promotes tumor progression by protecting tumor cells from necrosis and fulfilling their elevated metabolic demands (159, 160). Hypoxic microenvironment stimulates HIF-1α-induced autophagy and promotes tumor survival (164). Autophagy demonstrates a complex role in cancer. Therefore, understanding the mechanism of autophagy in cancer setting is required as it may serve as a potential tumor-suppressive target.

1.5.2.4. Autophagy and Cardiac Diseases

In myocardium, autophagy is thought to maintain normal cardiac structure and function; its inhibition or absence leads to cardiac hypertrophy and other cardiac pathologies (165). A growing body of evidence suggests that autophagy is induced in various heart diseases including, heart failure, cardiac hypertrophy, and myocardial I/R (166-168). Autophagic response is thought to act as a protective mechanism against ischemia-induced cardiac remodeling and dysfunction. Matsui et al. found that ischemia, due to glucose deprivation, stimulated autophagy through activating AMPK and inhibiting mTOR. Whereas reperfusion was accompanied by an increase of Beclin1 (166). In addition, Ma et al. found that autophagy was induced following I/R

in cardiomyocytes; however, autophagosome clearance was compromised, which led to cardiomyocyte death. Authors have found that the mechanism of cardiomyocyte death was through decreased lysosome-associated membrane protein-2 (LAMP2), upregulated Beclin1 and reactive-oxygen species (ROS) generation, and mitochondrial damage (169).

Unlike ischemia injury, autophagy-induced due to pressure overload could manifest as maladaptive and lead to detrimental effects to the heart. Zhu et al. found that the autophagy-induced, in cardiomyocytes, in response to pressure overload is through the upregulation of Beclin1. They also found that cardiac remodeling is reversed through inhibition of autophagy via heterozygous knockdown of Beclin1 (143). Moreover, Porrello et al. found that neurohormonal stimulation with angiotensin II (ANG II) upregulates autophagy in neonatal cardiomyocytes through ANG II type I receptor (AT1R), whereas ANG II type II receptor (AT2R) demonstrated anti-autophagic activity (170).

Dysregulated myocardial autophagy could result in age-related cardiomyopathy, cardiac hypertrophy, and heart failure. A previous study showed that cardiac specific Atg5-deficient mice, led to ventricular dilatation and dysfunction with increasing age (171). Moreover, Nakai et al. have found that cardiac specific Atg5-deficient mice promoted cardiac hypertrophy, LV dilatation, and cardiac dysfunction. Besides, Atg5-deficient heart showed disrupted sarcomere structure. Authors have examined the role of autophagy in neonatal cardiomyocyte; they demonstrated that Atg7 knockdown promote significant cardiac hypertrophy. Authors also suggested that basal autophagy is involved in maintaining homeostasis while upregulated autophagy, in failing heart, protects cardiomyocyte from hemodynamic stress (165). Furthermore, deficiency of LAMP2 causes Danon disease, which exhibits

accumulation of autophagic vacuoles and leads to heart failure (168, 172). Together, these findings show the different roles of autophagy in cardiac pathogenesis. Apart from its roles in cancer and cardiac diseases, autophagy has been implicated in TKIs-induced cardiotoxicity (146).

1.5.2.5. Autophagy in Small Molecule TKIs-Induced Cardiotoxicity

Many TKIs modulate autophagy in several types of tumor and non-tumor cells (146). For example, it was shown that imatinib induces cellular autophagy in mammalian cells (173). In isolated neonatal cardiomyocytes, it was found that imatinib induces cardiotoxicity by accumulating in lysosomes and disrupting autophagy. Authors found that imatinib increased LC3-II expression and increased p62 abundance, secondary to impairment of autophagy (174). In addition, autophagy was shown to play a role in sunitinib-induced cardiomyoblast loss. Exposure of H9c2, cardiomyoblast, cells to sunitinib increased LC3-II protein expression. Although autophagic flux was not assessed, the study showed that Beclin1 knockdown decreased H9c2 cell death associated with sunitinib treatment (101). A recent study found that sunitinib induced autophagic flux in H9c2 cardiomyoblast. Authors were able to attenuate sunitinib-induced cardiotoxicity by pretreatment with geldanamycin, a heat shock-protein 90 (Hsp90) inhibitor, which inhibited autophagy induction (175). Overall, these findings show that autophagy may play a role in TKIs-induced cardiotoxicity. However, Further studies are necessary to confirm the exact role of autophagy in ponatinib-mediate cardiotoxicity.

1.6. Thesis Rationale, Hypothesis and Objectives

1.6.1. Rationale

In recent years, the anticancer modalities have shifted towards a targeted approach which has remarkably prolonged the survival rates of cancer patients. Among the newly targeted anticancer therapies are TKIs. Although cancer prognosis has dramatically improved with TKIs, their use has been associated with undesirable cardiovascular toxicity. Cardiotoxicity is a well-known complication arisen during and/or after treatment with TKIs. Despite the high incidence of cardiotoxicity and the efforts to tackle it, the etiology remains unclear. Therefore, it is necessary to understand the molecular mechanisms of cardiotoxicity induced by TKIs, in order to inhibit or reverse their cardiotoxic effects without reducing TKIs efficacy.

Sunitinib and ponatinib are potent 2nd and 3rd generation TKIs used for the treatment of RCC and CML, respectively. Multiple signaling molecules have been implicated in sunitinib and ponatinib-induced cardiotoxicity. One of those mechanisms involves modulation of RSK. It was postulated that sunitinib induces cardiotoxic effects (such as, cardiomyocyte loss and hypertrophy) through inhibiting RSK activity. In human endothelial cells, ponatinib increased the phosphorylation of p90RSK expression, which probably mediates atherosclerotic effects. However, whether ponatinib induces or inhibits RSK in the cardiac setting is still unknown.

Besides RSK modulation, induction of autophagy plays a role in TKIs-induced cardiotoxicity. Autophagy was shown to mediate cardiomyocyte cell death following sunitinib treatment, which was rescued by autophagy inhibition. Whether the same effect is observed following ponatinib treatment in remains unclear. Hence, this study investigates RSK and autophagy as potential molecular mechanisms governing the cardiotoxicity induced by sunitinib and ponatinib.

1.6.2. Hypothesis

We hypothesize that the ribosomal S6 kinase (RSK) signaling pathway and/or autophagy activation mediate ponatinib and sunitinib-induced cardiotoxicity by inducing cardiomyocyte loss and cardiomyocyte hypertrophy. We examined the validity of this hypothesis by measuring the effect of RSK and autophagy inhibition on cardiomyocyte loss and cardiomyocyte hypertrophy (Figure 1.8).

1.6.3. Objectives

I. To evaluate cardiotoxic effects, manifested by H9c2 cardiomyoblast loss and cardiomyoblast hypertrophy, following ponatinib and sunitinib treatment.

II. To delineate the role of RSK and autophagy as potential molecular mechanisms mediating ponatinib and sunitinib-induced cardiotoxicity:

    a. Validate the role of RSK and autophagy inhibition in sunitinib-induced H9c2 cardiomyoblast loss and cardiomyoblast hypertrophy.

    b. Explore the role of RSK and autophagy inhibition in ponatinib-induced H9c2 cardiomyoblast loss and cardiomyoblast hypertrophy.

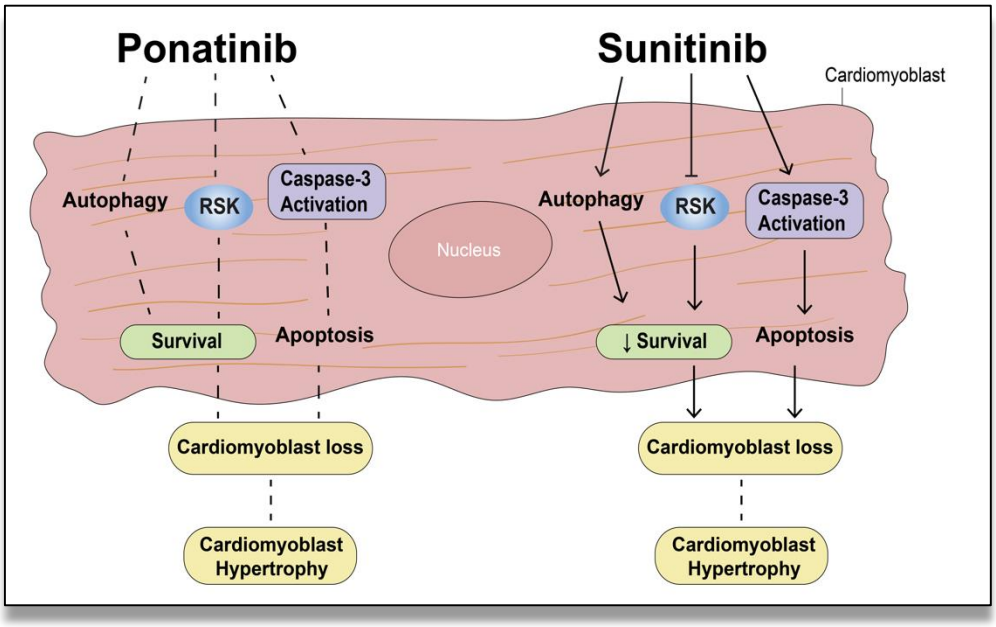

Figure 1.8. Hypothetical model of sunitinib and ponatinib-induced cardiotoxicity.

CHAPTER 2: MATERIALS AND METHODS

2.1. Materials

All routine chemicals and consumables were purchased from Fisher Scientific (Ottawa, ON), Gibco Life Technologies (Grand Island, NY), Sigma (St. Louis, MO), or BD Biosciences (San Jose, CA). Tyrosine kinase inhibitors, sunitinib, free base (S-8877), dasatinib, free base (D-3307), imatinib, free base (I-5577), and ponatinib, free base (P-7022), were purchased from LC Laboratories (Woburn, MA). The p90 ribosomal S6 kinas (p90RSK) inhibitor, BI-D1870 (BID), was purchased from the university of Dundee (Dundee, Scotland). The autophagy inhibitor, chloroquine diphosphate salt (CQ) (Sigma, C-6628), was a generous gift from Dr. Shahab Uddin from the Hamad Medical Corporation (Doha, Qatar). Primary antibodies used for immunoblotting including rabbit polyclonal p-p90RSK (9341S), LC3 A/B (CS-4108) and rabbit monoclonal caspase-3 were from Cell Signaling Technology (Danvers, MA). Goat polyclonal RSK-2 (sc-1430) and rabbit polyclonal cleaved caspase-3 was from Santa Cruz Biotechnology (Santa Cruz, CA). Primary rabbit polyclonal α-tubulin (Ab4074) and secondary goat polyclonal anti-rabbit IgG (Ab97051) were from Abcam (Cambridge, MA). Secondary donkey polyclonal anti-goat (705-035-003) was purchased from Jackson ImmunoResearch Laboratories (West Grove, PA) (Table 2.1).

Table 2.1.

List of the antibodies used to determine the protein expression.

Antibody against	**Type**	**Company and Catalog Number**	**Observed Band Size**
Phospho-p90RSK (P-p90RSK) (S380)	Primary Antibody; Rabbit polyclonal to Phosphorylated p90 ribosomal protein S6 kinase (p90RSK)	Cell Signaling Technology (Danvers, MA); 9341S	90 kDa
RSK-2 (C-19)	Primary Antibody; Goat polyclonal to Ribosomal protein S6 kinase alpha-3 (RSK)	Santa Cruz Biotechnology (Santa Cruz, CA); 1430	80 kDa
LC3 A/B	Primary Antibody; Rabbit polyclonal to microtubule associated light chain 3 (LC3 A/B)	Cell Signaling Technology (Danvers, MA); 4108	14 kDa (LC3 A/B II); 16 kDa (LC3 A/B I)
Cleaved Caspase-3 (CC3)	Primary Antibody; Rabbit polyclonal to Caspase-3	Santa Cruz Biotechnology (Santa Cruz, CA); 22171	11, 17, 20 kDa
Caspase-3 (C3)	Primary Antibody; Rabbit monoclonal to Caspase-3	Cell Signaling Technology (Danvers, MA); 14220	17, 19, 35 kDa

Antibody against	Type	Company and Catalog Number	Observed Band Size
α-tubulin	Primary Antibody; Rabbit polyclonal to α-tubulin	Abcam (Cambridge, MA); Ab4074	50 kDa
Goat anti-rabbit	Secondary Antibody; Goat polyclonal antibody to Rabbit IgG (HRP)	Abcam (Cambridge, MA); Ab97051	-
Donkey anti-goat	Secondary Antibody; Donkey polyclonal antibody to Goat IgG (HRP)	Jackson ImmunoResearch Laboratories (West Grove, PA); 705-035-003	-

2.2. Methods

2.2.1. Culturing and Maintaining Embryonic BDIX Rat Myoblast Cell Line (H9c2)

H9c2(2-1), a subclonal of the clonal cell line that is derived from BDIX embryonic rat cardiac tissue (176, 177) and was cultured in Dulbecco's Modified Eagle's Medium Ham's F-12 1:1 (DMEM/F-12) (Lonza; Basal, Switzerland) supplemented with 10% fetal bovine serum (FBS), 1% penicillin/streptomycin and incubated at 37°C in a humidified atmosphere (5% CO_2, 95% O_2) (177). H9c2 is a

well-characterized in vitro model that has been extensively used to study the molecular mechanism of anticancer therapy-induced cardiotoxicity, including TKIs (101, 178-181). Also, it has been utilized in investigating the cardioprotective effects of various compounds against TKIs-induced cardiotoxicity (175, 182). This wide utilization is due to its reproducible differentiation, preserved electrical, biochemical and hormonal signaling pathways (30, 176).

2.2.2. Drug Treatment

Stock solution of 50mM of sunitinib, dasatinib, imatinib, and ponatinib were dissolved separately in Dimethyl Sulfoxide Hybri-Max (DMSO) (Sigma Life Science; D2660). Stock solutions were further diluted in DMSO to 5mM, 10mM and finally to 500µM and 1000µM, respectively. The final concentration of the vehicle (DMSO) in the medium was 0.5%. Based on our inhouse, this concentration was not cytotoxic to H9c2 cardiomyoblasts

To provide an accurate comparison between groups, control group was treated with the same DMSO %v/v as in sunitinib or ponatinib treatment groups. In attempts to reduce the final concentration of DMSO, different dissolving and dilution methods were tried. The trials were done for the highest concentration of sunitinib (1^{st} dilution: 10mM and 2^{nd} dilution: 1000µM) (Table 2.2) and trial 5 was selected.

Ponatinib and sunitinib were used at a concentration of 2.5µM and 5µM to treat H9c2 cardiomyoblasts. Although the reported maximum plasma concentration (C_{max}) of ponatinib, following a daily dose of 45mg/day, is 0.145 µM and 0.12µM following 44mg/day dose of sunitinib (183, 184), the concentrations used in this study were in agreement with previous studies (74, 101, 178, 185, 186). A previous study examined ponatinib-induced cardiotoxicity in hiPSC-CM. The study revealed that 48-hours treatment with 5µM and 10µM ponatinib causes significant cell death. Authors

found that ponatinib caused 50% reduction in cell viability (IC_{50}) at a concentration of 6µM (74). Similarly, a study showed that 12-hours treatment with 2.5µM and 5µM sunitinib caused significant cardiac hypertrophy and increased H9c2 cell size (178).

Two pharmacological inhibitors, BI-D1870 (BID) and Chloroquine diphosphate (CQ) (Sigma, C-6628) were used to investigate the molecular mechanism of cardiotoxicity induced by sunitinib and ponatinib. BID and CQ were dissolved and diluted to make 2mM stock solutions. A final concentration of 10µM BID and 10µM CQ was used in the current research, which is in line with previous literature (105, 175, 187, 188). A previous study assessed the effect of different concentrations of BID on 54 protein kinases and showed that 10µM BID remarkably inhibited RSK1-4 isoforms (188). In another study, CQ, at a concentration of 10µM, was used to evaluate the autophagic flux following sunitinib treatment in H9c2 cardiomyoblasts (175).

Table 2.2.

Tyrosine kinase inhibitor dilution trials

Trial		**Dissolved**	**Precipitated**
1-	1st and 2nd dilutions prepared in 1:1 DMSO:Water	1000µM solution	10mM solution
2-	1st dilution prepared in DMSO and 2nd dilution prepared in 1:1 DMSO:Water	10mM, 1000µM	None
3-	1st and 2nd dilutions prepared in 2:1 DMSO:Water	None	10mM, 1000µM
4-	1st dilution prepared in DMSO and 2nd dilution prepared in 2:1 DMSO:Water	10mM, 1000µM	None
5-	1st and 2nd dilutions prepared in DMSO	10mM, 1000µM	None
6-	1st dilution prepared in DMSO and 2nd dilution prepared in water	10mM solution	1000µM solution

2.2.3. **Treatment Flow** (Experimental flow and methods can be found in figures 2.1 and 2.2)

Upon reaching confluency, cells were plated at an average seeding density of 3×10^5 cells in 35mm culture dishes. After 24 hours, serum free media was added and cells were treated as following:

1. Screening phase: cells were treated with sunitinib (2.5μM), sunitinib (5μM), dasatinib (2.5μM), dasatinib (5μM), imatinib (2.5μM), imatinib (5μM), ponatinib (2.5μM), and ponatinib (5μM) for 24 hours. Dimethyl sulfoxide (DMSO) was used as a control vehicle at a final concentration of 0.5%. DMSO concentration used did not show a significant difference in comparison with non-treated H9c2 cardiomyoblast cell viability (refer to section 3.1.1). In-house screening phase studies showed that sunitinib or ponatinib are the most cardiotoxic agents among the screened TKIs.
2. Determining sunitinib and ponatinib-induced cardiotoxicity at an early time point: cells were treated with sunitinib (2.5μM and 5μM) and ponatinib (2.5μM and 5μM) for 6 hours. Dimethyl sulfoxide (DMSO) was used as a control vehicle at a final concentration of 0.5%.
3. Investigating the role of p90RSK and autophagy in sunitinib and ponatinib-induced cardiotoxicity using pharmacological inhibitors: H9c2 cardiomyoblasts were pretreated for 30 minutes with BI-D1870 (10μM) or chloroquine (10μM), then treated with sunitinib (2.5μM and 5μM) and ponatinib (2.5μM and 5μM) treatment for an additional 6 hours.

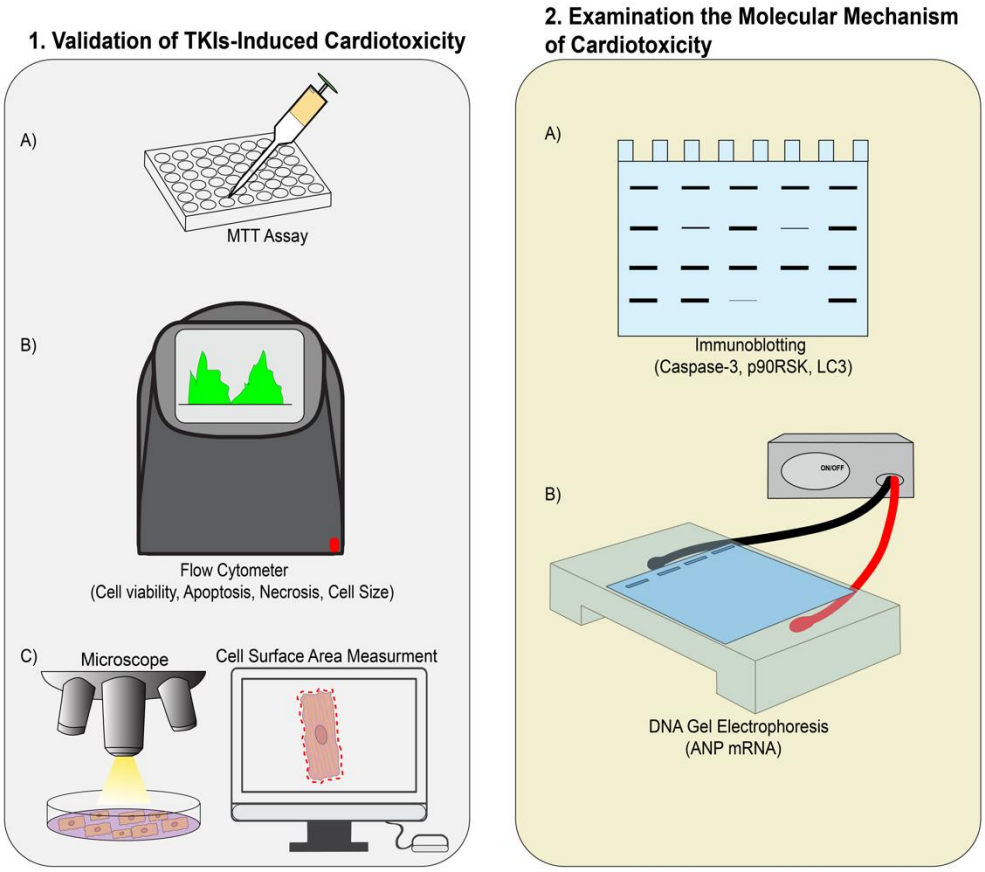

Figure 2.1. Experimental procedures used to determine tyrosine kinase inhibitors (TKIs)-induced cardiotoxicity. Step 1. Involves validating TKIs-induced cardiotoxicity by A) MTT B) flow cytometer analyses of cell viability, apoptosis, necrosis, and cell size, and C) cell surface area measurement. Step2. Involves an examination of molecular mechanisms of cardiotoxicity through A) quantifying protein expression of caspase-3, p90RSK, and LC3 by immunoblotting and B) quantifying gene expression of ANP by DNA gel electrophoresis. MTT, 3- (4,5-dimethylthiazol-2-yl)-2,5-diphenyltetrazolium bromide; p90RSK, p90 Ribosomal S6 kinase; LC3, Microtubule-associated protein 1 light chain 3; ANP, atrial natriuretic peptide; DNA, Deoxyribonucleic acid.

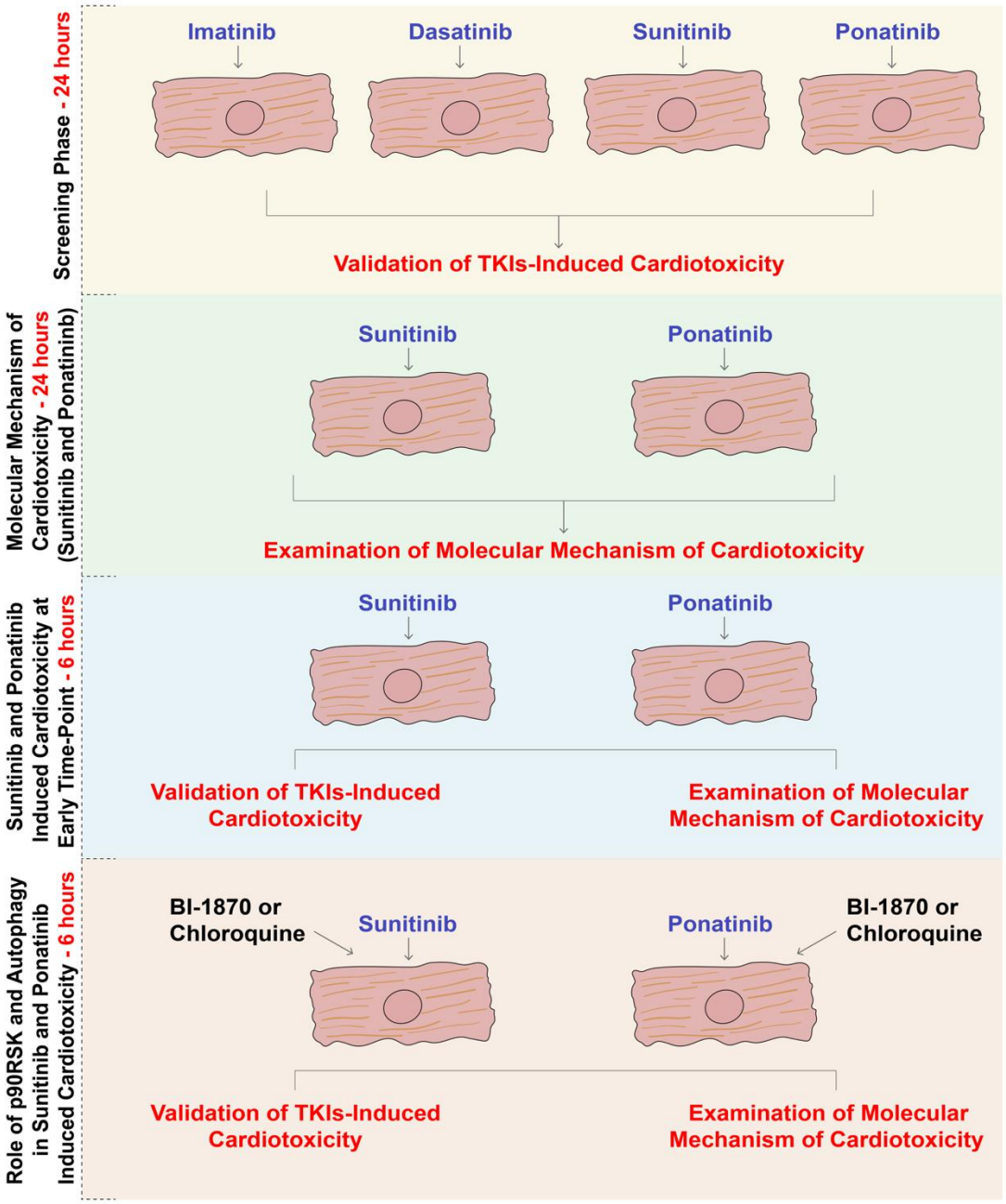

Figure 2.2. A summary of the experimental flow of TKIs treatment and parameters analyzed.

2.2.4. Cell Viability Assay (MTT Assay)

To study the cardiotoxicity of TKIs used to treat CML, we used a 1st generation TKI: imatinib, 2nd generation TKIs: dasatinib, sunitinib and a 3rd generation TKI: ponatinib on H9c2 rat cardiomyocytes. H9c2 cell viability was determined by 3-[4,5-dimethylthiazol-2-yl]-2,5 diphenyl tetrazolium bromide (MTT) assay (Sigma, cc1001830838). MTT assay is a widely used cytotoxic assay. It depends on mitochondrial dehydrogenase enzymes in viable cells to reduce MTT to violet colored formazan precipitate with absorbance at 570nm (189). Briefly, H9c2 cardiomyoblasts were seeded on 48-well plates at a seeding density of 4×10^4 cells/well. Following 24 hours of various treatments, the media was aspirated and 200µL of serum free media containing 0.5mg/mL of MTT solution was added to the plate and incubated for 3 hours at 37˚C. Following incubation, the media was carefully aspirated and 200µL of DMSO was added to solubilize the formazan crystals. The absorbance was measured at 570nm using a microplate reader (Epoch 2, BioTek).

2.2.5. Cardiomyocyte Hypertrophy Marker

In order to determine the role of TKIs on cardiomyoblast hypertrophic properties we used three distinctive makers: cell surface area, atrial natriuretic peptide (ANP) mRNA expression and cell size using flow cytometer. Hypertrophic stimuli increase H9c2 cardiomyoblast surface area, ANP and brain natriuretic peptide (BNP) mRNA expression and induce relative changes in cell size (178, 190, 191).

2.2.5.1. Cardiomyocyte Hypertrophy Marker: Cell Surface Area

In order to measure the cell surface area, an average of 10×10^4 per 35mm culture dish of H9c2 cardiomyoblasts were seeded for 24 hours. Following 24 hours, and upon reaching confluency, serum free media was added and cells were treated as

indicated in section 2.2.3. Next, the cells were washed with 1 x phosphate buffer saline, fixed with 4% formaldehyde and stained with 0.5% crystal violet. The cells were capture by AxioCam ERc5s (Carl Zeiss, Germany) using Axiovert 40 CFL inverted microscope. The surface area of an average of 15-30 of randomly selected cells were measured using the AxioVision Imaging software (Carl Zeiss Micro-imaging, USA).

2.2.5.2. Cardiac Hypertrophy Marker: ANP mRNA expression

2.2.5.2.1. Reverse Transcription Polymerase Chain Reaction (RT-PCR)

To measure ANP mRNA expression as another indicator of cardiac hypertrophy, an average of 3 x 10^5 of H9c2 cardiomyoblasts were plated in 35mm culture dishes for 24 hours. Upon confluency, serum free media was added and cells were treated as indicated in 2.2.3. RNA was isolated using Trizol RNA isolation procedure. 0.6 – 1μg of RNA was reverse transcribed, according to manufacturer's instructions, into complementary DNA (cDNA) using a High capacity cDNA Reverse Transcription Kit (Applied Biosystems) (Table 2.3). Then, PCR reaction was performed, using 200ng of the resulted cDNA, using the following conditions: 3 minutes initial denaturation step at 94°C, 45 seconds denaturation step at 94°C, 30 seconds annealing step at 60°C and 1 minute extending step at 72°C. Then the reaction was terminated at 72°C for 10 minutes for final extension following completion of 35 cycles of denaturing, annealing and extending (Table 2.4). ANP cDNA was amplified using the primer sequences (Table 2.5). All data was normalized to β-actin. The final product of PCR was assessed by 2% electrophoresis agarose gels stained with ethidium bromide. The mRNA bands were imaged using FluorChem M FM0564 system (Protein Simple, USA).

Table 2.3

Conditions of reverse transcription used to convert RNA into cDNA. RNA, ribonucleic acid and cDNA, complementary deoxyribonucleic acid.

	Step 1	**Step 2**	**Step 3**	**Step 4**
Temperature (˚C)	25˚C	37˚C	85˚C	4˚C
Duration (minutes)	10	120	5	indefinite

Table 2.4.

Conditions of semi-quantitative Reverse Transcription-PCR (qPCR).

	Temperature (˚C)	**Duration**	**cycles**
Initial Denaturation	94˚C	3 minutes	-
Denaturation	94˚C	45 seconds	35 cycles
Annealing	60˚C	30 seconds	
Extension	72˚C	1 minute	
Final Extension	72˚C	10 minutes	-
Hold	4˚C	indefinite	-

Table 2.5.

List of primes used for semi-quantitative Reverse Transcription-PCR (qPCR).

Gene	Primer Sequence
Rat ANP	
Forward	5'-CTG CTA GAC CAC CTG GAG GA-3'
Reverse	5'-AAG CTG TTG CAG CCT AGT CC-3'
Rat β-Actin	
Forward	5'-CGT CAT CCA TGG CGA ACT GG-3'
Reverse	5'-ACG CAG CTC AGT AAC AGT CC-3'

2.2.6. Flow Cytometer Studies

Mitochondria has a major role in apoptotic cell death by releasing pro-apoptotic proteins from intermembrane space into the cytoplasm (192). To determine the type of cell death seen in H9c2 treated with TKIs, H9c2 cardiomyoblasts were seeded at an average density of 3 x 10^5 on 35mm cell culture dishes in DMEM-F-12 medium supplemented with 10% FBS and 1% penicillin/streptomycin and incubated for 24 hours. Upon confluency, cells were treated with CQ, BID, ponatinib and sunitinib with or without CQ and BID at previously mentioned concentrations and time points. Treatment vehicle was used as a control. Following treatment, cells were harvested, washed with PBS, centrifuged and equalized. Cells were then stained with annexin-v and propidium iodide (PI) dual staining (BD Biosciences) in 1x annexin binding buffer (ABB) for 30 minutes. Flow cytometry (BD LSRFortessa™ cell analyzer, BD Biosciences) was used to measure the cell viability ($PI^{negative}$, Annexin-$FITC^{negative}$), early ($PI^{negative}$, Annexin-$FITC^{positive}$) and late ($PI^{positive}$, Annexin-

FITC^{positive}) phase apoptosis and necrosis (PI^{positive}, Annexin-FITC^{negative}) as previously described (193, 194). Cell size was measured with forward light scatter using flow cytometer. Percentage of cells in early and late apoptosis were also expressed as total apoptosis.

2.2.7. Immunoblotting

Western blotting was used to measure P-p90RSK, RSK-2, LC3 A/B, cleaved caspase-3, and caspase-3 protein expression levels following treatment of H9c2 cardiomyoblasts with the indicated treatment groups and time points. Briefly, at the treatment endpoint, H9c2 cardiomyoblasts were lysed using radio-immunoprecipitation protein assay (RIPA) and centrifuged at 12,000-14,000 rpm at 4˚C for 15 minutes, as described in (195). Then, the supernatant was collected. The protein concentration was calculated using the DC protein assay kit (Biorad). Equal amount of protein was resolved on 9% or 15% SDS-PAGE (sodium dodecyl sulfate polyacrylamide gel electrophoresis). Then, nitrocellulose membrane incubated with primary antibodies (P-p90RSK, RSK-2, LC3A/B, Cleaved Caspase-3, and Caspase-3) at 4°C overnight. All primary antibodies were used at a dilution of 1:1000 and secondary antibodies at a dilution of 1:4000. Anti-α-tubulin was used as a loading control. Visualization was performed using chemiluminescence reaction and imaged using FluorChem M FM0564 system (Protein Simple, California, USA). ImageJ software (National Institutes of Health, USA) was used to quantify the resulted bands.

2.2.8. Evaluation of Autophagic Flux

As discussed previously in section 1.5.2.1, LC3-II is known to present in autophagosomal membrane, and thus, is a commonly used marker for autophagosomes. However, increased level of autophagosomes does not solely correlate with increased autophagic activity; thus, it is important to monitor

autophagic flux (147, 148). To evaluate whether treatment with ponatinib and sunitinib alter the autophagic activity in H9c2 cardiomyoblast, the protein expression of LC3-II was measured in the presence or absence of CQ (147, 175). CQ, an anti-malaria agent, increases the pH in the lysosomes, and thus, inhibits the last stage of autophagy, autophagosome-lysosome fusion, and inhibits the degradation of LC3-II (147, 196). Here, H9c2 cardiomyoblasts were pretreated with 10μM CQ for 30 minutes followed by additional 6-hours treatment with ponatinib and sunitinib. LC3-II protein expression was assessed by immunoblotting.

2.3. Statistical Analysis

All values are compared to vehicle-treated group (control) and expressed as mean ± SEM. The statistical significance between individual groups was assessed using unpaired student's t-test where P-value of less than or equal to 0.05 was considered as statistically significant. One-way analysis of variance (ANOVA) followed by Bonferroni correction were used to assess the multiple group comparisons. The Bonferroni correction is performed by dividing the α error level by the total number of comparisons. Herein, α error level = 0.05 (197).

CHAPTER 3: RESULTS

3.1. Screening for Cardiotoxicity Induced by Various Tyrosine Kinase Inhibitors

3.1.1. Cell Viability: MTT Assay

In order to determine the cardiotoxicity induced by TKIs, we measured cell viability of H9c2 cardiomyoblasts using MTT (3-(4,5-dimethylthiazol-2-yl)-2,5-diphenyltetrazolium bromide) assay, following 24-hours treatment with different concentrations of sunitinib, dasatinib, imatinib, ponatinib and DMSO (vehicle control). Treatment with 2.5µM or 5µM sunitinib caused a significant dose-dependent decrease in cell viability, by 4% and 22%, respectively as compared to control (95.68 ± 0.46 % and 78.12 ± 1.27 % of control; $p < 0.01$). Treatment with 5µM dasatinib resulted in a 23% reduction in cell viability (77.22 ± 2.37 % of control; $p < 0.01$). Treatment with ponatinib resulted in a severe reduction in cell viability as compared to control. Treatment with 2.5µM ponatinib reduced H9c2 cell viability by 22% (78.25 ± 3.8% of control; $p < 0.05$), while at 5µM, ponatinib resulted in 40% reduction in H9c2 cell viability (61.46 ± 1.49 % of control; $p < 0.01$). In contrast, imatinib was the safest to H9c2 cardiomyoblasts among screened TKIs. Treatment with 2.5µM imatinib resulted in a 9% increase in cell viability (109.19 ± 2.35% of control; $p < 0.05$) (Figure 3.1). In addition, we determined the effect of the vehicle control (DMSO) on H9c2 cardiomyoblast cell viability. In comparison with non-treated H9c2 cardiomyoblasts, 0.5% of DMSO did not show a significant change in cell viability (Figure 3.2). Taken together, cell viability analyses using MTT assay show that treatment with ponatinib is associated with higher cell death as compared to control and other TKIs.

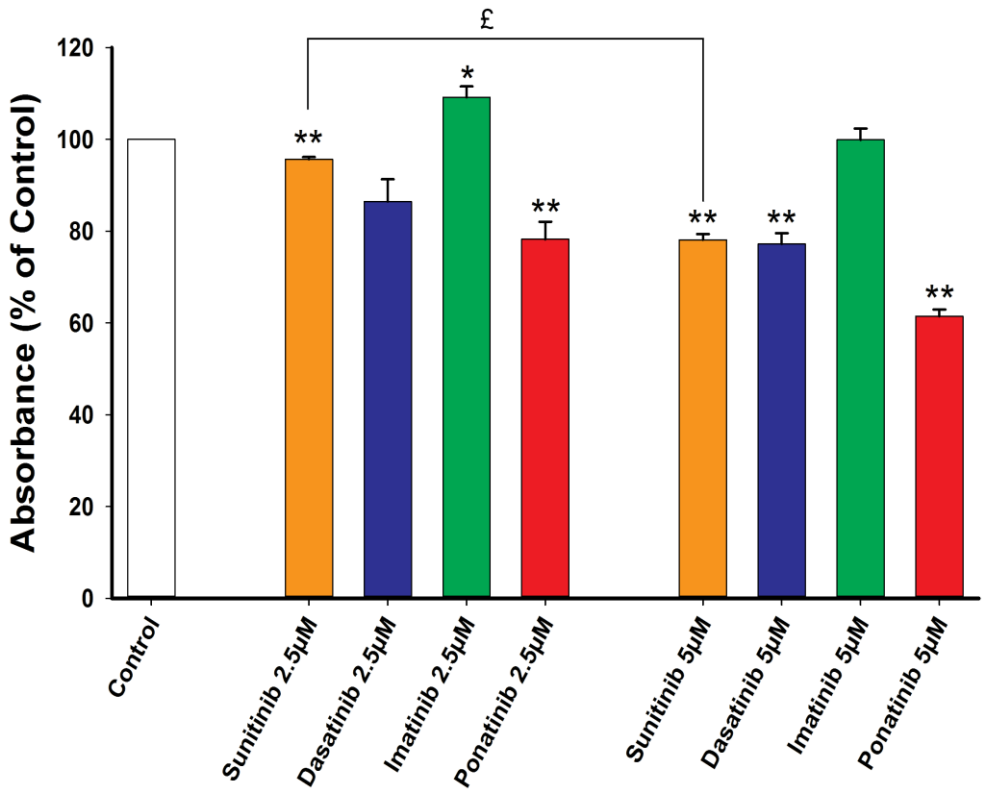

Figure 3.1. The effect of various tyrosine kinase inhibitors on the cell viability of H9c2 cardiomyoblasts. The cell viability of H9c2 cardiomyoblasts, treated for 24-hours with sunitinib, dasatinib, imatinib or ponatinib, at concentrations of 2.5µM or 5µM, was measured using MTT assay. Values are expressed as % of control (mean ± SEM, n= 3-4). *P-value < 0.05 vs control, **P-value < 0.01 vs. control and £P-value < 0.001 vs sunitinib 2.5µM.

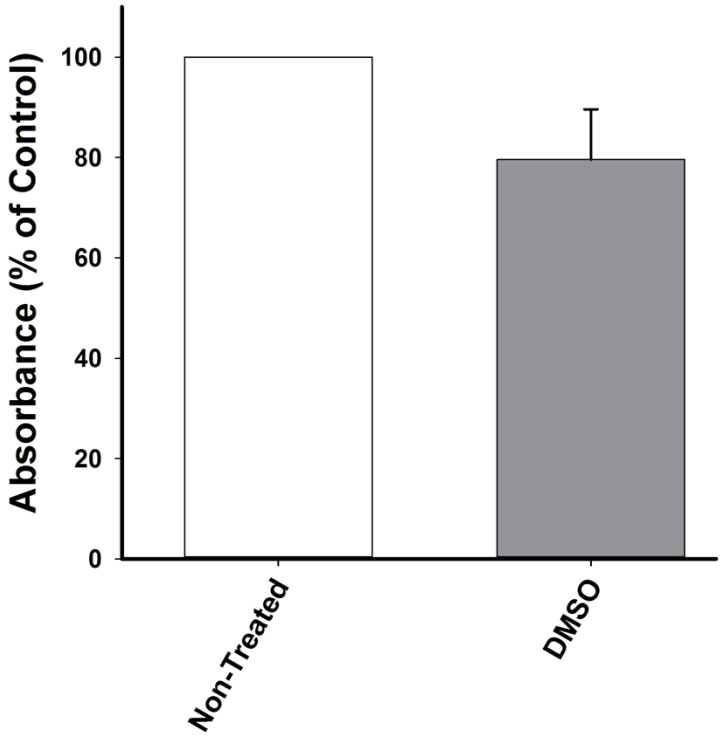

Figure 3.2. The effect of dimethyl sulfoxide (DMSO) on H9c2 cell viability. The cell viability of non-treated and treated H9c2 cardiomyoblasts with 0.5% DMSO for 24 hours, was measured using MTT assay. Values are expressed as % of control (mean ± SEM, n= 3).

3.1.2. Cell Viability: Flow Cytometer

To further confirm the effect of TKIs on H9c2 cardiomyoblasts, we analyzed the cell viability following 24-hours treatment with various TKIs using flow cytometer. Our results revealed that sunitinib treatment (2.5μM or 5μM) led to severe cell death and resulted in more than 90% reduction in cell viability. Similarly, cellular exposure to ponatinib (2.5μM) caused a significant reduction in cell viability by 35% (64.80 ± 7.14 % of control; $p < 0.05$). Also, treatment with 5μM of ponatinib led to an 80% reduction in cell viability (21.83 ± 12.74 % of control; $p < 0.01$). Treatment with dasatinib or imatinib (2.5μM or 5μM) for 24 hours did not induce cell death as compared to control (Figure 3.3). Taken together, cell viability analyses using flow cytometer show that treatment with sunitinib or ponatinib causes significant cell death as compared to control and other TKIs. While treatment with dasatinib or imatinib at comparable concentrations is not associated with H9c2 cell death.

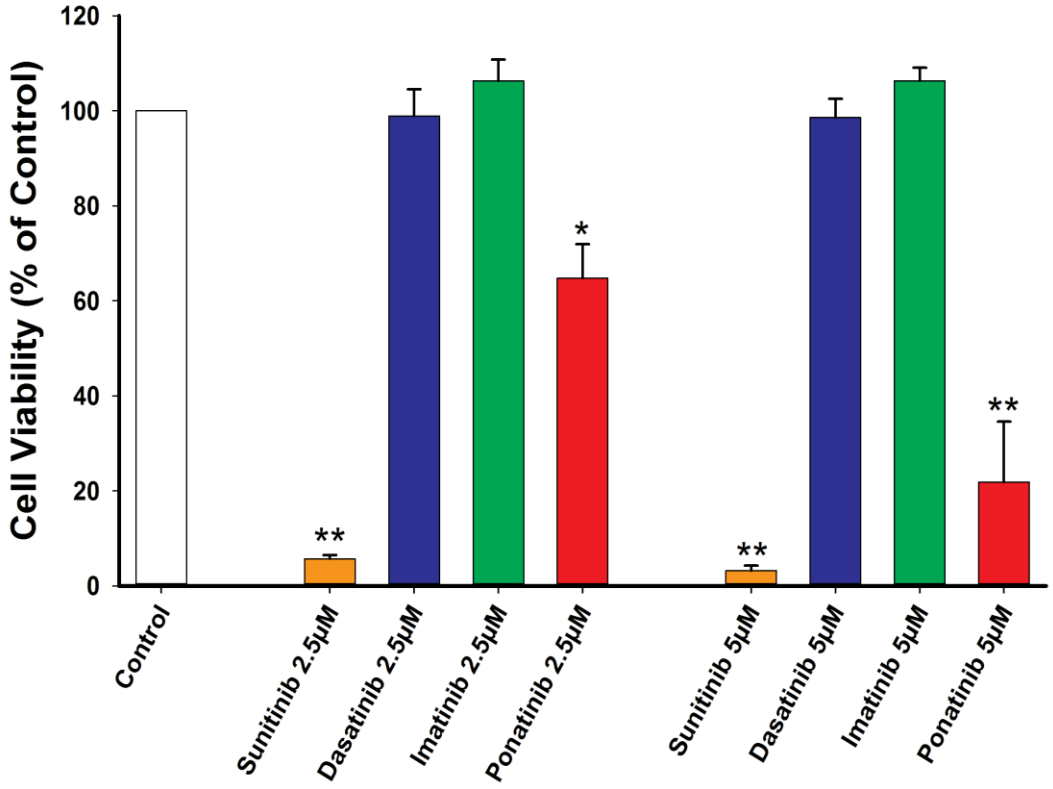

Figure 3.3. The effect of sunitinib or ponatinib treatment on H9c2 cardiomyoblast cell viability. The cell viability of H9c2 cardiomyoblasts, treated for 24-hours with sunitinib, dasatinib, imatinib or ponatinib at concentrations of 2.5µM or 5µM, was measured by flow cytometer using propidium iodide (PI) staining solution. Values are expressed as % of control (mean ± SEM, n= 3-4). *P-value < 0.05 vs control and **P-value < 0.01 vs control.

3.1.3. Cell Death: Necrosis and Apoptosis

We next determined the mechanism of cell death induced. We examined whether the treatment with 2.5µM or 5µM of sunitinib, dasatinib, imatinib or ponatinib for 24-hours, induce necrotic and/or apoptotic cell death. Although no significant change was observed for necrosis in all treatment groups (data not shown), apoptosis was the major mediator of sunitinib or ponatinib-induced cell death. Treatment with 2.5µM or 5µM sunitinib induced 300% increase in total apoptosis (392.28 ± 42.39% and 385.95 ± 49.56% of control; $p < 0.05$). Similarly, treatment with ponatinib induced apoptotic cell death by 72% and 200%, respectively, as compared to control (172.48 ± 17.47% and 299.59 ± 24.96% of control; $p < 0.05$ and $p < 0.01$). Treatment with dasatinib or imatinib (2.5µM or 5µM) did not induce apoptotic cell death (Figure 3.4). Overall, these results show that sunitinib or ponatinib induced-cell death in H9c2 cardiomyoblasts is mediated through apoptosis.

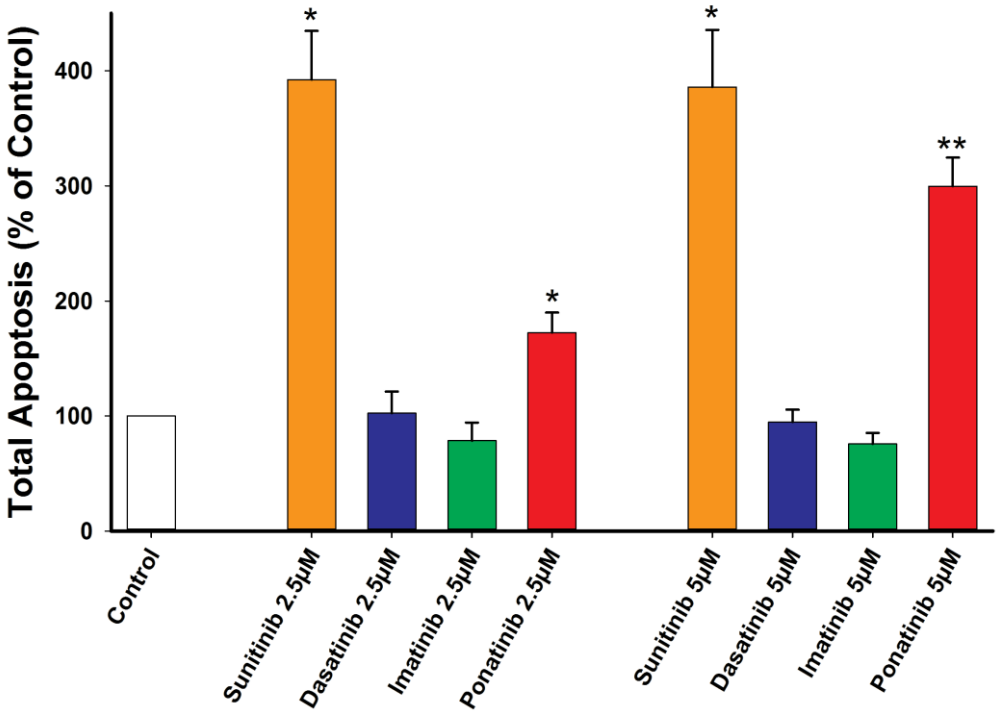

Figure 3.4. Sunitinib or ponatinib induce H9c2 cardiomyoblasts apoptotic cell death. Total apoptosis was analyzed by measuring annexin-v FITC expression and PI staining following 24-hours treatment with sunitinib, dasatinib, imatinib or ponatinib, at concentrations of 2.5µM or 5µM. Values are expressed as % of control (mean ± SEM, n= 3-4). *P-value < 0.05 vs control and **P-value < 0.01 vs control.

3.1.4. Cell Morphology and Cardiac Hypertrophy Markers: Cell Surface Area

Next, we examined the effect of various TKIs on cell morphology and cardiomyocyte hypertrophic markers, including cell surface area and cell size. Our results showed that exposure of H9c2 cardiomyoblasts to sunitinib (5μM) for 24 hours led to a significant increase in H9c2 cardiomyoblast cell surface area as compared to control (115.87 ± 5.26% vs. 100% control; $P < 0.05$). Whereas, exposure to ponatinib (2.5μM) induced significant H9c2 cardiomyoblast shrinkage (69.23 ± 9.86% vs. control; $P < 0.05$) (Figure 3.5 and Figure 3.6).

Treatment with 2.5μM or 5μM ponatinib led to reduced cellular density and increased cellular detachment as compared to control. In addition, ponatinib induced cellular shrinkage (Figure 3.6).

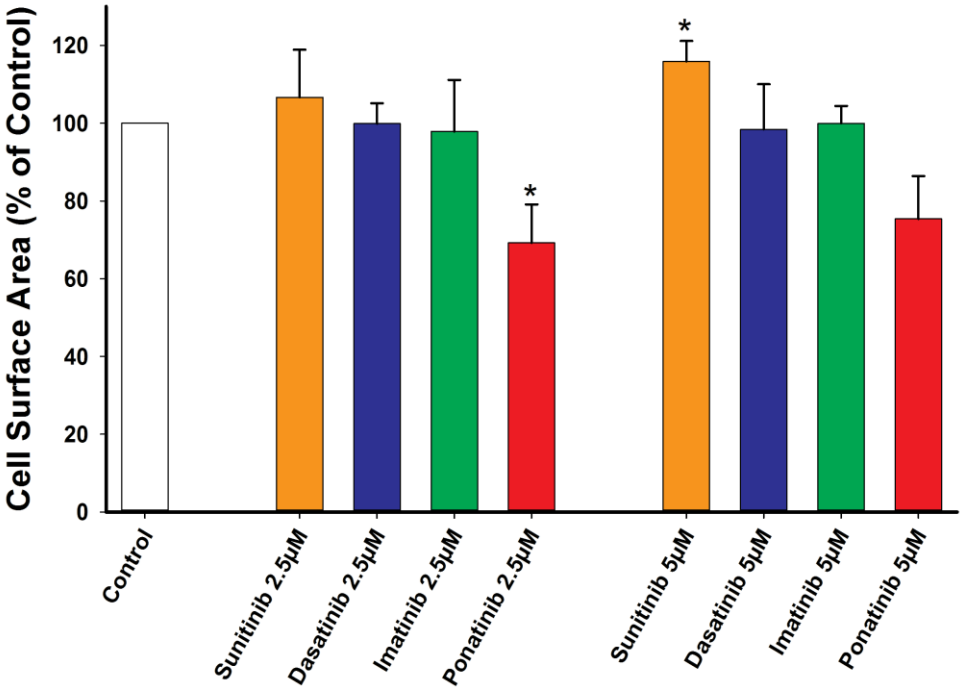

Figure 3.5. Sunitinib-induced H9c2 cardiomyoblast hypertrophy and ponatinib-induced H9c2 cardiomyoblast shrinkage. Measurement of cell surface area of an average of 15-30 H9c2 cardiomyoblasts treated with various TKIs following 24 hours treatment, using AxioVison software. Values are expressed as % of control (mean ± %SEM, n= 5-6). *P-value < 0.05 vs control.

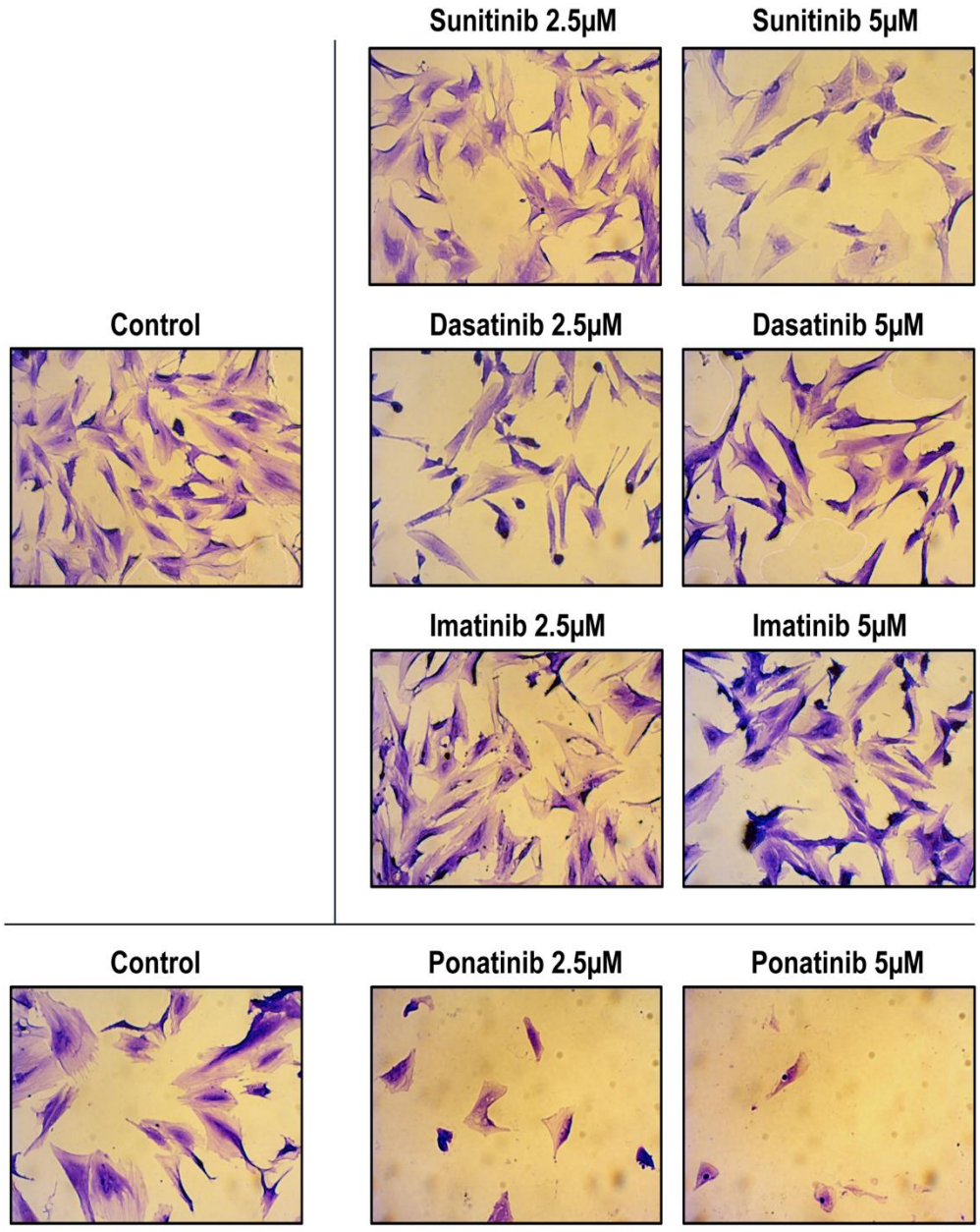

Figure 3.6. Sunitinib-induced H9c2 cardiomyoblast hypertrophy and ponatinib-induced cellular detachment and cardiomyoblast loss. Representative images of H9c2 cardiomyoblasts stained with crystal violet following 24-hours treatment with various TKIs, at concentrations ranging from 2.5µM – 5µM (n=5-6). Images were captured with Carl Zeiss AxioVision imaging system at a magnification of 20x.

3.1.5. Cell Morphology and Cardiomyocyte Hypertrophic Markers: Cell Size

To further confirm the effect of TKIs on H9c2 cardiomyocyte cell morphology and cell surface area, we assessed the cell size using flow cytometer. H9c2 cardiomyoblasts were treated for 24 hours with 2.5μM or 5μM of sunitinib, dasatinib, imatinib and ponatinib. In agreement with our previous data, treatment with 2.5μM or 5μM ponatinib led to a significant cellular shrinkage (37.59 ± 14.35% vs. control; $P < 0.05$ and 1.26 ± 0.22% vs. control; $P < 0.01$). Moreover, in contrast to our previous data, sunitinib treatment (5μM) led to significant cell shrinkage (41.55 ± 6.27% vs. control; $P < 0.01$). No significant cell size change was observed following dasatinib or imatinib treatment (Figure 3.7). **Overall, based on our data, we found that sunitinib or ponatinib are the most cardiotoxic among the screened TKIs.** As a result, we selected sunitinib or ponatinib for further investigations to understand their molecule mechanisms of cardiotoxicity.

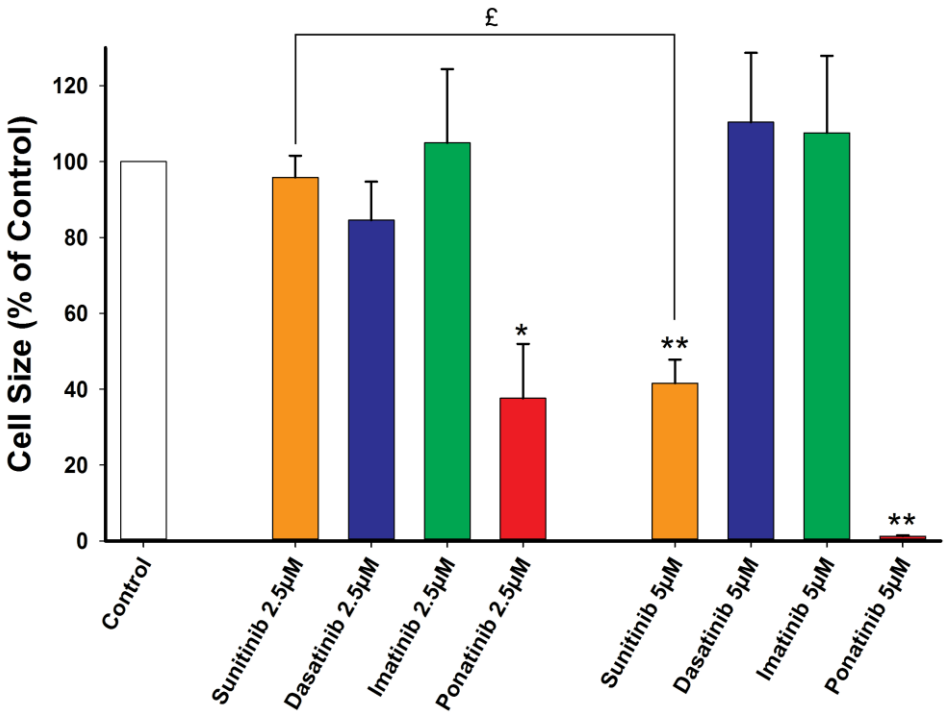

Figure 3.7. Sunitinib and ponatinib treatment causes H9c2 cardiomyoblast shrinkage. The cell size of H9c2 cardiomyoblasts, following 24-hours treatment with various TKIs, was measured by forward scatter using flow cytometer analyses. Values are expressed as % of control (mean ± %SEM, n= 5-6). *P-value < 0.05 vs control, **P-value < 0.01 vs control, and £P-value < 0.001 vs sunitinib 2.5µM.

3.2. Studies on Sunitinib and Ponatinib

3.2.1. Cardiomyocyte Hypertrophic Markers – Atrial Natriuretic Peptide (ANP) mRNA Expression

To Further investigate the hypertrophic effects of sunitinib and ponatinib in H9c2 cardiomyoblasts, we measured ANP mRNA expression. H9c2 cardiomyoblasts with treated with sunitinib or ponatinib (2.5µM or 5µM) for 24 hours. Our preliminary result suggested that ANP mRNA following 24-hours exposure to sunitinib (2.5µM) slightly increases when compared to control and other treatment groups (Figure 3.8).

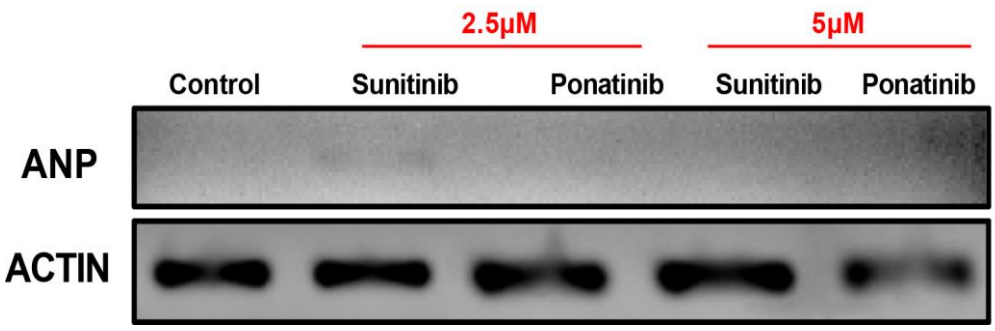

Figure 3.8. Sunitinib treatment for 24 hours induces atrial natriuretic peptide (ANP) mRNA expression in H9c2 cardiomyoblast. Representative agarose DNA gel of ANP mRNA expression in H9c2 cardiomyoblasts treated with sunitinib or ponatinib (2.5µM or 5µM) for 24 hours. RNA was isolated from H9c2 cardiomyoblasts, reverse transcribed and amplified against ANP and β-actin primers (n=1).

3.2.2. Apoptosis – Caspase-3 Activation

Next, we determined whether sunitinib or ponatinib-induced apoptosis is through a caspase-dependent pathway. Treatment with 2.5μM sunitinib for 24 hours showed no change in caspase-3 protein expression (84.06 ± 7.60% vs. control; not significant). While treatment with 5μM sunitinib or ponatinib (2.5μM or 5μM) for 24 hours showed 26%, 64% and 80% reduction in caspase-3 protein expression, respectively (74.04 ± 7.31% vs. control; $P < 0.05$, 35.96 ± 11.9% vs. control; $P < 0.01$, and 21.71 ± 4.3% vs. control; $P < 0.01$) (Figure 3.9).

Similarly, upon treatment with 5μM sunitinib or 2.5μM ponatinib, the cleaved caspase-3 protein expression was regressed by 46% and 67%, respectively (54.24 ± 9.96% vs. control; $P < 0.05$, and 33.93 ± 9.29% vs. control; $P < 0.01$). While treatment with 2.5μM sunitinib or 5μM ponatinib showed no significant change in cleaved caspase-3 protein expression (70.76 ± 11.27% vs. control; not significant, and 29.57 ± 20.17% vs. control; not significant). Together, these results show that sunitinib or ponatinib-induced apoptosis in H9c2 cardiomyoblasts is not mediated through a caspase-3 dependent pathway.

A)

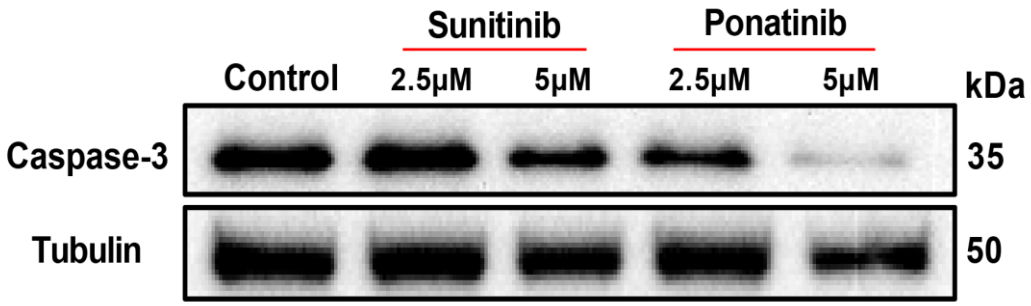

B)

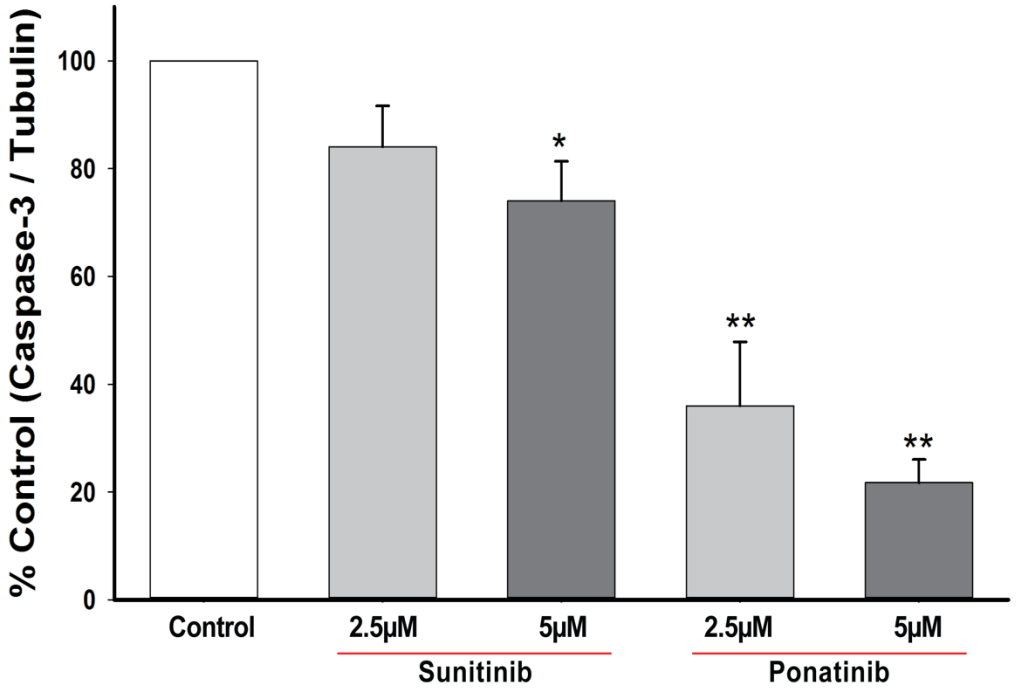

Figure 3.9. Sunitinib or ponatinib-induced apoptosis is not mediated through a caspase-3 pathway in H9c2 cardiomyoblasts. H9c2 cardiomyoblasts were treated with sunitinib or ponatinib (2.5µM or 5µM) for 24 hours and caspase-3 protein expression was measured by immunoblotting. A) Representative caspase-3 western blot and B) Quantification of caspase-3 protein expression after normalization to α-tubulin. Values are expressed as % of control (mean ± %SEM, n=3-4). *P-value < 0.05 vs control and **P-value < 0.01 vs control.

3.3. Molecular Mechanisms of Cardiotoxicity Induced by Sunitinib and Ponatinib

3.3.1. Role of p90 Ribosomal S6 Kinase (p90RSK) Activation in Sunitinib and Ponatinib-Induced Cardiotoxicity

We next examined the potential molecular mechanism mediating sunitinib or ponatinib cardiotoxicity. H9c2 cardiomyoblasts were treated with sunitinib or ponatinib (2.5μM or 5μM) for 24 hours and P-p90RSK and RSK-2 protein expression were measured by immunoblotting. Treatment with sunitinib (2.5μM or 5μM) showed no change in P-p90RSK protein expression (118.5 ± 22.29% vs. 100% control; not significant and 168 ± 22.84% vs. 100% control; not significant). In contrast, treatment with 2.5μM ponatinib for 24 hours significantly increased p90RSK phosphorylation (606.18 ± 99.71% vs. 100% control; $P < 0.01$) (Figure 3.10).

In terms of total RSK2 protein expression, treatment with sunitinib (2.5μM) led to 14% increase in the expression (114.25 ± 4.59% vs. 100% control; $P < 0.05$). In contrast, treatment with 2.5μM of ponatinib regressed RSK2 expression by 50% (47.3 ± 8.57% vs. 100% control; $P < 0.01$).

Cellular exposure to 2.5μM sunitinib led to a significant decrease in p90RSK/RSK2 ratio (83.45 ± 2.06% vs. 100% control; $P < 0.05$), whereas, treatment with 2.5μM ponatinib significantly induced p90RSK/RSK2 ratio (2060.14 ± 570.3% vs. 100% control; $P < 0.05$). It is noteworthy that 24-hours treatment with high concentrations of ponatinib resulted in lower tubulin protein expression compared to control, which is indicative of a lower protein lysate concentration. Collectively, our results suggest that ponatinib mediates p90RSK phosphorylation which might be implicated in its cardiotoxicity. **Further studies employing lower concentrations or shorter time points are necessary to maximize the protein lysate concentrations.**

A)

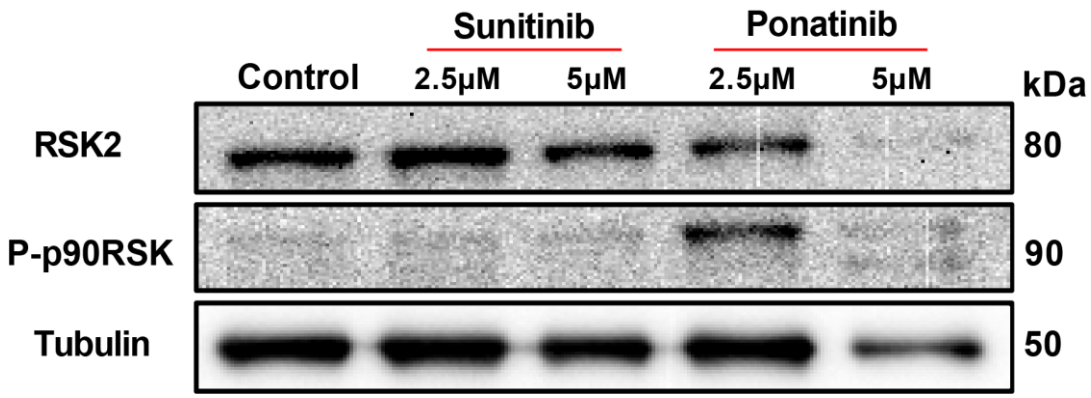

B)

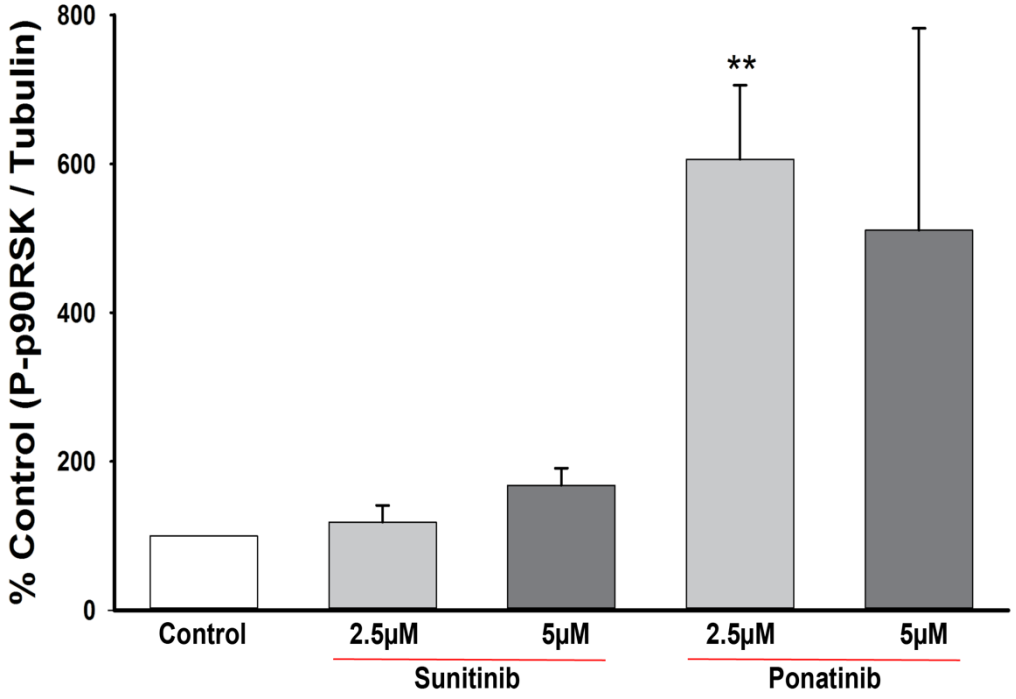

Figure 3.10. Ponatinib induces p90 Ribosomal S6 kinase (p90RSK) phosphorylation in H9c2 cardiomyoblasts. H9c2 cardiomyoblasts were treated with 2.5μM or 5μM of sunitinib or ponatinib for 24 hours. A) Representative phospho-p90RSK (P-p90RSK) and RSK2 western blots and B) Quantification of P-p90RSK protein expression after normalization to α-tubulin. Values are expressed as % of control (mean ± %SEM, n=3-4). **P-value < 0.01 vs control.

3.3.2. Role of Autophagy in Sunitinib and Ponatinib-Induced Cardiotoxicity

We also examined the role of autophagy in sunitinib or ponatinib-mediated cardiotoxicity by measuring the protein expression of LC3-I and LC3-II following 24-hours. Treatment with 2.5μM ponatinib led to a significant increase of LC3-II:LC3-I ratio as compared to control (526.72 ± 101.1% vs. 100% control; $P < 0.05$). Treatment with 5μM ponatinib showed non-significant increase in LC3-II:LC3-I protein expression (2439.43 ± 875.97% vs. 100% control; not significant). Whereas sunitinib treatment (2.5μM or 5μM) showed no significant alteration in autophagy as compared to control (125.8 ± 13.84% vs. 100% control; not significant and 168.87 ± 44.4% vs. 100% control; not significant) (Figure 3.11). Taken together, these results show that ponatinib modulate cardiac autophagy and could be a potential mechanism of ponatinib-mediated cardiotoxicity. Further studies are needed to confirm whether ponatinib induces or regresses autophagic flux.

A)

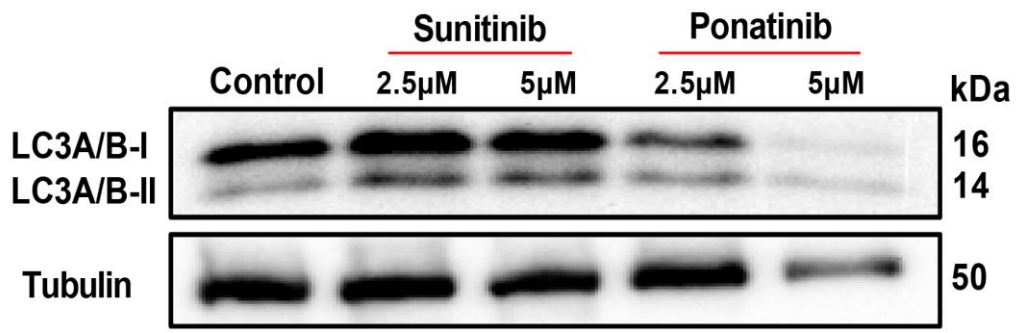

B)

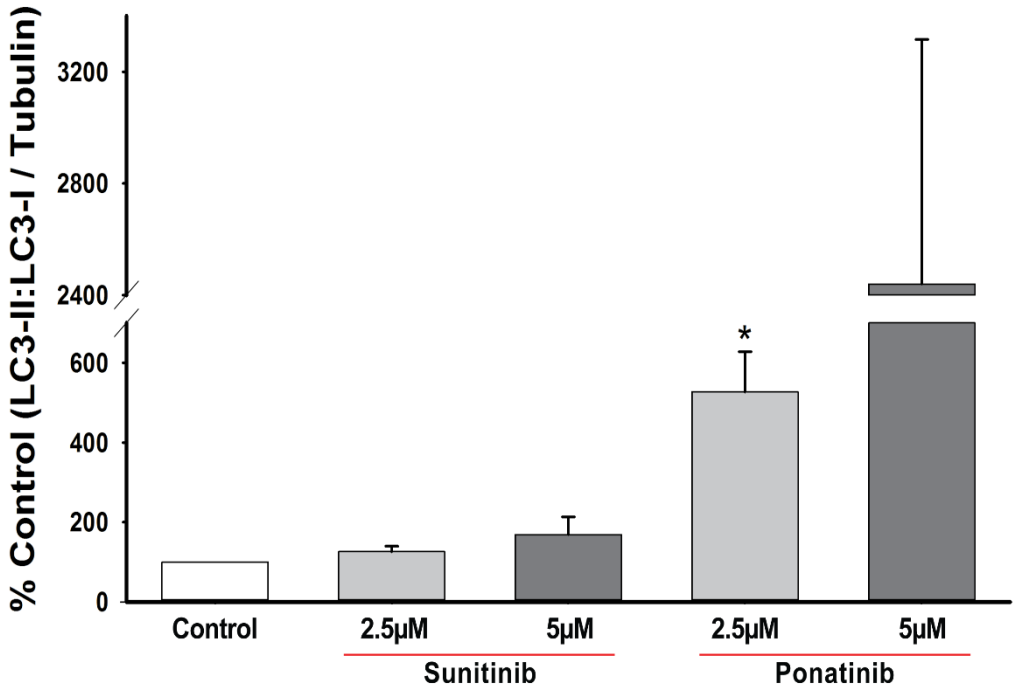

Figure 3.11. Ponatinib treatment activates cellular autophagy in H9c2 cardiomyoblasts. H9c2 cardiomyoblasts were treated with 2.5µM or 5µM of sunitinib or ponatinib for 24 hours. LC3 protein expression was measured by immunoblotting techniques. A) Representative LC3-I and LC3-II western blot and B) Quantification of LC3-II:LC3-I protein expression after normalization to α-tubulin. Values are expressed as % of control (mean ± %SEM, n=3-4). *P-value < 0.05 vs control.

Table 3.1.

Summary of Findings – Sunitinib or ponatinib-Induced Cardiotoxicity: 24 hours. Arrows denote significance compared to control (↑: increase; ↓: decrease; -: no change; N/A: not applicable).

Parameter	**Sunitinib 2.5μM**	**Sunitinib 5μM**	**Ponatinib 2.5μM**	**Ponatinib 5μM**
Cell Viability				
MTT	↓	↓	↓	↓
Flow Cytometer	↓	↓	↓	↓
Mechanism of Cell Death				
Apoptosis	↑	↑	↑	↑
Caspase-3	-	↓	↓	↓
Necrosis	-	-	-	-
Cardiac Hypertrophy				
Cell Area	-	↑	↓	-
Cell Size	-	↓	↓	↓
ANP (n=1)	↑	N/A	N/A	N/A
p90 Ribosomal S6 Kinase Pathway				
P-p90RSK	-	-	↑	-
RSK2	↑	-	↓	-
P-p90RSK:RSK2	↓	-	↑	-
Autophagy Pathway				
LC3-I	-	-	↓	-
LC3-II	-	-	-	-
LC3-II:LC3-I	-	-	↑	-

3.4. Cardiotoxic Studies of Sunitinib and Ponatinib – Reduced Treatment Duration

Due to severe cardiotoxicity induced by sunitinib or ponatinib following 24 hours treatment in H9c2 cardiomyoblasts as manifested by cardiomyoblast loss and low protein lysate concentration, we studied the cardiotoxic parameters following 6-hours treatment.

3.4.1. Cell Viability

To determine the effect of 6-hours treatment with sunitinib or ponatinib, we measured the H9c2 cardiomyoblast cell viability using flow cytometer analyses. Sunitinib treatment led to a significant dose-dependent reduction in H9c2 cell viability by 7% and 13%, respectively (93.21 ± 0.38% of control; $p < 0.01$ and 86.73 ± 0.69% of control; $p < 0.01$). Similarly, ponatinib treatment (2.5μM) induced a 7% reduction in cell viability (92.31 ± 0.56% of control; $p < 0.01$) while treatment with 5μM resulted in a 14% cell viability reduction as comparted to control (86.04 ± 2.02% of control; $p < 0.05$) (Figure 3.12). Together, our results suggest that sunitinib or ponatinib-induced cardiotoxicity starts at an early time-point, which is less detrimental as compared to 24-hours treatment.

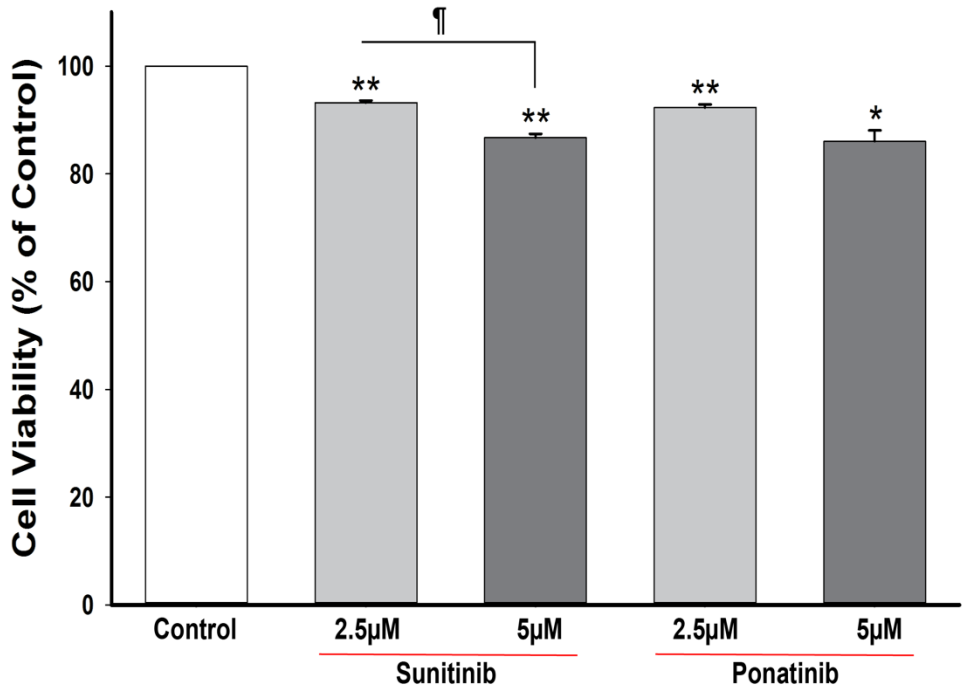

Figure 3.12. Sunitinib and ponatinib treatment reduced H9c2 cardiomyoblast cell viability following 6-hours treatment. The cell viability of H9c2 cardiomyoblasts, treated for 6 hours with sunitinib or ponatinib (2.5µM or 5µM), was measured by flow cytometer analysis using annexin-v FITC and PI dual staining. Values are expressed as % of control (mean ± %SEM, n= 3-4). *P-value < 0.05 vs control, **P-value < 0.01 vs control, and ¶P-value < 0.01 vs sunitinib 2.5µM.

3.4.2. Cell Death: Necrosis and Apoptosis

We examined whether exposure to sunitinib or ponatinib in H9c2 cardiomyoblasts for 6 hours induces necrotic and/or apoptotic cell death. Similar to treatment of H9c2 cardiomyoblasts with sunitinib or ponatinib for 24 hours, no significant difference was seen between the most treatment groups and the respective concentrations vs. control in relation to necrosis. However, treatment with sunitinib (2.5μM) induced a significant reduction in necrosis (34.54 ± 13.4% of control; $p < 0.05$); indicating that necrosis is not a key cell death mechanism induced by sunitinib or ponatinib (Figure 3.13, A).

In terms of apoptosis, treatment with sunitinib or ponatinib (2.5μM or 5μM) led to a significant increase in total apoptosis following 6-hours treatment (Figure 3.13, B). Overall, our results suggest that apoptosis is a key mechanism of H9c2 cardiomyoblasts cell death induced by sunitinib or ponatinib following 6 hours of treatment.

A)

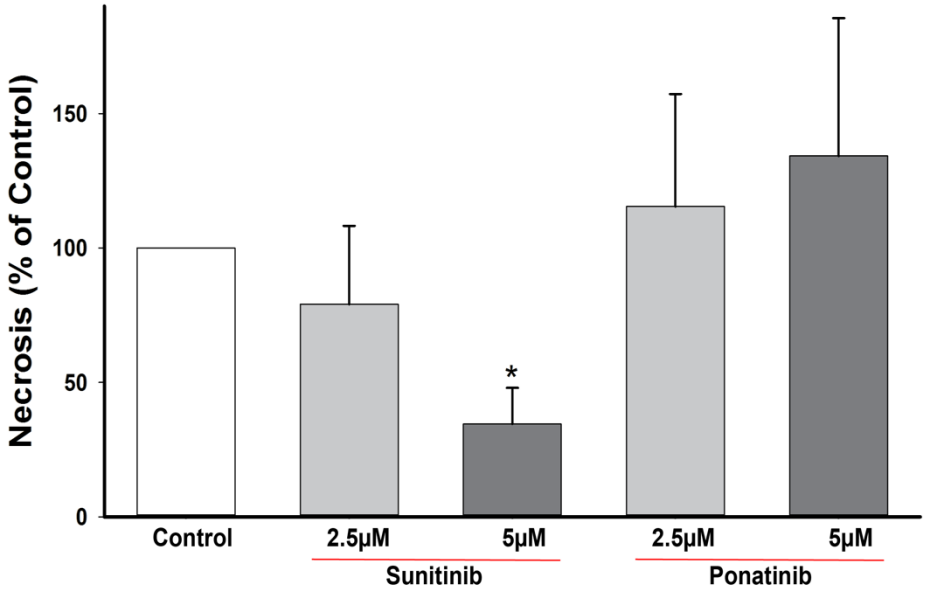

B)

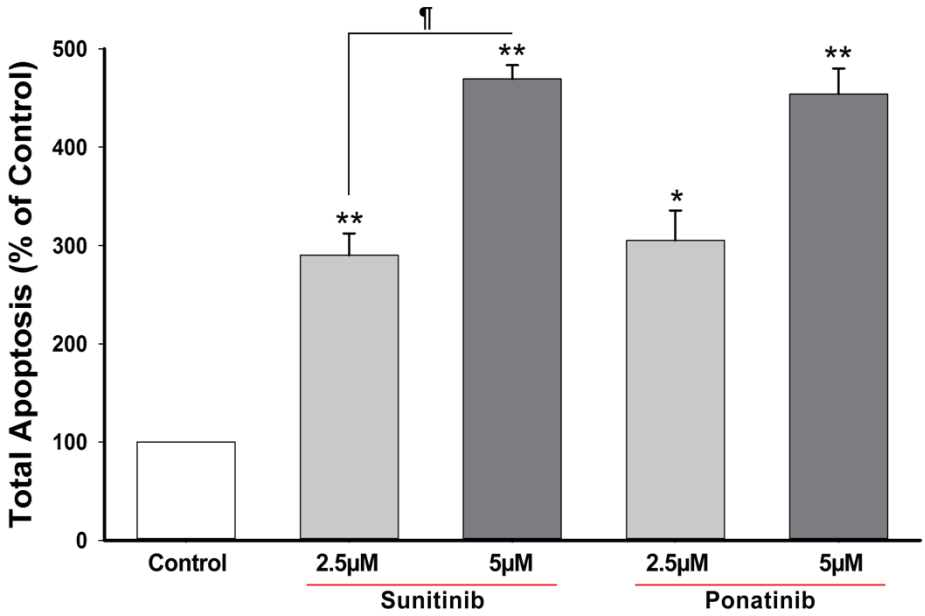

Figure 3.13. Sunitinib or ponatinib treatment for 6 hours regresses necrosis and induces apoptosis. H9c2 cardiomyoblasts were treated with 2.5µM or 5µM. A) Necrosis and B) total apoptosis parameters were analyzed using annexin-v FITC and PI dual staining. Values are expressed as % of control (mean ± %SEM, n= 3-4). *P-value < 0.05 vs control, **P-value < 0.01 vs control, and ¶P-value < 0.01 vs sunitinib 2.5µM.

3.4.3. Cell Morphology and Cardiomyocyte Hypertrophic Markers: Cell Size

To verify whether 6-hours treatment with sunitinib or ponatinib alter H9c2 cardiomyoblast morphology and hypertrophic makers, we first examined the effect on cell size using flow cytometer. In contrast to 24 hours, 6-hours exposure to sunitinib or ponatinib (2.5µM or 5µM) did not show a significant change in cell size (Figure 3.14).

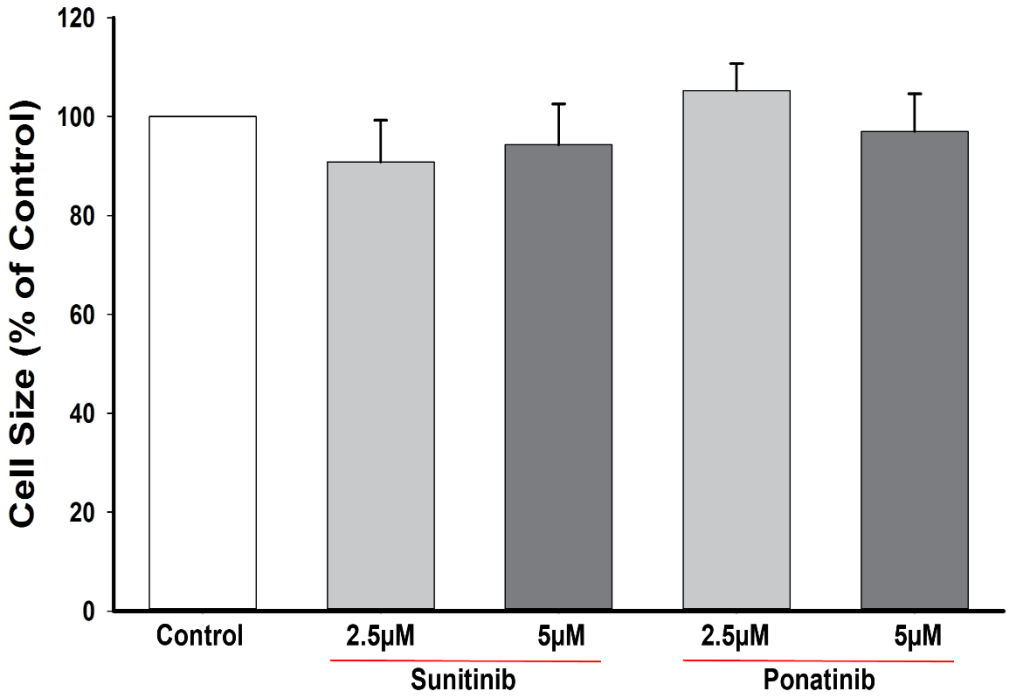

Figure 3.14. Effect of 6 hours treatment with sunitinib or ponatinib on H9c2 cardiomyoblast cell size. Forward scatter flow cytometer analyses were conducted following 6-hours treatment with sunitinib and ponatinib (2.5µM or 5µM) to measure H9c2 cell size. Values are expressed as % of control (mean ± %SEM, n= 3).

3.4.4. Cell Morphology and Cardiomyocyte Hypertrophic Markers: Atrial natriuretic peptide (ANP) mRNA Expression

We also examined the effect of 6-hours treatment with sunitinib or ponatinib on ANP mRNA expression in H9c2 cardiomyoblasts. Our preliminary result showed a high expression of ANP mRNA following ponatinib treatment (5μM). In contrast to our 24-hours, sunitinib did not show ANP mRNA expression, which might indicate a time-dependent effect of sunitinib or ponatinib (Figure 3.15).

Together, our data suggest that 6-hours treatment with sunitinib and ponatinib might induce a time-dependent H9c2 cardiomyoblast hypertrophy. Further studies are required to confirm this notion.

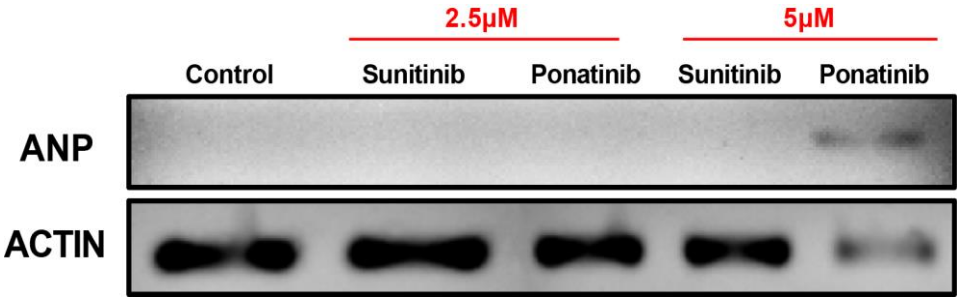

Figure 3.15. Ponatinib treatment for 6 hours induces atrial natriuretic peptide (ANP) mRNA expression. An agarose DNA gel of ANP mRNA expression in H9c2 cardiomyoblasts treated with 2.5μM or 5μM of sunitinib or ponatinib for 6 hours. RNA was isolated from H9c2 cardiomyoblasts, reverse transcribed and amplified against ANP and β-actin primers (n=1).

Table 3.2.

Summary of Findings – Sunitinib or ponatinib-Induced Cardiotoxicity: 6 hours. Arrows denote significance compared to control (↑: increase; ↓: decrease; -: no change; N/A: not applicable).

Parameter	**Sunitinib 2.5µM**	**Sunitinib 5µM**	**Ponatinib 2.5µM**	**Ponatinib 5µM**
Cell viability	↓	↓	↓	↓
Mechanism of Cell Death				
Apoptosis	↑	↑	↑	↑
Necrosis	-	↓	-	-
Cardiac Hypertrophy				
Cell Size	-	-	-	-
ANP	-	-	-	↑

3.5. Molecular Mechanisms of Cardiotoxicity Induced by Sunitinib and Ponatinib – Role of p90 Ribosomal S6 Kinase (p90RSK) and Autophagy Inhibition

3.5.1. p90 Ribosomal S6 Kinase Activity

In order to clearly understand the role of RSK and autophagy in the sunitinib and ponatinib, we treated H9c2 cardiomyoblasts with sunitinib or ponatinib the in the presence and absence of pharmacological inhibitors of RSK and autophagy using BID and CQ, respectively.

Firs, we examined the inhibitory effect of BID (RSK inhibitor) on P-p90RSK and RSK2 under our experimental conditions. H9c2 cardiomyoblasts were pretreated with 10μM BID for 30 minutes and subsequently treated with sunitinib or ponatinib for additional 6 hours.

3.5.1.1. Sunitinib-Mediated Regression of p90 Ribosomal S6 Kinase

In comparison to control, treatment with 10μM BID showed no significant change in P-p90RSK protein expression (144.8 ± 21.94% of control; not significant). Sunitinib treatment (2.5μM) led to a significant decrease of phosphorylated p90RSK as compared to control (87.04 ± 5.44% of control; $p < 0.05$), while pretreatment with 10μM BID showed no significant change (114.6 ± 27.42% of control; not significant). In addition, treatment with 5μM sunitinib in the presence or absence of BID showed no significant change in P-p90RSK protein expression (100.65 ± 9.54% of control and 118.58 ± 29.77% of control; not significant). Furthermore, pretreatment with 10μM BID followed with treatment with sunitinib (2.5μM or 5μM), showed a non-significant trend towards an increase in P-p90RSK protein expression as compared to treatment with sunitinib (2.5μM or 5μM) alone. This may indicate the presence of synergistic effect between both compounds.

In terms of total RSK2, treatment with 10μM BID significantly reduced RSK2 protein expression in comparison to control (62.16 ± 2.44% of control; $p < 0.01$). Treatment with 2.5μM sunitinib in the presence or absence of BID showed no significant change (95.18 ± 6.04% of control and 71.73 ± 11.26% of control; not significant). Similarly, treatment with 5μM sunitinib in the absence of 10μM BID showed no significant change in RSK2 protein expression (92.38 ± 5.97% of control; not significant) whereas in presence of 10μM BID caused a 33% reduction in RSK2 protein expression as compared to control (66.90 ± 8.83% of control; $p < 0.05$). Moreover, pretreatment with 10μM BID followed with treatment with sunitinib (2.5μM or 5μM), showed a non-significant trend towards a decrease in RSK2 protein expression as compared to treatment with sunitinib (2.5μM or 5μM) alone. This may indicate the presence of synergistic effect between both agents.

Furthermore, treatment with 10μM BID showed no significant change in P-p90RSK:RSK2 protein expression (262.71 ± 54.05% of control; not significant). In addition, treatment with 2.5μM sunitinib led to a significant reduction in P-p90RSK:RSK2 protein expression (83.90 ± 5.06% of control; $p < 0.05$), whereas no significant was observed in the presence of BID (144.51 ± 38.82% of control; not significant). Moreover, treatment with 5μM sunitinib in the presence or absence of 10μM BID showed no significant change in P-p90RSK:RSK2 protein expression (100.24 ± 9.05% of control; and 140.90 ± 36.2% of control; not significant) (Figure 3.16). Furthermore, pretreatment with 10μM BID followed with treatment with sunitinib (2.5μM or 5μM), showed a non-significant trend towards an increase in P-p90RSK:RSK2 protein expression as compared to treatment with sunitinib (2.5μM or 5μM) alone. This may indicate the presence of synergistic effect between both agents. Together, these results suggest that 10μM BID is able to regress RSK expression.

Also, our findings confirm that treatment with sunitinib at 2.5µM but not at 5µM inhibits p90RSK phosphorylation.

A)

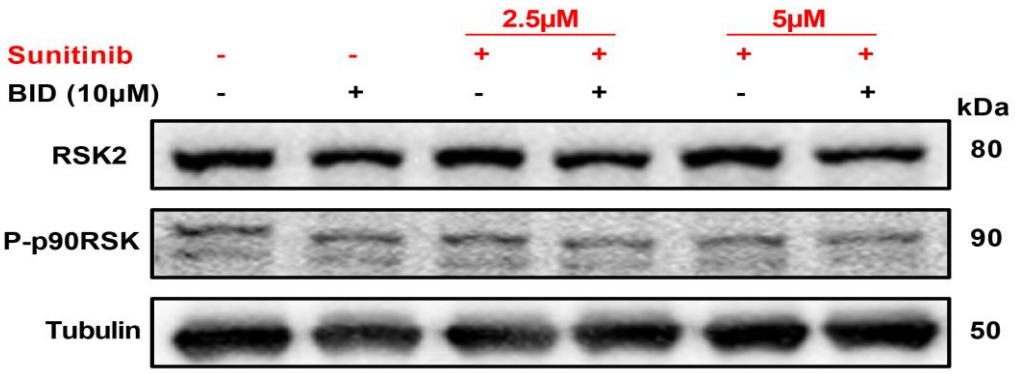

B)

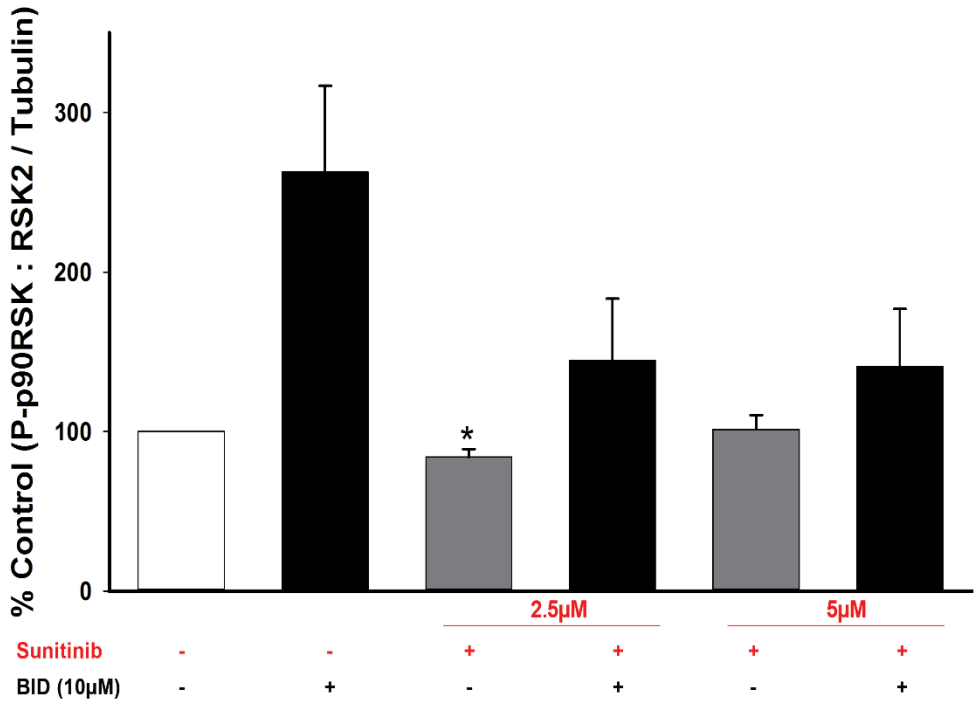

Figure 3.16. Sunitinib treatment for 6 hours reduces phosphorylation of p90RSK protein expression. H9c2 cardiomyoblasts were pretreated with 10μM BID for 30 minutes and subsequently incubated with 2.5μM or 5μM sunitinib for 6 hours. RSK2 phospho-p90RSK (P-p90RSK) protein expression was measured by immunoblotting. A) Representative P-p90RSK and RSK-2 western blots and B) Quantification of P-p90RSK:RSK2 blot after normalization to α-tubulin. Values are expressed as % of control (mean ± %SEM, n=3-11). *P-value < 0.05 vs control.

3.5.1.2. Ponatinib-Mediated Induction of p90 Ribosomal S6 Kinase

In comparison to control, treatment with 10µM BID significantly increased the P-p90RSK protein expression (164.58 ± 5.08% of control; $p < 0.01$). Similarly, treatment with ponatinib (2.5µM or 5µM) induced the phosphorylated form of p90RSK by 74% and 97%, as compared to control, respectively (174.32 ± 20.90% of control; $p < 0.01$ and 197.62 ± 20.70% of control; $p < 0.01$). Treatment with ponatinib (2.5µM or 5µM) in the presence of 10µM BID did not show a significant change in P-p90RSK protein expression in comparison to ponatinib alone.

In terms of total RSK2 protein expression, 10µM of BID was enough to significantly regress RSK2 protein expression by 40% as compared to control (64.97 ± 6.50% of control; $p < 0.01$). In comparison to control, treatment with 2.5µM ponatinib in the presence or absence of 10µM BID reduced the protein expression of RSK2 (86.16 ± 5.13% of control and 65.14 ± 10.18% of control; $p < 0.05$, respectively). Likewise, treatment with 5µM ponatinib in the presence or absence of 10µM BID caused a reduction in RSK2 protein expression as compared to control (68.54 ± 9.05% of control and 55.8 ± 5.6% of control; $p < 0.01$, respectively). Moreover, pretreatment with 10µM BID followed with treatment with ponatinib (2.5µM or 5µM), showed a non-significant trend towards a decrease in RSK2 protein expression as compared to treatment with ponatinib (2.5µM or 5µM) alone. This shows a possibility of synergistic effect between ponatinib and BID.

In terms of p90RSK:RSK2 ratio, treatment with ponatinib (2.5µM or 5µM) led to a significant increase of p90RSK:RSK2 protein expression (184.18 ± 24.35% and 265.5 ± 39.98% of control; $p < 0.01$). Similarly, treatment with BID alone or in combination with 2.5µM or 5µM ponatinib caused a significant increase of p90RSK:RSK2 ratio (294.87 ± 36.9% of control; $p < 0.05$; 221.8 ± 34.31% of control;

$p < 0.05$; and 215.07 ± 9.45% of control; $p < 0.01$), respectively. Furthermore, pretreatment with 10µM BID followed with treatment with ponatinib (2.5µM), showed a non-significant increase in P-p90RSK:RSK2 protein expression as compared to treatment with ponatinib (2.5µM) alone, which may indicate a possible synergistic effect between the two compounds. In contrast, pretreatment with 10µM BID followed with treatment with 5µM ponatinib, showed a non-significant decrease in P-p90RSK:RSK2 protein expression as compared to treatment with 5µM ponatinib alone (Figure 3.71). Collectively, our results indicate that, in contrast to sunitinib, ponatinib treatment induces p90RSK phosphorylation while stabilizing RSK2 expression.

A)

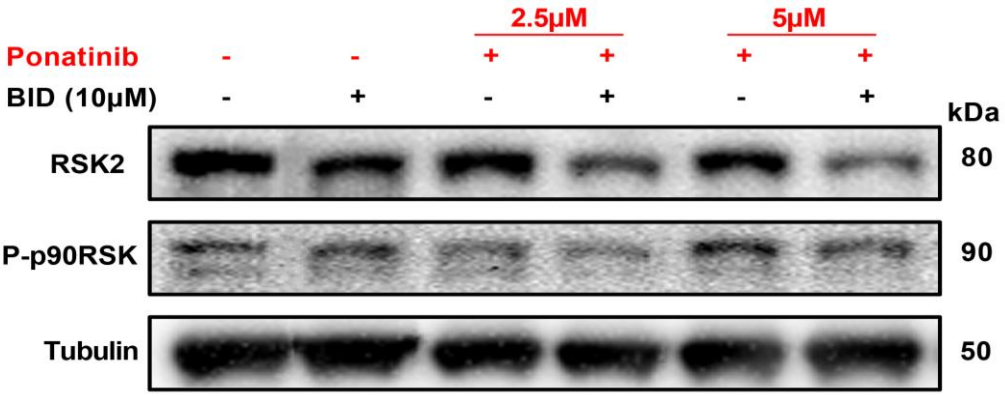

B)

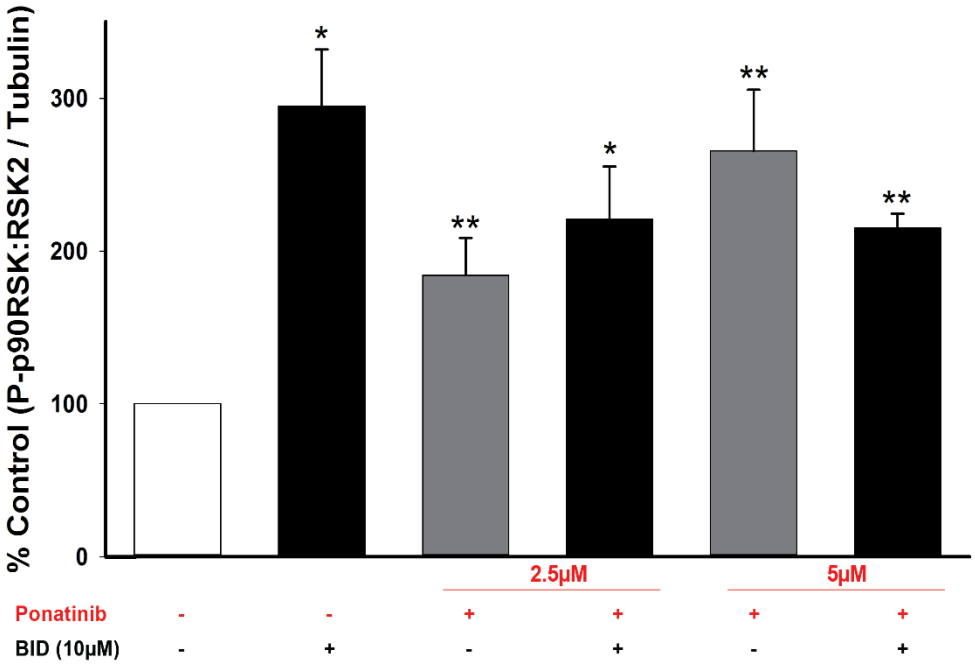

Figure 3.17. Ponatinib treatment for 6 hours induces phosphorylation of p90RSK protein expression. H9c2 cardiomyoblasts were pretreated with 10μM BID for 30 minutes and subsequently incubated with 2.5μM or 5μM ponatinib for 6 hours. RSK2 phospho-p90RSK (P-p90RSK) protein expression was measured by immunoblotting. A) Representative P-p90RSK and RSK2 western blots and B) Quantification of P-p90RSK:RSK2 blot after normalization to α-tubulin. Values are expressed as % of control (mean ± %SEM, n=3-10). *P-value < 0.05 vs control and **P-value < 0.01 vs control.

3.5.2. Evaluation of Autophagic flux

Our previous findings revealed a trend towards an increase of LC3-II:LC3-I protein expression following 24-hours treatment with sunitinib and a significant increase following treatment with 2.5µM ponatinib. However, whether sunitinib or ponatinib alters the autophagic flux following 6-hours treatment is not known. Herein, we characterized the effect of sunitinib or ponatinib on autophagic activity using autophagosome-lysosome fusion inhibitor, CQ. To evaluate autophagic flux, H9c2 cardiomyoblast were pretreated with 10µM CQ for 30-minutes and then incubated with sunitinib or ponatinib for additional 6-hours, protein expression of LC3-II was then analyzed.

Increased LC3-II protein expression following drug treatment in the presence of CQ suggests that the drug induces autophagic flux. Whereas unchanged LC3-II protein expression suggests that the drug accumulates autophagosome by blocking autophagic degradation.

3.5.2.1. Sunitinib-Mediated Induction of Autophagy

Treatment with 2.5µM or 5µM sunitinib for 6-hours led to a significant increase in LC3-II protein expression as compared to control (169.45 ± 19.45% of control; $p < 0.01$ and 217.93 ± 28.25% of control; $p < 0.01$). Treatment with 10µM did not cause a significant change in LC3-II as compared with control (146.41 ± 33.11% of control; not significant). Likewise, in comparison to control, treatment with sunitinib (2.5µM or 5µM) in the presence of CQ did not show a significant change in LC3-II protein expression. As compared to sunitinib (2.5µM or 5µM) alone, pretreatment with 10µM CQ, showed a non-significant trend towards an increase of LC3-II protein expression, which may indicate a possible induction of autophagic flux (Figure 3.18). Taken together, our results show that

sunitinib might induce autophagy.

A)

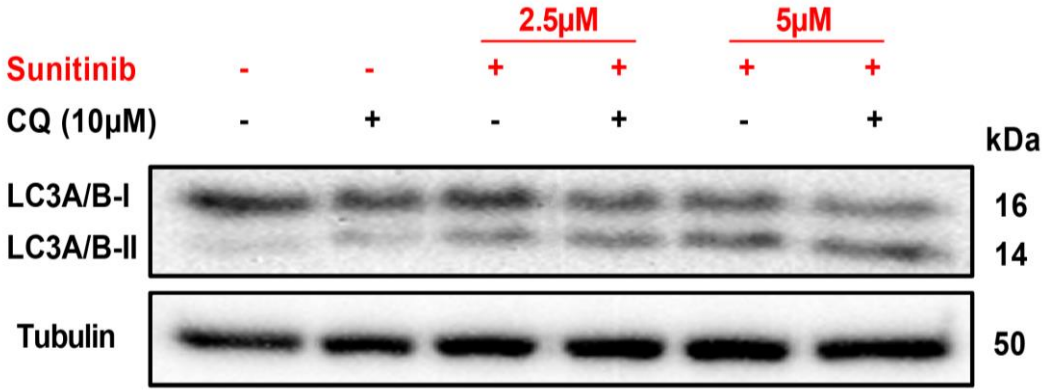

B)

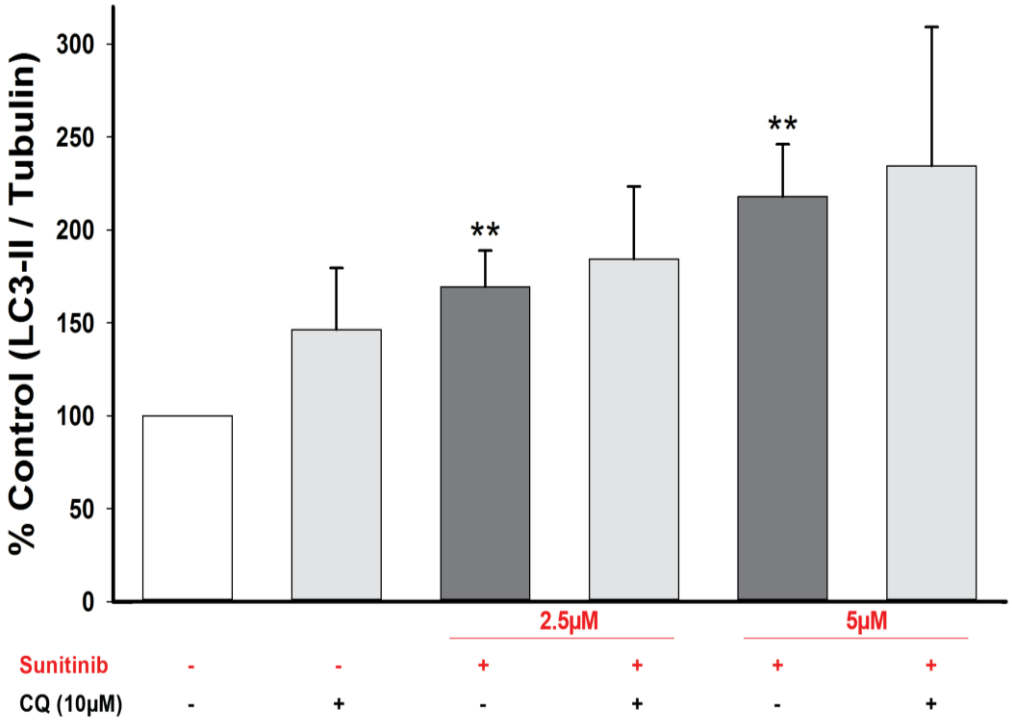

Figure 3.18. The effect of 6-hours treatment sunitinib on autophagic flux. H9c2 cardiomyoblasts were pretreated with 10μM CQ for 30 minutes and subsequently treated with 2.5μM or 5μM of sunitinib for 6 hours. A) Representative LC3-I and LC3-II western blot and B) Quantification of LC3-II blot after normalization to α-tubulin. Values are expressed as % of control (mean ± %SEM, n=3-8). *P-value < 0.05 vs control and **P-value < 0.01 vs control.

3.5.2.2. Ponatinib-Mediated Induction of Autophagy

Treatment with 2.5μM or 5μM ponatinib for 6-hours significantly increased LC3-II protein expression, as compared to control (228.11 ± 27.74% and 322.9 ± 53.06% of control; $p < 0.01$). Similarly, treatment with 10μM CQ increased LC3-II protein expression as compared to control (181.44 ± 23.46% of control; $p < 0.05$). In comparison to control, treatment with ponatinib (2.5μM or 5μM) in the presence of CQ caused a significant increase in LC3-II protein expression (254.98 ± 48.23% of control and 510.9 ± 132.1% of control; $p < 0.05$, respectively). As compared to ponatinib (2.5μM or 5μM) alone, pretreatment with 10μM CQ, showed a non-significant trend towards an increase of LC3-II protein expression, which may indicate a possible induction of autophagic flux (Figure 3.19). Taken together, our results show that ponatinib might induce autophagy.

A)

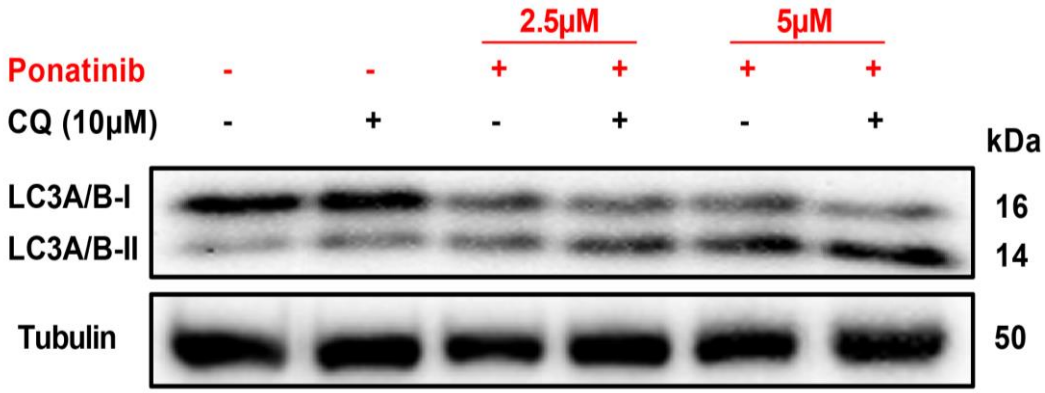

B)

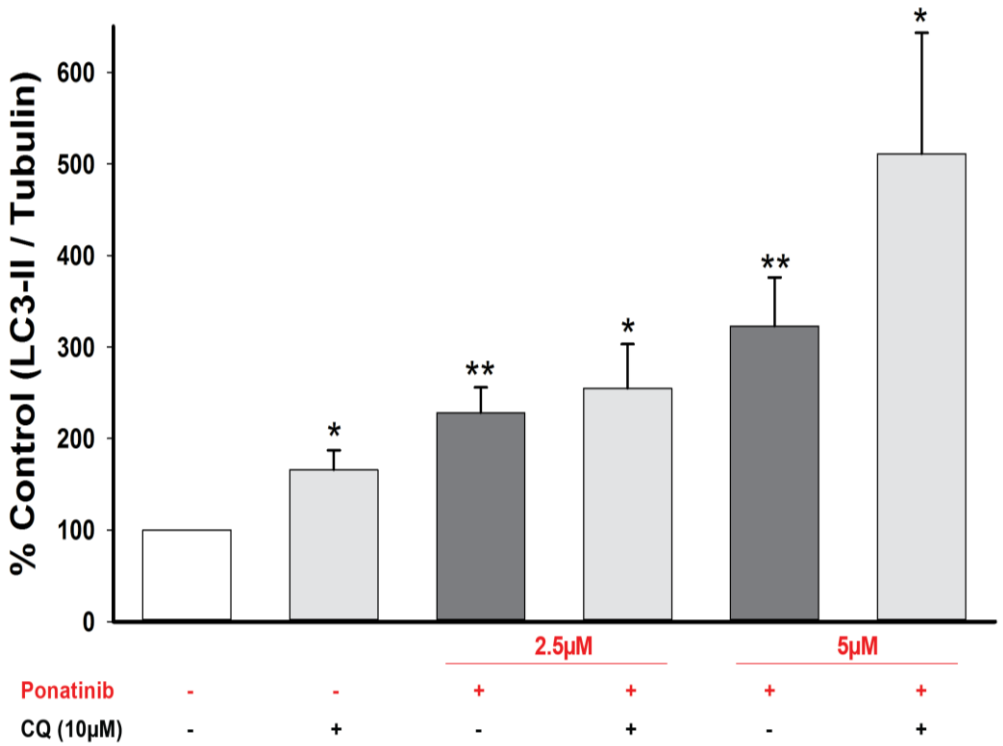

Figure 3.19. The effect of 6-hours treatment ponatinib on autophagic flux. H9c2 cardiomyoblasts were pretreated with 10μM CQ for 30 minutes and subsequently treated with 2.5μM or 5μM of ponatinib for 6 hours. A) Representative LC3-I and LC3-II western blot and B) Quantification of LC3-II blot after normalization to α-tubulin. Values are expressed as % of control (mean ± %SEM, n=4-9). *P-value <

0.05 vs control and **P-value < 0.01 vs control.

3.5.3. Cell Viability

Next, we examined the role of RSK and autophagy inhibition, by BID and CQ, respectively, in cardiotoxicity induced by sunitinib or ponatinib. H9c2 cardiomyoblasts were pretreated with 10μM BID or CQ for 30 minutes and subsequently treated with sunitinib or ponatinib (2.5μM or 5μM) for additional 6 hours. H9c2 cardiomyoblast cell viability was measured using PI staining solution by flow cytometer.

Treatment with 10μM BID led to a significant reduction in H9c2 cardiomyoblast cell viability as compared to control (77.81 ± 1.6% of control; $p < 0.01$). Treatment with 10μM CQ did not show a significant change in H9c2 cardiomyoblast cell viability. In comparison to control, treatment with sunitinib or ponatinib (2.5μM or 5μM) significantly reduced H9c2 cardiomyoblast cell viability. In addition, pretreatment with 10μM BID or 10μM CQ followed with sunitinib or ponatinib (2.5μM or 5μM) treatment resulted in a significant reduction in H9c2 cell viability as compared with control. Moreover, pretreatment with 10μM BID followed with 2.5μM ponatinib resulted in a significant reduction in H9c2 cell viability as compared with ponatinib (2.5μM) treatment alone. A similar non-significant trend was observed with sunitinib (2.5μM or 5μM) or ponatinib (5μM) treatment in the presence of 10μM BID. While pretreatment with 10μM CQ followed with treatment with ponatinib or sunitinib (2.5μM or 5μM) showed no significant change in H9c2 cell viability as compared to ponatinib or sunitinib (2.5μM or 5μM) alone (Figure 3.20). Taken together, RSK inhibition exacerbates ponatinib and sunitinib-induced cell death.

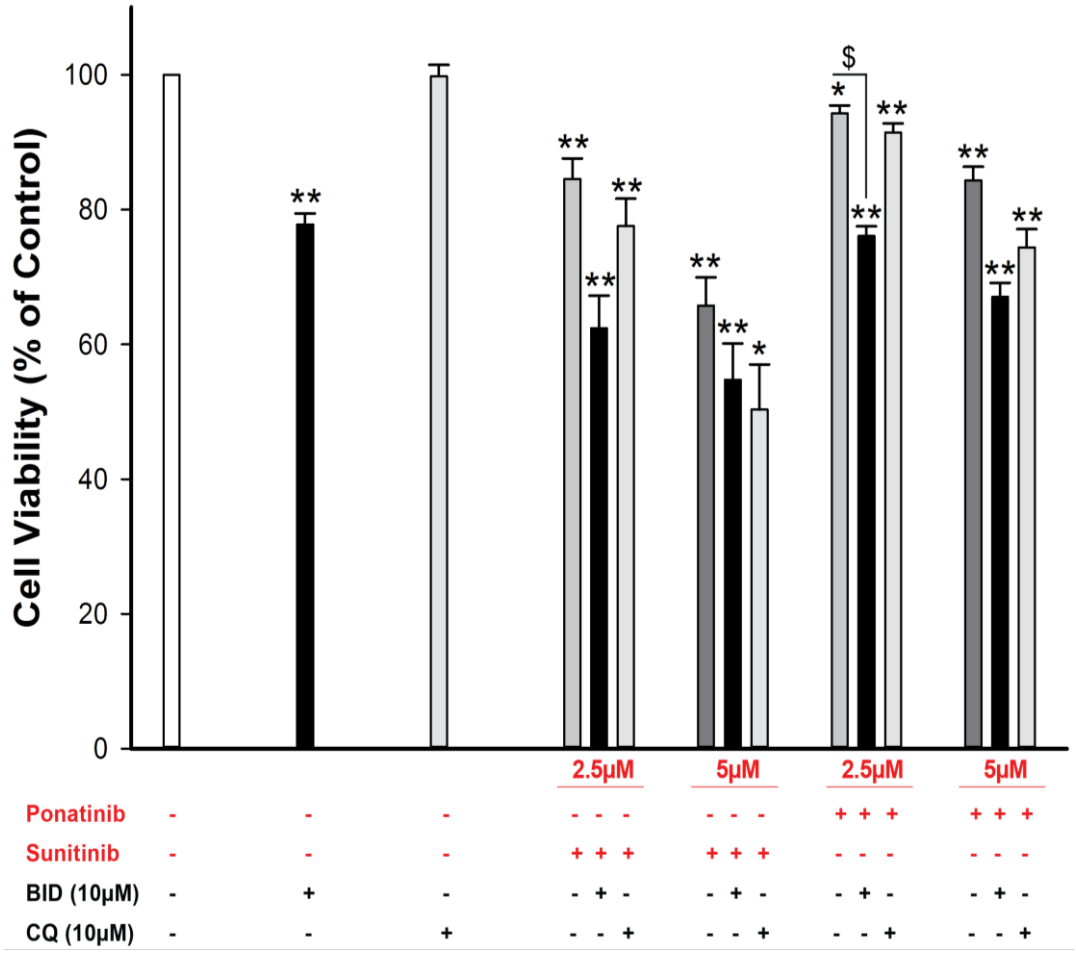

Figure 3.20. Effect of RSK and autophagy inhibition on sunitinib or ponatinib on H9c2 cardiomyoblast cell viability. H9c2 cardiomyoblasts were pretreated with 10μM of BID or CQ for 30 minutes and subsequently treated with 2.5μM or 5μM of ponatinib for 6 hours. The cell viability was measured by flow cytometer analysis using annexin-v FITC and PI dual staining. Values are expressed as % of control (mean ± %SEM, n= 4). *P-value < 0.05 vs control, **P-value < 0.01 vs control, $P-value < 0.0001 vs cells treated with ponatinib 2.5μM.

3.5.4. Cell Death: Necrosis and Apoptosis

Next, we examined the effect RSK and autophagy inhibition (using BID or CQ) on the mechanism of cell death induced by sunitinib or ponatinib treatment. H9c2 cardiomyoblasts were pretreated with BID or CQ for 30 minutes and subsequently treated with 2.5μM or 5μM sunitinib or ponatinib for an additional 6 hours. Necrotic and apoptotic H9c2 cardiomyoblast death was measured by flow cytometer.

Treatment with 10μM BID led to necrotic cell death as compared to control (180.71 ± 17.2% of control; $p < 0.05$). Although treatment with 2.5μM ponatinib caused a significant reduction in necrosis, in comparison to control (83.41 ± 3.03% of control; $p < 0.05$), pretreatment with 10μM BID significantly increased necrotic cell death, as compared to control (178.91 ± 23.75% of control; $p < 0.05$). Pretreatment with 10μM BID followed with treatment with ponatinib or sunitinib (2.5μM or 5μM) showed a non-significant increase in necrotic cell death as compared to ponatinib or sunitinib (2.5μM or 5μM) alone, which indicates that RSK inhibition might mediate necrotic cell death.

Treatment with 10μM CQ did not induce a significant change in necrosis, as compared to control (83.97 ± 8.63% of control; not significant). In addition, pretreatment with 10μM CQ followed with treatment with ponatinib or sunitinib (2.5μM or 5μM) showed no significant change in necrotic cell death as compared to ponatinib or sunitinib (2.5μM or 5μM) alone (Figure 3.21).

Moreover, treatment with 10μM BID significantly induced apoptotic cardiomyoblast cell death (241.88 ± 24.5% of control; $p < 0.01$). In addition, pretreatment with BID followed with ponatinib or sunitinib (2.5μM or 5μM) showed

a trend towards an increase in apoptotic cell death compared to treatment with ponatinib or sunitinib alone. In addition, treatment with 10µM CQ showed no change in apoptotic cell death as compared to control (105.30 ± 12.27% of control; not significant). However, pretreatment with 10µM CQ followed with treatment with 2.5µM or 5µM ponatinib or sunitinib showed a tread towards an increase in total apoptosis as compared to treatment with ponatinib or sunitinib alone (Figure 3.22). Taken together, our results show that RSK inhibition by BID mediates both necrotic and apoptotic H9c2 cardiomyoblast cell death, while inhibition of autophagy by CQ may potentiate ponatinib and sunitinib-induced apoptotic H9c2 cell death.

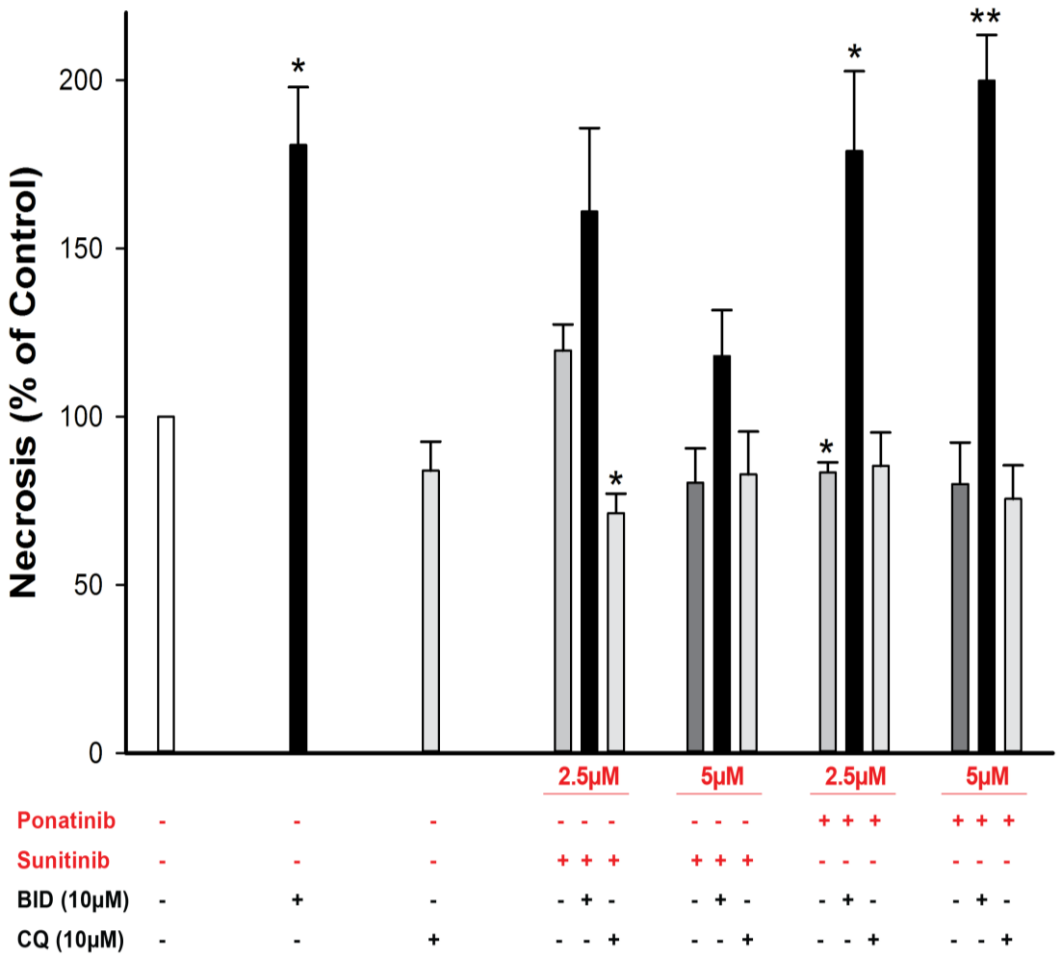

Figure 3.21. Effect of RSK and autophagy inhibition on necrotic cell death following ponatinib or sunitinib. H9c2 cardiomyoblasts were pretreated with 10μM of BID or CQ for 30 minutes and subsequently treated with 2.5μM or 5μM of ponatinib for 6 hours. Necrosis was measured by flow cytometer analysis using annexin-v FITC and PI dual staining. Values are expressed as % of control (mean ± %SEM, n= 3-4). *P-value < 0.05 vs control and **P-value < 0.01 vs control.

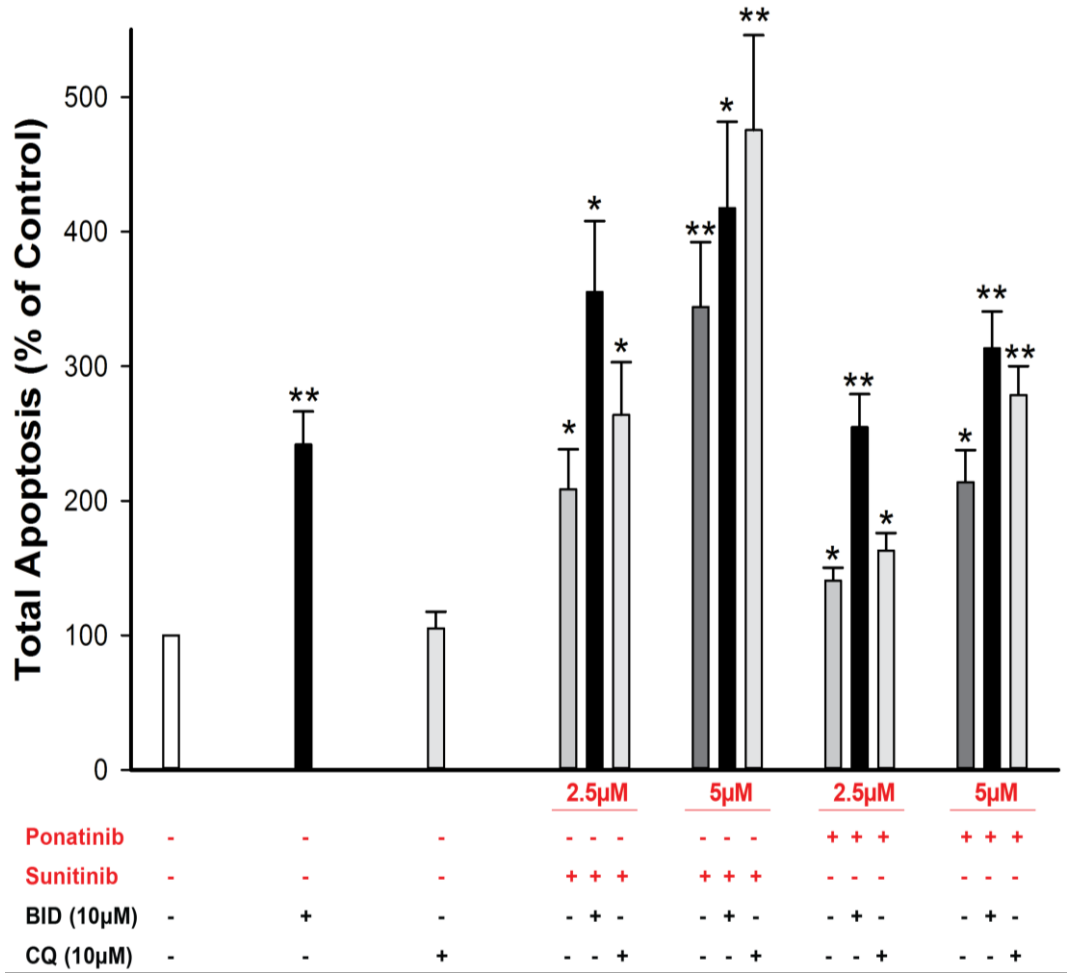

Figure 3.22. Effect of RSK and autophagy inhibition on apoptotic cell death following ponatinib or sunitinib. H9c2 cardiomyoblasts were pretreated with 10μM of BID or CQ for 30 minutes and subsequently treated with 2.5μM or 5μM of ponatinib for 6 hours. Total apoptosis was measured by flow cytometer analysis using Annexin-v FITC and PI dual staining. Values are expressed as % of control (mean ± %SEM, n= 4). *P-value < 0.05 vs control and **P-value < 0.01 vs control.

3.5.5. Apoptosis – Caspase-3 Activation

Next, we determined whether effect of RSK and autophagy inhibition on apoptotic marker, caspase-3. H9c2 cardiomyoblast were pretreated with 10µM BID or 10µM CQ for 30-minutes and then incubated with sunitinib or ponatinib for additional 6-hours.

1.6.3.1. Sunitinib or Ponatinib-Mediated Caspase-3 Regression

Exposure to RSK or autophagy inhibitors alone did not alter caspase-3 protein expression in comparison to control. Treatment with 10µM BID or CQ resulted in no effect in caspase-3 protein expression. Pretreatment with 10µM CQ followed with treatment with 5µM sunitinib reduced caspase-3 protein expression as compared to control (72.35 ± 6.7% of control; $p < 0.05$). Pretreatment with 10µM BID followed with treatment with 2.5µM or 5µM sunitinib showed no change in caspase-3 protein expression as compared to sunitinib alone (Figure 3.23).

Similarly, pretreatment with BID or CQ followed with treatment with 2.5µM or 5µM showed no significant change in caspase-3 protein expression (Figure 3.24).

Together, these findings demonstrate that sunitinib and ponatinib-induced H9c2 cardiomyoblast apoptotic death is not mediated via a caspase-deponent pathway. Further studies investigating the involvement of caspase-independent in this setting is required.

A)

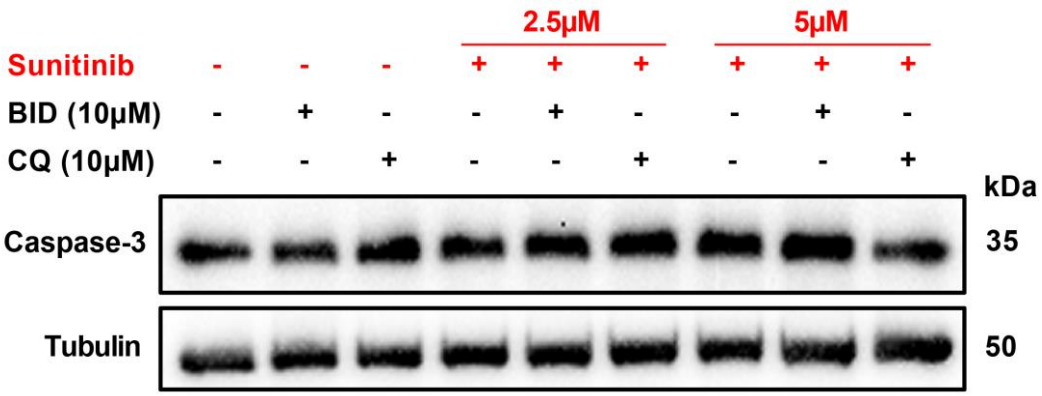

B)

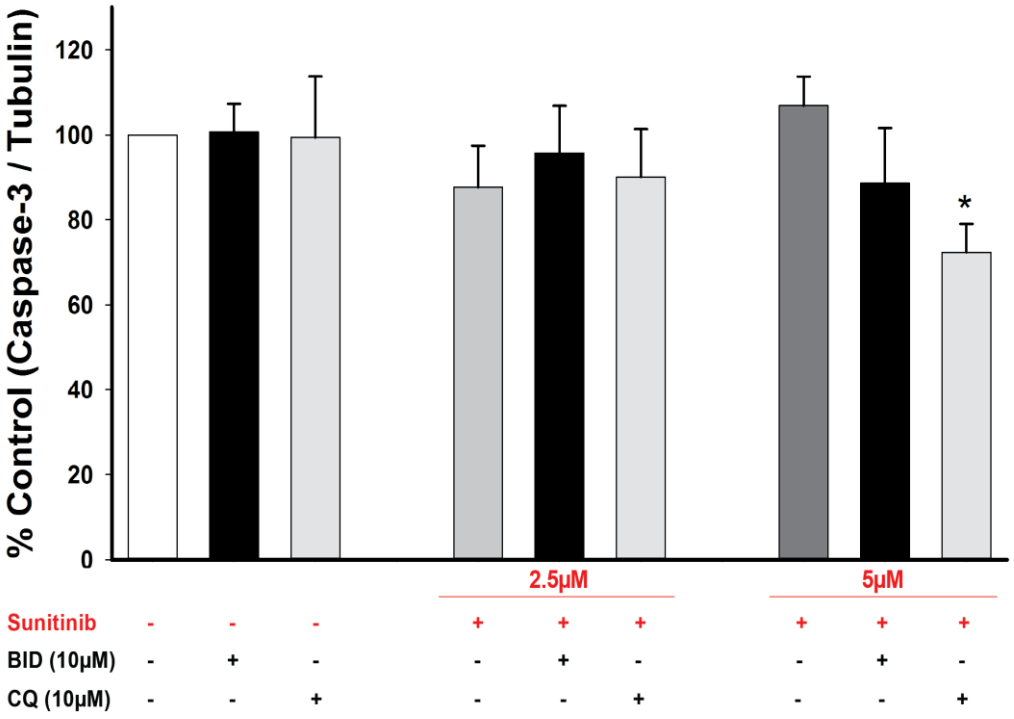

Figure 3.23. The effect of RSK and autophagy inhibition on caspase-3 protein expression following sunitinib treatment. H9c2 cardiomyoblasts were pretreated with 10μM of BID or CQ for 30 minutes and subsequently treated with 2.5μM or 5μM sunitinib for an additional 6 hours. A) Representative caspase-3 western blot and B) Quantification of caspase-3 blot after normalization to α-tubulin. Values are expressed as % of control (mean ± %SEM, n=3-6). *P-value < 0.05 vs control.

A)

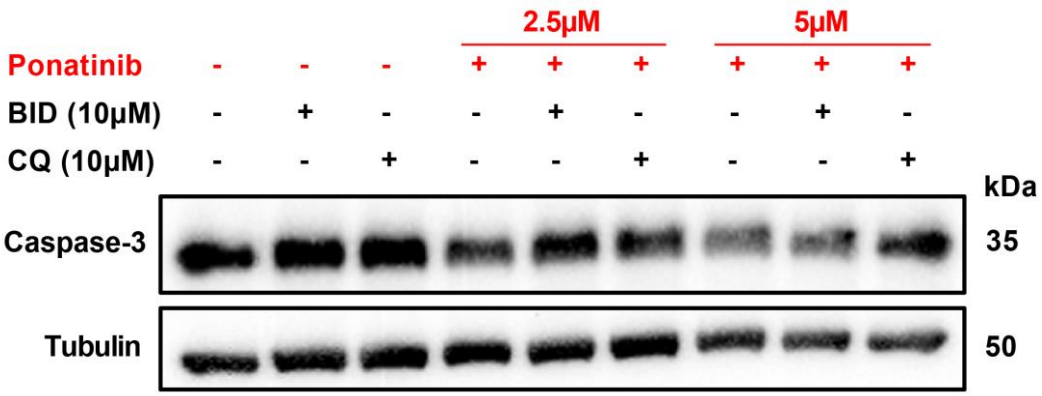

B)

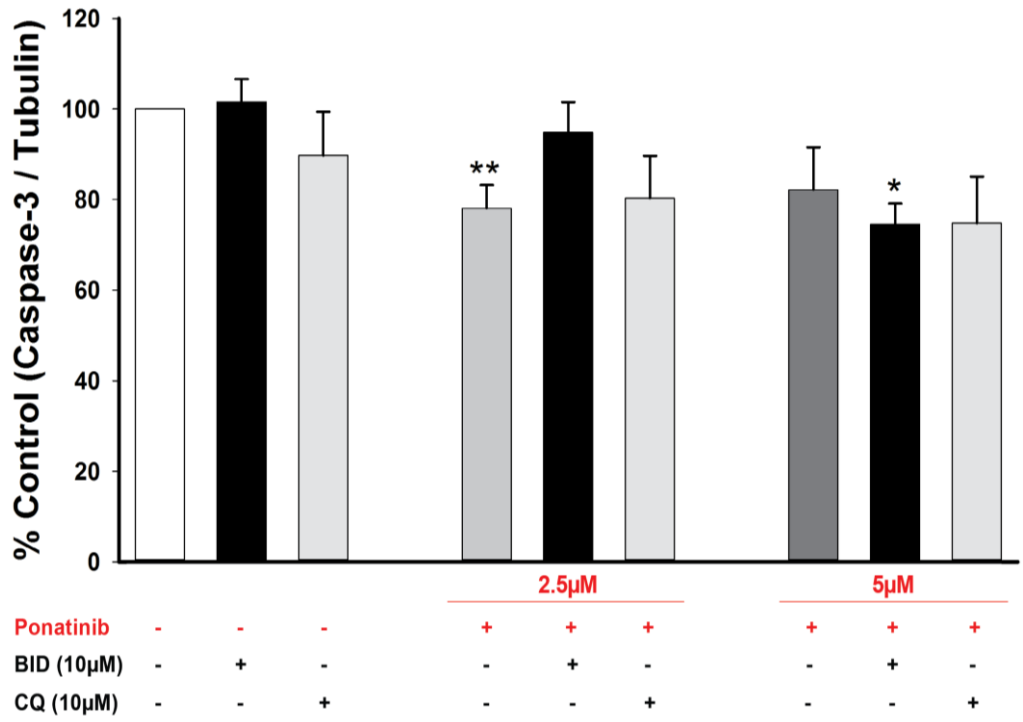

Figure 3.24. The effect of RSK and autophagy inhibition on caspase-3 protein expression following ponatinib treatment. H9c2 cardiomyoblasts were pretreated with 10μM of BID or CQ for 30 minutes and subsequently treated with 2.5μM or 5μM ponatinib for an additional 6 hours. A) Representative caspase-3 western blot and B) Quantification of caspase-3 blot after normalization to α-tubulin. Values are expressed as % of control (mean ± %SEM, n=3-5). *P-value < 0.05 vs control and **P-value < 0.01 vs control.

3.5.6. Cardiac Hypertrophy and Cell Morphology

3.5.6.1. Cell Surface Area and Cell Size

We also examined the effect of RSK and autophagy inhibition on ponatinib and sunitinib-induced cardiac hypertrophy and cardiomyoblast damage. H9c2 cardiomyoblasts cell surface area using crystal violet staining was measured, as an indication of cardiac hypertrophy, and cell size was assessed, as an indication of cellular morphology, using flow cytometer.

Treatment with sunitinib or ponatinib (2.5µM or 5µM) in the presentence or absence of 10µM BID or 10µM CQ, showed no change in H9c2 cell surface area (Data not shown).

Exposure to 10µM BID or 10µM CQ did not impair H9c2 cardiomyoblast cell size. Pretreatment with 10µM BID followed with treatment with sunitinib or ponatinib (2.5µM or 5µM) showed a non-significant trend towards a decrease in H9c2 cell size as compared to sunitinib or ponatinib treatment alone. In addition, Pretreatment with 10µM CQ followed with treatment with sunitinib or ponatinib (2.5µM or 5µM) resulted in no effect in H9c2 cell size as compared to sunitinib or ponatinib treatment alone. (Figure 3.25). Collectively, RSK inhibition by BID might induce H9c2 cellular shrinkage.

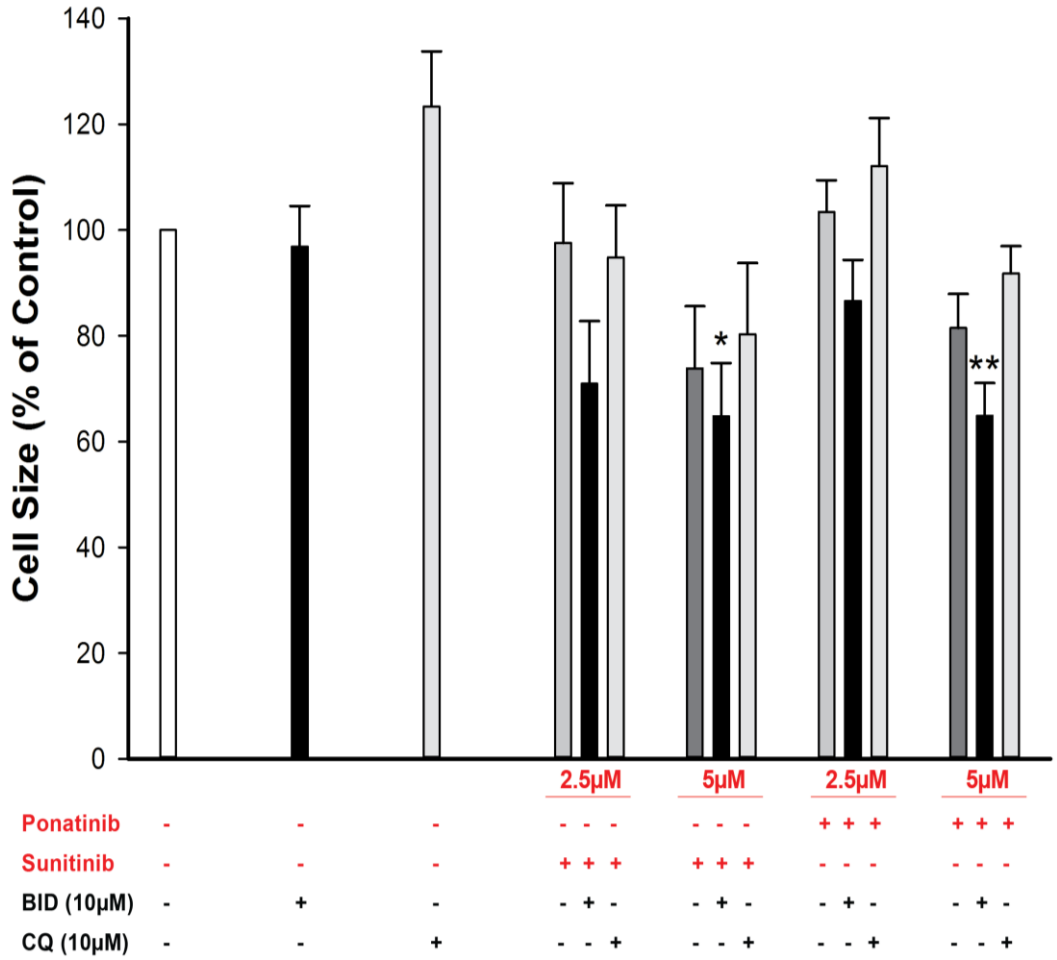

Figure 3.25. The effect of RSK or autophagy inhibition on ponatinib or sunitinib-induced cardiomyoblast damage. H9c2 cardiomyoblasts were pretreated with 10μM of BID or CQ for 30 minutes and subsequently treated with 2.5μM or 5μM of ponatinib for an additional 6 hours. H9c2 cell size was measured by forward scatter using flow cytometer. Values are expressed as % of control (mean ± %SEM, n= 4). *P-value < 0.05 vs control and **P-value < 0.01 vs control.

CHAPTER 4: DISCUSSION

Cardio-oncology is a multi-disciplinary field that focuses on the detection and treatment of cardiovascular adverse events caused by cancer therapy (7). Understanding the cancer pathophysiology has shifted cancer management towards a targeted approach. Multi-targeted TKIs, including sunitinib and ponatinib are used extensively in RCC and CML patients, respectively. Despite their superb anticancer efficacy, their use has been associated with increased risk of cardiotoxicity (30, 65, 91, 94). Thus, it is crucial to understand the underlying molecular mechanism of TKIs-induced cardiotoxicity to identify novel protective measures during clinical use. Inhibition of RSK signaling pathway is thought to play a role in sunitinib-induced cardiotoxicity. Force et.al have hypothesized that sunitinib-induced RSK inhibition promote mitochondrial damage, cardiomyocyte apoptosis, cardiac hypertrophy and ventricular dysfunction (31, 35, 38). Another major factor to sunitinib-mediated cardiotoxicity involves the induction of cardiomyocyte autophagic activity, which mediates cardiomyocyte cell death (101, 175). A recent study has revealed that ponatinib treatment stimulates p90RSK phosphorylation in human endothelial cell models (137). The activation of p90RSK is thought to play a role in atherosclerosis and vascular adverse effects through inhibition of ERK5 atheroprotective effect (137, 198).

While the involvement of RSK pathway and upregulation of autophagy, in sunitinib-mediated cardiotoxicity, are well-addressed (31, 35, 100, 101); their involvement in ponatinib-mediated cardiotoxicity remains unknown. In the current study, we hypothesize that the RSK signaling and/or autophagy upregulation promote ponatinib and sunitinib-induced cardiotoxicity via inducing cardiomyocyte loss and hypertrophy. The objectives of this study are to: 1) evaluate the cardiotoxic effects of

ponatinib and sunitinib in H9c2 cardiomyoblasts; 2) explore the effect of RSK and autophagy inhibition in ponatinib-mediated cardiotoxicity; and 3) validate the role of RSK and autophagy inhibition in sunitinib-mediated cardiotoxicity.

In the present study, 4 TKIs were screened (imatinib, dasatinib, sunitinib, and ponatinib) for cardiotoxicity in H9c2 cardiomyoblasts. We considered two criteria for cardiotoxicity; cardiomyoblast loss and cardiomyoblast hypertrophy. At comparable treatment concentrations, we found that imatinib was the safest, to H9c2 cardiomyoblasts, among the screened TKIs, while dasatinib caused minimal damage to cardiomyoblast. We found that ponatinib and sunitinib were the most toxic TKIs to H9c2 cardiomyoblasts and were selected for further investigations. Ponatinib and sunitinib were recognized as the most cardiotoxic agents, among different TKIs, in previous studies (73, 76, 185).

At the initial phase, we employed ponatinib and sunitinib at concentrations of 2.5μM and 5μM for 24 hours. However, the treatment duration was soon reduced to 6 hours due to server myocyte loss and low protein lysate concentrations obtained (Figures 3.6, 3.10, and 3.11). We then examined the effect of 6-hours ponatinib and sunitinib treatment on H9c2 cardiomyoblast and evaluated the role of RSK and autophagy as a potential mechanism governing cardiotoxicity induced.

4.1. Ponatinib and Sunitinib-Induced Cardiomyoblast Loss and Hypertrophy

In this study, we employed H9c2 embryonic rat cardiac tissue, which is a well-characterized in vitro model that has been used to study the molecular mechanism of anticancer therapy-induced cardiotoxicity, including TKIs (101, 178, 179). The reported C_{max} of ponatinib, following a daily dose of 45mg/day, is 0.145 μM and 0.12μM following 44mg/day dose of sunitinib (183, 184). Although the concentrations used in this study (2.5μM and 5μM) were higher compared to C_{max}

levels, these concentrations are in agreement with previous studies (74, 101, 178, 185, 186).

Cytotoxic compounds are those that affect the cellular morphology, cellular growth and attachment, or reduce cellular viability (199). Cardiomyocyte loss mediates the pathogenesis of heart failure. In failing heart, cardiomyocyte loss occurs by apoptosis, necrosis, and autophagy (200, 201). Similarly, pathological cardiac hypertrophy, stimulated by increased pressure and neurohormonal activation, leads to heart failure. A hallmark feature of cardiac hypertrophy is increased expression of ANP, BNP, and β-MHC and enlarged cardiomyocyte size (202, 203). Therefore, we determined the effect of ponatinib and sunitinib treatment on H9c2 cardiomyoblast loss and hypertrophy markers.

4.1.1. Cardiomyoblast Loss

Cell Viability

Cardiomyocyte loss in failing hearts occurs due to apoptotic, necrotic, and autophagic cell death (200, 201). Cell viability measures the number of intact and viable cells in a sample (199), which also can indicate cellular loss. Our in vitro H9c2 cardiomyoblast model, treated for 6 hours with ponatinib or sunitinib (2.5µM or 5µM), caused a decrease in cell viability by 7% -14% (Figure 3.12). Results of the MTT assay, following 24 hours treatment with sunitinib or ponatinib, showed a maximum decline of 20% and 40% in cell viability, respectively (Figure 3.1). Various in vitro studies showed comparable results (74, 75, 101, 178, 185, 199). A previous study assessed hiPSC-CMs cell viability following 48-hours treatment with ponatinib using Hoechst dye. Authors found that the treatment with 5µM and 10µM ponatinib induced 15% and 95% reduction in cell viability, respectively (74). In comparison to our findings, a 48-hours treatment with 5µM ponatinib caused lesser cell death; this

inconsistency could be attributed to the type of cells and cell viability assay used. Using similar in vitro model and cell viability assay, Korashy et al. found similar pattern of H9c2 cell viability reduction following 24-hours treatment with 1µM, 2.5µM, 5µM and 10µM sunitinib (178). Moreover, using the same model and experimental procedure, Zhao et al. found that 48-hours treatment with 4µM sunitinib reduced H9c2 cell viability by approximately 45% (101). This discrepancy in comparison to our results could be due to the duration of treatment, which could further reduce the cell viability. Thus, we can conclude that the experimental differences, including the cell type, experimental procedure, treatment duration, and treatment concentration could affect the cardiotoxic effects induced by sunitinib and ponatinib.

To accurately determine the cell viability following ponatinib and sunitinib treatment we used flow cytometer assays. Our flow cytometer results showed more than 90% and 35% - 80% reduction in H9c2 cell viability following 24-hours treatment with sunitinib and ponatinib, respectively (Figure 3.3). The discrepancy between our MTT and flow cytometer results may be attributed, in part, to the experimental procedure used. Flow cytometer is an effective, accurate, and reliable method for single-cell analyses. However, MTT assay is a simple and inexpensive method that depends on an enzymatic reaction and may generate a false positive result (189, 199). Therefore, herein, we used MTT assay as a preliminary screening assay whereas we used flow cytometer cell viability assay as a secondary validation of results obtained. Together, these findings confirm that treatment of H9c2 cells with ponatinib and sunitinib treatment reduces cell viability, which may in turn be associated with the cardiotoxic effects.

Mechanism of Cell Death

We further characterized the type of cell death induced by ponatinib and sunitinib. Our study showed that 6 and 24-hours treatment with ponatinib and sunitinib induce apoptotic cell death (Figure 3.4 and 3.13). We also demonstrated that apoptotic cell death at 24-hours treatment occurred via a caspase-3 independent pathway (Figure 3.9). These findings are in alignment with Zhao et al.'s study. They found that 48-hours treatment with increasing concentrations of sunitinib (1.3μM, 2.5μM, 5μM, and 10μM) showed no change in cleaved caspase-3 and cleaved PARP protein expression. Using similar in vitro model, they also found that pretreatment with caspase inhibitor did not attenuate sunitinib-induced cell death. In this study, Zhao et al. demonstrated that sunitinib treatment induces autophagic cell death but not apoptotic cell death (101). In addition, Doherty et al. examined whether 24-hours treatment with 0.3μM – 10μM sunitinib was associated with caspase dependent apoptotic cell death, using caspase3/7 assay. They found that sunitinib-mediated human cardiac myocyte (HCM) cell death was through a caspase-independent pathway (185), which is in agreement with our results. In contrary, it was shown that 24-hours treatment with increasing concentrations of ponatinib (50nM, 100nM, 500nM, and 1000nM) promotes cleaved casapase-3 protein expression in NRVMs (76). This inconsistency in comparison to our results may be due to the cell-model and treatment concentration used. Collectively, our study demonstrated that sunitinib and ponatinib treatment induced caspase-independent apoptotic H9c2 cell death. Further studies using lower treatment concentrations and/or employing a caspase inhibitor are needed to confirm our results. In addition, there is a need to examine the involvement of caspase-independent effect following ponatinib and sunitinib treatment.

4.1.2. Cardiomyoblast Hypertrophy, Cell Morphology, and Cell Size

Our study showed that 24-hours treatment with ponatinib induces significant cardiomyoblast shrinkage and cellular detachment. Whereas, 24-hours treatment with 5µM sunitinib showed a significant increase in cardiomyoblast cell surface area (Figure 3.5 and 3.6). Morphologically, cellular shrinkage is indicative of apoptosis (203, 204), while increased cardiomyoblast cell surface area is indicative of cardiomyocyte hypertrophy (190). In agreement to our findings, a previous study found that ponatinib-treated NRVMs exhibits morphological changes, manifested by reduced myocyte cellular density. Hasinoff et al. found that 72-hours treatment with 2µM ponatinib led to detachment of damaged cardiomyocyte (75). Similarly, treatment with sunitinib induced morphological changes in cardiac cells. It was shown that 48-hours treatment with 3µM sunitinib resulted in hypertrophied HCM cells (185). Cardiomyocyte shrinkage and hypertrophy are known characteristics of ponatinib and sunitinib treatment, respectively. It is therefore important to identify the molecular mechanisms that lead to such phenotypes.

To further validate the effect of ponatinib and sunitinib on cardiomyocyte hypertrophy, we measured the expression of ANP mRNA. Our preliminary findings demonstrated, for the first time, that 6-hours treatment with 5µM ponatinib expresses ANP mRNA (Figure 3.15). In addition, 24-hours treatment with 2.5µM sunitinib slightly expresses ANP mRNA (Figure 3.8). Although these results were not replicated, previous studies showed that treatment with sunitinib results in cardiomyocytes hypertrophy (178, 205). Maayah et al. showed that sunitinib treatment induced cardiac hypertrophy in adult albino rats in vivo model and H9c2 cardiomyoblast in vitro model. Authors found that 12-hours treatment with 5µM sunitinib induced ANP mRNA expression in H9c2 cardiomyoblasts. In addition,

their study showed similar results in rat model (205). Similarly, Korashy et al. found that 12-hours treatment with 2.5μM and 5μM sunitinib-induced BNP, β-myosin heavy chain (β-MHC) mRNA and protein expression in H9c2 cardiomyoblasts (178). Together, it is well established that sunitinib treatment induces cardiomyocyte hypertrophy, while it is not yet validated whether ponatinib induces cardiomyocyte hypertrophy. Thus, further studies are required to confirm ponatinib-induced cardiomyocyte hypertrophy.

Also, we determined H9c2 cell size using forward light scatter by flow cytometer. Flow cytometer is a rapid tool to assess physical changes during apoptotic cell death. A decrease in forward light scatter is indicative of cellular shrinkage, a hallmark of apoptosis (204, 206, 207). We found that 24-hours treatment with ponatinib (2.5μM or 5μM) and sunitinib (5μM) reduced H9c2 cardiomyoblast cell size (Figure 3.7). Whereas no change was observed following 6-hours treatment (Figure 3.14). Overall, our study provides an evidence that ponatinib and sunitinib treatment is associated with cardiotoxic side effects manifested by reduced in cardiomyoblast viability, cell death, morphological changes, and cardiomyoblast hypertrophy.

Sunitinib Versus Ponatinib-Induced Cardiotoxicity

Ponatinib-induced cardiotoxic effects differ from sunitinib's. In terms of cardiomyoblast loss, we found that 24-hours treatment with sunitinib treatment was associated with higher reduction in cardiomyoblast cell viability compared with ponatinib. Treatment with 5μM ponatinib caused 80% reduction in H9c2 cell viability compared to control, while 5μM sunitinib reduced H9c2 cell viability by 97% (Figure 3.3). Treatment with 5μM sunitinib induced 400% apoptotic cell death compared with control, while 5μM ponatinib treatment induced 300% apoptotic cell death (Figure

3.4). In terms of cardiomyoblast size and hypertrophy, we found that 24-hours treatment with 5µM sunitinib induced cardiomyoblast hypertrophy, while 5µM ponatinib treatment was associated with cellular shrinkage and cellular detachment (Figures 3.5, 3.6, and 3.7). At 6-hours treatment, both sunitinib and ponatinib were associated with comparable cardiotoxic effects (cardiomyoblast loss, hypertrophy, and cellular morphology). Therefore, there is a need to identify the molecular mechanisms that are governing ponatinib and sunitinib-induced cardiotoxic effects.

4.2. Role of p90RSK and Autophagy in Ponatinib and Sunitinib-Induced Cardiomyoblast Loss and Hypertrophy

p90RSK

Our study found that 24-hours treatment with ponatinib induces phosphorylation of p90RSK protein expression, whereas treatment with sunitinib reduces p90RSK phosphorylation. This finding is in agreement with previous studies (35, 100, 137, 138). Recently, it was shown that treatment with 150nM ponatinib induced p90RSK phosphorylation in human aortic endothelial cells (137). This agrees with a previous study which examined the biochemical inhibitory activity of 25 kinase inhibitors on 313 protein kinases. Treatment with 1µM ponatinib resulted in a weak inhibition of RSK1, 2, 3, and 4 by 32%, 30%, 62%, and 13%, respectively. Whereas treatment with 1µM sunitinib resulted in potent inhibition of RSK1-4 by 95-97% (138). In addition, a kinase map interaction published by Karaman et al., showed that the K_d for RSK1 following treatment with 10µM sunitinib was 0.14µM, 0.017µM for RSK2, and 0.58µM for RSK3 (35). Furthermore, Hasinoff et al. showed that treatment with 0.36µM Sunitinib results in 50% inhibition of RSK1 in NRVMs (100). Therefore, our findings indicate that ponatinib is an inducer of p90RSK whereas sunitinib is a potent inhibitor. Thus, it is

important to identify the role of p90RSK as a potential mechanism of cardiotoxicity induced by ponatinib or sunitinib.

To determine the role of p90RSK in ponatinib and sunitinib-induced cardiotoxicity, we examined ponatinib and sunitinib-induced cardiotoxic effects following p90RSK inhibition by BID (will be discussed in section 4.3). Our findings showed that treatment with 10µM BID was enough to reduce RSK2 protein expression (Figure 3.16). This is in agreement with a previous study which showed that 10µM BID was able to completely inhibit RSK1-4 isoforms (188).

Autophagy

In addition to p90RSK, we also examined the role of autophagy as another potential mechanism in cardiotoxicity induced by ponatinib and sunitinib. Our findings demonstrated that 24-hours treatment with 2.5µM ponatinib increased LC3-II:LC3-I protein expression, whereas treatment with sunitinib did not induce a significant change (Figure 3.11). In agreement with our results, a previous study detected autophagic effect of 0.0098µM ponatinib using green fluorescent protein-tagged LC3-B assay. Treatment with ponatinib was able to activate autophagy in imatinib-resistant leukemic K562 cells (208). Another study has shown that sunitinib treatment activates autophagy. Zhao et al. demonstrated that 48-hours treatment with increasing concentrations of sunitinib, (1.3µM, 2.5µM, 5µM, and 10µM), increased the expression of autophagy-related proteins (LC3-II and Beclin-1) in H9c2 cardiomyoblasts. In addition, 24-hours treatment with 2.5µM sunitinib induced autophagy, which was manifested by visible acidic vacuoles following acridine orange staining (101); however, authors did not confirm whether treatment with sunitinib modulates the autophagic activity. Since autophagy is highly dynamic activity, an increase in LC3-II expression could be interpreted as both induced

autophagosome formation and/or dysregulated autophagosome degradation. Thus, it is significantly important to estimate the autophagic flux as a method of monitoring autophagy (146-149), which was discussed in an earlier section (1.5.2.1). Our findings demonstrated that treatment with ponatinib for 24 hours might modulate cardiac autophagy. To understand the exact effect of ponatinib and sunitinib on cardiac autophagy, estimating the autophagic flux is required.

Moreover, we examined the autophagic flux, following ponatinib and sunitinib treatment, using an autophagy inhibitor, chloroquine (CQ). CQ acts as an autophagy inhibitor by blocking the final step of autophagy, i.e. autophagosome-lysosome fusion (209). Our study showed that 30-minute pretreatment with 10μM CQ and 6-hours treatment with ponatinib or sunitinib (2.5μM and 5μM) induced a trend towards an increase in autophagic flux (figure 3.18 and 3.19). Our results are consistent with Kimura et al.'s study, which found that 6-hours treatment with 15μM sunitinib in the presence of 10μM CQ induced autophagic flux in H9c2 cardiomyoblasts (175). In comparison to Kimura et al., our study did not show a significant increase in LC3-II protein expression. This inconsistency between the two studies could be due to high concentration of sunitinib used in their study, experimental conditions, and/or statistical measure used. In their study, authors used student-t test for multiple-group comparisons, which might generate false-positive results (197). In this case, ANOVA, followed by suitable post-hoc analysis would be considered an appropriate statistical measure for multiple-group comparisons (197). Overall, these findings show the effect of ponatinib and sunitinib treatment on cardiac autophagy.

4.3. Role of Inhibiting p90RSK and Autophagy in Ponatinib and Sunitinib-Induced Cardiomyoblast Loss and Hypertrophy

4.3.1. Cardiomyoblast Loss

Cell Viability

In the current study, we found that p90RSK activity is essential for H9c2 cardiomyoblast survival. Six-hours treatment with 2.5µM ponatinib in the presence of a p90RSK inhibitor (BID) caused a significant reduction in H9c2 cell viability as compared to treatment with 2.5µM ponatinib alone. This observation was not surprising as RSK regulates different cellular activities, including cell survival and proliferation (104-106, 108). In fact, p90RSK inhibition showed anti-tumor activity. It was shown that BID inhibited triple-negative breast cancer cells proliferation and metastatic activity (210).

Additionally, our study demonstrated that treatment with CQ alone did not reduce H9c2 cell viability, whereas a reduction was observed in combination treatment with sunitinib or ponatinib. This finding was supported by a previous study which found that CQ and sunitinib co-treatment reduces H9c2 cell viability in comparison to sunitinib alone (175). Furthermore, in a previous study, which examined whether CQ is able to modulate sunitinib-mediated cytotoxicity, authors found that CQ synergistically enhanced sunitinib-induced cytotoxicity in several tumor cell lines. In addition, they found that co-treatment with CQ further decreased PCNA (proliferating cell nuclear antigen, a proliferation marker) in murine tumor cell line as compared to sunitinib treatment alone (211).

In contrast, multiple studies have shown that inhibition of autophagy attenuates sunitinib-induced reduction in H9c2 cell viability (101, 175). Zhao et al. demonstrated that Beclin1 knockdown reduced sunitinib-induced H9c2 cell death

(101). In addition, Kimura et al. examined the protective effect of autophagy inhibition on sunitinib-induced cardiotoxicity. Authors showed that silencing ULK1 (an important regulator of autophagy induction) attenuated sunitinib-mediated reduction in H9c2 cell viability (175). Also, they demonstrated that 3-methyladenine (3-MA) effectively attenuated sunitinib-induced cardiotoxicity as compared to bafilomycin A1 and NH_4Cl (175).

These contradicting findings associated with CQ co-treatment may be dependent on autophagy phase being inhibited. Kimura et al. suggested that the protective effect of 3-MA was achieved by inhibiting the early phases of autophagy that involves PI3K (175). On the other hand, CQ inhibits the last phase of autophagy by inhibiting the lysosomal acidification (140). Together, these results suggest that RSK and autophagy inhibition, by BID and CQ, respectively, may promote ponatinib and sunitinib-induced cardiotoxicity via increasing cardiomyoblast death.

Mechanism of Cell Death

In the current study, we demonstrated the effect of p90RSK and autophagy inhibition in ponatinib and sunitinib-induced cardiomyoblast death. We found that RSK inhibition alone, by 10µM BID, or in combination with ponatinib induced necrotic cell death. In contrast, 10µM CQ alone or in combination with ponatinib and sunitinib did not activate necrotic H9c2 cell death (Figure 3.21). Our findings also demonstrated that p90RSK and autophagy inhibition by BID and CQ, respectively may potentiate ponatinib and sunitinib-induced apoptotic cell death (Figure 3.22). Multiple studies reported the anti-tumor effects of BID and CQ (209, 210), which explains their toxic effects. A previous study demonstrated that CQ potentiates the anti-tumor efficacy of sunitinib. It was shown that combining 25µM CQ with 5µM and 10µM sunitinib treatment resulted in improved sunitinib-induced

apoptotic RCC cell death (209). Another study showed that p90RSK inhibition is associated with anti-tumor activity. It was shown that BID inhibited triple-negative breast cancer cells proliferation and metastatic activity (210).

4.3.2. Cardiomyoblast Hypertrophy, Cell Morphology, and Cell Size

Our study suggested that treatment with ponatinib or sunitinib and sunitinib in the presence of 10μM BID may result in a decrease in H9c2 cell size, which is an indicative marker of cell size shrinkage and apoptosis (Figure 3.25).

Whilst many studies have linked active p90RSK to cardiomyocyte hypertrophy (130, 131), our findings showed no effect of p90RSK or autophagy inhibition (by BID or CQ, respectively) on cardiomyocyte hypertrophy following ponatinib or sunitinib treatment. Therefore, further research should be undertaken to confirm the effect of p90RSK inhibition on hypertrophic markers.

CHAPTER 5: CONCLUSION

The current research indicates that the treatment with ponatinib and sunitinib is associated with high cardiotoxic effects manifested by increased in cardiomyoblast loss, morphological changes, and cardiomyocyte hypertrophy. Ponatinib and sunitinib treatment possessed different time and concentration-dependent cardiotoxic effects. Treatment with ponatinib was associated with cardiomyocyte loss, cellular shrinkage, and cell detachment, whereas treatment with sunitinib was associated with cardiomyocyte death and hypertrophy. Our in vitro H9c2 cardiomyoblast model suggested that treatment with ponatinib and sunitinib may induce cardiomyocyte hypertrophy and modulate autophagy. This study also focused on examining p90RSK and autophagy alterations as potential molecular mechanisms of cardiotoxicity. Ponatinib treatment induced p90RSK phosphorylation and autophagy, while sunitinib treatment inhibited p90RSK activity and induced autophagy. Inhibition of p90RSK or autophagy by BID or CQ, respectively may further increase cardiomyoblast loss induced by sunitinib or ponatinib. Additional studies are warranted to validate the role p90RSK and autophagy in cardiomyoblast hypertrophy.

5.1. LIMTATIONS

1. One of the limitations associated with this study was the use of BI-D1870 (BID), which at 10μM is able to potently inhibit RSK1-4 isoforms. Besides RSK inhibition, BID also inhibits other protein kinases, including GSK3, PLK1, and MELK (121, 188, 212). Additionally, non-selective pharmacological RSK inhibition will poorly define the role of individual isoforms in cardiac dysfunction induced by ponatinib and sunitinib. Thus, for further investigations and to confirm our findings, specific p90RSK isoform gene silencing could be considered.
2. In the present research, chloroquine (CQ) was used as an autophagy inhibitor. CQ is an autophagosome-lysosome fusion, inhibitor, it is also known to potentiate the cytotoxic effects of sunitinib in cancer setting (147, 196, 209). In a previous study, it was shown that CQ exacerbated sunitinib-induced cardiomyocyte death as compared to other autophagy inhibitors (175).
3. In addition, the present study did not confirm whether ponatinib and sunitinib induce autophagic flux. Optimizing treatment conditions, including TKIs and pharmacological inhibitor concentration, and treatment time are necessary to understand the role of autophagy in cardiotoxicity mediated by ponatinib and sunitinib.
4. Herein, we examined the caspase-dependent apoptotic cell death pathway. To draw a solid conclusion, further research that examines the total apoptosis following ponatinib or sunitinib treatment in the presence or the absence of a pan-caspase inhibitor (for example z-VAD-fmk) is required (213). In addition, to understand the mechanism of ponatinib and sunitinib-induced cell death, it is significantly important to investigate the role of caspase-independent pathway.

5.2. FUTURE DIRECTIONS

1. An in vivo, animal model could be used to validate the cardiotoxic effects of ponatinib and sunitinib.
2. In line with our results, recently, it was shown that ponatinib phosphorylates p90RSK in human aortic endothelial cells (137). This activation is thought to enhance endothelial cell apoptosis, eNOS reduction, and formation of atherosclerosis lesion (134). Moreover, it was demonstrated that p90RSK inhibition induces anti-atherosclerosis effects (136). Therefore, it would be interesting to investigate whether p90RSK inhibition would attenuate ponatinib-induced vascular adverse events in endothelial setting.
3. Using an early-stage autophagy inhibitor (such as, 3-MA) or introducing autophagy-related gene knockdown might provide a better insight on the role of autophagy in ponatinib and sunitinib-mediated cardiotoxicity.
4. It is warranted to confirm the effect of ponatinib and sunitinib on cardiomyocyte hypertrophic markers (including ANP, BNP, or β-MHC) in the presence or absence of p90RSK and autophagy inhibitors.
5. To determine the effects of clinically relevant concentrations of sunitinib and ponatinib on H9c2 cells, use a wider range of concentrations starting from 50nM – 150nM (clinically relevant concentrations) for longer treatment duration and compare the results with 6 hours and 24 hours data.

REFERENCES

1. Heron M. Deaths: Leading Causes for 2016. National vital statistics reports : from the Centers for Disease Control and Prevention, National Center for Health Statistics, National Vital Statistics System. 2018;67(6):1-77.

2. Curigliano G, Cardinale D, Dent S, Criscitiello C, Aseyev O, Lenihan D, et al. Cardiotoxicity of anticancer treatments: Epidemiology, detection, and management. CA: a cancer journal for clinicians. 2016;66(4):309-25.

3. Sheppard RJ, Berger J, Sebag IA. Cardiotoxicity of cancer therapeutics: current issues in screening, prevention, and therapy. Frontiers in pharmacology. 2013;4:19.

4. Han X, Zhou Y, Liu W. Precision cardio-oncology: understanding the cardiotoxicity of cancer therapy. NPJ precision oncology. 2017;1(1):31.

5. Cardinale D. A new frontier: cardio-oncology. Cardiologia (Rome, Italy). 1996;41(9):887-91.

6. Teske AJ, Linschoten M, Kamphuis JAM, Naaktgeboren WR, Leiner T, van der Wall E, et al. Cardio-oncology: an overview on outpatient management and future developments. Netherlands heart journal : monthly journal of the Netherlands Society of Cardiology and the Netherlands Heart Foundation. 2018;26(11):521-32.

7. Wickramasinghe CD, Nguyen KL, Watson KE, Vorobiof G, Yang EH. Concepts in cardio-oncology: definitions, mechanisms, diagnosis and treatment strategies of cancer therapy-induced cardiotoxicity. Future oncology (London, England). 2016;12(6):855-70.

8. Zamorano JL, Lancellotti P, Rodriguez Muñoz D, Aboyans V, Asteggiano R, Galderisi M, et al. 2016 ESC Position Paper on cancer treatments and cardiovascular toxicity developed under the auspices of the ESC Committee for Practice Guidelines:

The Task Force for cancer treatments and cardiovascular toxicity of the European Society of Cardiology (ESC). European Heart Journal. 2016;37(36):2768-801.

9. Virani SA, Dent S, Brezden-Masley C, Clarke B, Davis MK, Jassal DS, et al. Canadian Cardiovascular Society Guidelines for Evaluation and Management of Cardiovascular Complications of Cancer Therapy. Canadian Journal of Cardiology. 2016;32(7):831-41.

10. Lenneman Carrie G, Sawyer Douglas B. Cardio-Oncology. Circulation Research. 2016;118(6):1008-20.

11. Khouri Michel G, Douglas Pamela S, Mackey John R, Martin M, Scott Jessica M, Scherrer-Crosbie M, et al. Cancer Therapy–Induced Cardiac Toxicity in Early Breast Cancer. Circulation. 2012;126(23):2749-63.

12. Moudgil R, Yeh ET. Mechanisms of Cardiotoxicity of Cancer Chemotherapeutic Agents: Cardiomyopathy and Beyond. The Canadian journal of cardiology. 2016;32(7):863-70.e5.

13. Institute NC. NCI Dictionary of Cancer Terms [Available from: https://www.cancer.gov/publications/dictionaries/cancer-terms/def/cardiotoxicity?redirect=true.

14. Bloom MW, Hamo CE, Cardinale D, Ky B, Nohria A, Baer L, et al. Cancer Therapy-Related Cardiac Dysfunction and Heart Failure: Part 1: Definitions, Pathophysiology, Risk Factors, and Imaging. Circulation Heart failure. 2016;9(1):e002661.

15. Seidman A, Hudis C, Pierri MK, Shak S, Paton V, Ashby M, et al. Cardiac Dysfunction in the Trastuzumab Clinical Trials Experience. Journal of Clinical Oncology. 2002;20(5):1215-21.

16. Plana JC, Galderisi M, Barac A, Ewer MS, Ky B, Scherrer-Crosbie M, et al. Expert Consensus for Multimodality Imaging Evaluation of Adult Patients during and after Cancer Therapy: A Report from the American Society of Echocardiography and the European Association of Cardiovascular Imaging. Journal of the American Society of Echocardiography. 2014;27(9):911-39.

17. Zheng PP, Li J, Kros JM. Breakthroughs in modern cancer therapy and elusive cardiotoxicity: Critical research-practice gaps, challenges, and insights. Medicinal research reviews. 2018;38(1):325-76.

18. Vallakati A, Konda B, Lenihan DJ, Baliga RR. Management of Cancer Therapeutics-Related Cardiac Dysfunction. Heart failure clinics. 2018;14(4):553-67.

19. Finet JE, Tang WHW. Protecting the heart in cancer therapy. F1000Research. 2018;7.

20. Koutsoukis A, Ntalianis A, Repasos E, Kastritis E, Dimopoulos MA, Paraskevaidis I. Cardio-oncology: A Focus on Cardiotoxicity. European cardiology. 2018;13(1):64-9.

21. Ewer MS, Lippman SM. Type II chemotherapy-related cardiac dysfunction: time to recognize a new entity. Journal of clinical oncology : official journal of the American Society of Clinical Oncology. 2005;23(13):2900-2.

22. Friedman MA, Bozdech MJ, Billingham ME, Rider AK. Doxorubicin cardiotoxicity. Serial endomyocardial biopsies and systolic time intervals. Jama. 1978;240(15):1603-6.

23. Mackay B, Ewer MS, Carrasco CH, Benjamin RS. Assessment of anthracycline cardiomyopathy by endomyocardial biopsy. Ultrastructural pathology. 1994;18(1-2):203-11.

24. Raschi E, De Ponti F. Cardiovascular toxicity of anticancer-targeted therapy: emerging issues in the era of cardio-oncology. Internal and emergency medicine. 2012;7(2):113-31.

25. Swain SM, Whaley FS, Ewer MS. Congestive heart failure in patients treated with doxorubicin: a retrospective analysis of three trials. Cancer. 2003;97(11):2869-79.

26. Alvarez JA, Russell RR. Cardio-oncology: the Nuclear Option. Current cardiology reports. 2017;19(4):31.

27. Ewer MS, Vooletich MT, Durand JB, Woods ML, Davis JR, Valero V, et al. Reversibility of trastuzumab-related cardiotoxicity: new insights based on clinical course and response to medical treatment. Journal of clinical oncology : official journal of the American Society of Clinical Oncology. 2005;23(31):7820-6.

28. Herrmann J, Lerman A, Sandhu NP, Villarraga HR, Mulvagh SL, Kohli M. Evaluation and management of patients with heart disease and cancer: cardio-oncology. Mayo Clinic proceedings. 2014;89(9):1287-306.

29. Larsen CM, Mulvagh SL. Cardio-oncology: what you need to know now for clinical practice and echocardiography. Echo research and practice. 2017;4(1):R33-r41.

30. Sheng CC, Amiri-Kordestani L, Palmby T, Force T, Hong CC, Wu JC, et al. 21st Century Cardio-Oncology: Identifying Cardiac Safety Signals in the Era of Personalized Medicine. JACC Basic to translational science. 2016;1(5):386-98.

31. Gorini S, De Angelis A, Berrino L, Malara N, Rosano G, Ferraro E. Chemotherapeutic Drugs and Mitochondrial Dysfunction: Focus on Doxorubicin, Trastuzumab, and Sunitinib. Oxidative medicine and cellular longevity. 2018;2018:7582730.

32. Greineder CF, Kohnstamm S, Ky B. Heart failure associated with sunitinib: lessons learned from animal models. Current hypertension reports. 2011;13(6):436-41.

33. Chen MH, Kerkelä R, Force T. Mechanisms of cardiac dysfunction associated with tyrosine kinase inhibitor cancer therapeutics. Circulation. 2008;118(1):84-95.

34. Mellor HR, Bell AR, Valentin JP, Roberts RR. Cardiotoxicity associated with targeting kinase pathways in cancer. Toxicological sciences : an official journal of the Society of Toxicology. 2011;120(1):14-32.

35. Karaman MW, Herrgard S, Treiber DK, Gallant P, Atteridge CE, Campbell BT, et al. A quantitative analysis of kinase inhibitor selectivity. Nature biotechnology. 2008;26(1):127-32.

36. Shah DR, Shah RR, Morganroth J. Tyrosine kinase inhibitors: their on-target toxicities as potential indicators of efficacy. Drug safety. 2013;36(6):413-26.

37. Gupta R, Maitland ML. Sunitinib, hypertension, and heart failure: a model for kinase inhibitor-mediated cardiotoxicity. Current hypertension reports. 2011;13(6):430-5.

38. Force T, Krause DS, Van Etten RA. Molecular mechanisms of cardiotoxicity of tyrosine kinase inhibition. Nature reviews Cancer. 2007;7(5):332-44.

39. Muller MC, Cervantes F, Hjorth-Hansen H, Janssen J, Milojkovic D, Rea D, et al. Ponatinib in chronic myeloid leukemia (CML): Consensus on patient treatment and management from a European expert panel. Critical reviews in oncology/hematology. 2017;120:52-9.

40. Motzer RJ, Escudier B, Gannon A, Figlin RA. Sunitinib: Ten Years of Successful Clinical Use and Study in Advanced Renal Cell Carcinoma. The oncologist. 2017;22(1):41-52.

41. Jabbour E, Kantarjian H. Chronic myeloid leukemia: 2018 update on diagnosis, therapy and monitoring. American journal of hematology. 2018;93(3):442-59.

42. Jain P, Kantarjian H, Cortes J. Chronic myeloid leukemia: overview of new agents and comparative analysis. Current treatment options in oncology. 2013;14(2):127-43.

43. Fitzmaurice C, Dicker D, Pain A, Hamavid H, Moradi-Lakeh M, MacIntyre MF, et al. The Global Burden of Cancer 2013. JAMA oncology. 2015;1(4):505-27.

44. Radich J. Structure, function, and resistance in chronic myeloid leukemia. Cancer cell. 2014;26(3):305-6.

45. Hehlmann R, Hochhaus A, Baccarani M. Chronic myeloid leukaemia. Lancet (London, England). 2007;370(9584):342-50.

46. Maru Y. Molecular biology of chronic myeloid leukemia. Cancer science. 2012;103(9):1601-10.

47. Apperley JF. Chronic myeloid leukaemia. Lancet (London, England). 2015;385(9976):1447-59.

48. Jabbour E, Cortes JE, Kantarjian HM. Molecular monitoring in chronic myeloid leukemia: response to tyrosine kinase inhibitors and prognostic implications. Cancer. 2008;112(10):2112-8.

49. Chen Y, Peng C, Li D, Li S. Molecular and cellular bases of chronic myeloid leukemia. Protein & cell. 2010;1(2):124-32.

50. Skorski T, Bellacosa A, Nieborowska-Skorska M, Majewski M, Martinez R, Choi JK, et al. Transformation of hematopoietic cells by BCR/ABL requires activation of a PI-3k/Akt-dependent pathway. The EMBO Journal. 1997;16(20):6151.

51. Carlesso N, Frank DA, Griffin JD. Tyrosyl phosphorylation and DNA binding activity of signal transducers and activators of transcription (STAT) proteins in hematopoietic cell lines transformed by Bcr/Abl. The Journal of Experimental Medicine. 1996;183(3):811.

52. Mandanas RA, Leibowitz DS, Gharehbaghi K, Tauchi T, Burgess GS, Miyazawa K, et al. Role of p21 RAS in p210 bcr-abl transformation of murine myeloid cells. Blood. 1993;82(6):1838-47.

53. Dao K-HT, Tyner JW. Next-Generation Medicine: Combining BCR-ABL and Hedgehog-Targeted Therapies. Clinical Cancer Research. 2013;19(6):1309.

54. Pophali PA, Patnaik MM. The Role of New Tyrosine Kinase Inhibitors in Chronic Myeloid Leukemia. Cancer journal (Sudbury, Mass). 2016;22(1):40-50.

55. O'Brien SG, Guilhot F, Larson RA, Gathmann I, Baccarani M, Cervantes F, et al. Imatinib compared with interferon and low-dose cytarabine for newly diagnosed chronic-phase chronic myeloid leukemia. The New England journal of medicine. 2003;348(11):994-1004.

56. Saussele S, Pfirrmann M. Clinical trials in chronic myeloid leukemia. Current hematologic malignancy reports. 2012;7(2):109-15.

57. Jabbour E, Kantarjian H, Cortes J. Use of second- and third-generation tyrosine kinase inhibitors in the treatment of chronic myeloid leukemia: an evolving treatment paradigm. Clinical lymphoma, myeloma & leukemia. 2015;15(6):323-34.

58. Rossari F, Minutolo F, Orciuolo E. Past, present, and future of Bcr-Abl inhibitors: from chemical development to clinical efficacy. Journal of hematology & oncology. 2018;11(1):84.

59. Tan FH, Putoczki TL, Stylli SS, Luwor RB. Ponatinib: a novel multi-tyrosine kinase inhibitor against human malignancies. OncoTargets and therapy. 2019;12:635-45.

60. Musumeci F, Greco C, Grossi G, Molinari A, Schenone S. Recent Studies on Ponatinib in Cancers Other Than Chronic Myeloid Leukemia. Cancers (Basel). 2018;10(11).

61. Moslehi JJ, Deininger M. Tyrosine Kinase Inhibitor-Associated Cardiovascular Toxicity in Chronic Myeloid Leukemia. Journal of clinical oncology : official journal of the American Society of Clinical Oncology. 2015;33(35):4210-8.

62. Huang WS, Metcalf CA, Sundaramoorthi R, Wang Y, Zou D, Thomas RM, et al. Discovery of 3-[2-(imidazo[1,2-b]pyridazin-3-yl)ethynyl]-4-methyl-N-{4-[(4-methylpiperazin-1-y l)methyl]-3-(trifluoromethyl)phenyl}benzamide (AP24534), a potent, orally active pan-inhibitor of breakpoint cluster region-abelson (BCR-ABL) kinase including the T315I gatekeeper mutant. Journal of medicinal chemistry. 2010;53(12):4701-19.

63. Cortes JE, Kim DW, Pinilla-Ibarz J, le Coutre P, Paquette R, Chuah C, et al. A phase 2 trial of ponatinib in Philadelphia chromosome-positive leukemias. The New England journal of medicine. 2013;369(19):1783-96.

64. Sanford D, Kantarjian H, Skinner J, Jabbour E, Cortes J. Phase II trial of ponatinib in patients with chronic myeloid leukemia resistant to one previous tyrosine kinase inhibitor. Haematologica. 2015;100(12):e494-e5.

65. Cortes JE, Kim D-W, Pinilla-Ibarz J, Le Coutre P, Paquette R, Chuah C, et al. Long-Term Follow-up of Ponatinib Efficacy and Safety in the Phase 2 PACE Trial. Blood. 2014;124(21):3135.

66. Damrongwatanasuk R, Fradley MG. Cardiovascular Complications of Targeted Therapies for Chronic Myeloid Leukemia. Current treatment options in cardiovascular medicine. 2017;19(4):24.

67. Hoeper MM, Barst RJ, Bourge RC, Feldman J, Frost AE, Galie N, et al. Imatinib mesylate as add-on therapy for pulmonary arterial hypertension: results of the randomized IMPRES study. Circulation. 2013;127(10):1128-38.

68. Shah AM, Campbell P, Rocha GQ, Peacock A, Barst RJ, Quinn D, et al. Effect of imatinib as add-on therapy on echocardiographic measures of right ventricular function in patients with significant pulmonary arterial hypertension. Eur Heart J. 2015;36(10):623-32.

69. Giles FJ, Mauro MJ, Hong F, Ortmann CE, McNeill C, Woodman RC, et al. Rates of peripheral arterial occlusive disease in patients with chronic myeloid leukemia in the chronic phase treated with imatinib, nilotinib, or non-tyrosine kinase therapy: a retrospective cohort analysis. Leukemia. 2013;27(6):1310-5.

70. Tajiri K, Aonuma K, Sekine I. Cardiovascular toxic effects of targeted cancer therapy. Japanese journal of clinical oncology. 2017;47(9):779-85.

71. Zhu X, Stergiopoulos K, Wu S. Risk of hypertension and renal dysfunction with an angiogenesis inhibitor sunitinib: Systematic review and meta-analysis. Acta Oncologica. 2009;48(1):9-17.

72. Agarwal M, Thareja N, Benjamin M, Akhondi A, Mitchell GD. Tyrosine Kinase Inhibitor-Induced Hypertension. Current oncology reports. 2018;20(8):65.

73. Sharma A, Burridge PW, McKeithan WL, Serrano R, Shukla P, Sayed N, et al. High-throughput screening of tyrosine kinase inhibitor cardiotoxicity with human induced pluripotent stem cells. Science translational medicine. 2017;9(377).

74. Talbert DR, Doherty KR, Trusk PB, Moran DM, Shell SA, Bacus S. A multi-parameter in vitro screen in human stem cell-derived cardiomyocytes identifies ponatinib-induced structural and functional cardiac toxicity. Toxicological sciences : an official journal of the Society of Toxicology. 2015;143(1):147-55.

75. Hasinoff BB, Patel D, Wu X. The Myocyte-Damaging Effects of the BCR-ABL1-Targeted Tyrosine Kinase Inhibitors Increase with Potency and Decrease with Specificity. Cardiovascular toxicology. 2017;17(3):297-306.

76. Singh AP, Glennon MS, Umbarkar P, Gupte M, Galindo CL, Zhang Q, et al. Ponatinib-induced cardiotoxicity: delineating the signalling mechanisms and potential rescue strategies. 2019.

77. Network CGAR. Comprehensive molecular characterization of clear cell renal cell carcinoma. Nature. 2013;499(7456):43-9.

78. Choueiri TK, Motzer RJ. Systemic Therapy for Metastatic Renal-Cell Carcinoma. New England Journal of Medicine. 2017;376(4):354-66.

79. Miller KD, Siegel RL, Lin CC, Mariotto AB, Kramer JL, Rowland JH, et al. Cancer treatment and survivorship statistics, 2016. CA: a cancer journal for clinicians. 2016;66(4):271-89.

80. Siegel RL, Miller KD, Jemal A. Cancer statistics, 2016. CA: a cancer journal for clinicians. 2016;66(1):7-30.

81. Ridge CA, Pua BB, Madoff DC. Epidemiology and staging of renal cell carcinoma. Seminars in interventional radiology. 2014;31(1):3-8.

82. Inamura K. Renal Cell Tumors: Understanding Their Molecular Pathological Epidemiology and the 2016 WHO Classification. International journal of molecular sciences. 2017;18(10).

83. Hancock SB, Georgiades CS. Kidney Cancer. Cancer journal (Sudbury, Mass). 2016;22(6):387-92.

84. Shingarev R, Jaimes EA. Renal cell carcinoma: new insights and challenges for a clinician scientist. American journal of physiology Renal physiology. 2017;313(2):F145-f54.

85. Schwandt A, Wood LS, Rini B, Dreicer R. Management of side effects associated with sunitinib therapy for patients with renal cell carcinoma. OncoTargets and therapy. 2009;2:51-61.

86. Graves A, Hessamodini H, Wong G, Lim WH. Metastatic renal cell carcinoma: update on epidemiology, genetics, and therapeutic modalities. ImmunoTargets and therapy. 2013;2:73-90.

87. Hurtado-de-Mendoza D, Loaiza-Bonilla A, Bonilla-Reyes PA, Tinoco G, Alcorta R. Cardio-Oncology: Cancer Therapy-related Cardiovascular Complications in a Molecular Targeted Era: New Concepts and Perspectives. Cureus. 2017;9(5):e1258.

88. Aparicio-Gallego G, Blanco M, Figueroa A, García-Campelo R, Valladares-Ayerbes M, Grande-Pulido E, et al. New Insights into Molecular Mechanisms of Sunitinib-Associated Side Effects. Molecular Cancer Therapeutics. 2011;10(12):2215.

89. Faivre S, Demetri G, Sargent W, Raymond E. Molecular basis for sunitinib efficacy and future clinical development. Nature reviews Drug discovery. 2007;6(9):734-45.

90. Motzer RJ, Hutson TE, Tomczak P, Michaelson MD, Bukowski RM, Rixe O, et al. Sunitinib versus Interferon Alfa in Metastatic Renal-Cell Carcinoma. New England Journal of Medicine. 2007;356(2):115-24.

91. Sayed-Ahmed MM, Alrufaiq BI, Alrikabi A, Abdullah ML, Hafez MM, Al-Shabanah OA. Carnitine Supplementation Attenuates Sunitinib-Induced Inhibition of AMP-Activated Protein Kinase Downstream Signals in Cardiac Tissues. Cardiovascular toxicology. 2019.

92. Hao Z, Sadek I. Sunitinib: the antiangiogenic effects and beyond. OncoTargets and therapy. 2016;9:5495-505.

93. Khakoo AY, Kassiotis CM, Tannir N, Plana JC, Halushka M, Bickford C, et al. Heart failure associated with sunitinib malate. Cancer. 2008;112(11):2500-8.

94. Chu TF, Rupnick MA, Kerkela R, Dallabrida SM, Zurakowski D, Nguyen L, et al. Cardiotoxicity associated with tyrosine kinase inhibitor sunitinib. Lancet (London, England). 2007;370(9604):2011-9.

95. Rock EP, Goodman V, Jiang JX, Mahjoob K, Verbois SL, Morse D, et al. Food and Drug Administration drug approval summary: Sunitinib malate for the treatment of gastrointestinal stromal tumor and advanced renal cell carcinoma. The oncologist. 2007;12(1):107-13.

96. Motzer RJ, Rini BI, Bukowski RM, Curti BD, George DJ, Hudes GR, et al. Sunitinib in patients with metastatic renal cell carcinoma. Jama. 2006;295(21):2516-24.

97. Chintalgattu V, Ai D, Langley RR, Zhang J, Bankson JA, Shih TL, et al. Cardiomyocyte PDGFR-β signaling is an essential component of the mouse cardiac response to load-induced stress. The Journal of clinical investigation. 2010;120(2):472-84.

98. Robinson ES, Khankin EV, Choueiri TK, Dhawan MS, Rogers MJ, Karumanchi SA, et al. Suppression of the nitric oxide pathway in metastatic renal cell

carcinoma patients receiving vascular endothelial growth factor-signaling inhibitors. Hypertension (Dallas, Tex : 1979). 2010;56(6):1131-6.

99. Kerkela R, Woulfe KC, Durand JB, Vagnozzi R, Kramer D, Chu TF, et al. Sunitinib-induced cardiotoxicity is mediated by off-target inhibition of AMP-activated protein kinase. Clinical and translational science. 2009;2(1):15-25.

100. Hasinoff BB, Patel D, O'Hara KA. Mechanisms of myocyte cytotoxicity induced by the multiple receptor tyrosine kinase inhibitor sunitinib. Molecular pharmacology. 2008;74(6):1722-8.

101. Zhao Y, Xue T, Yang X, Zhu H, Ding X, Lou L, et al. Autophagy plays an important role in sunitinib-mediated cell death in H9c2 cardiac muscle cells. Toxicology and applied pharmacology. 2010;248(1):20-7.

102. Anjum R, Blenis J. The RSK family of kinases: emerging roles in cellular signalling. Nature reviews Molecular cell biology. 2008;9(10):747-58.

103. Carriere A, Ray H, Blenis J, Roux PP. The RSK factors of activating the Ras/MAPK signaling cascade. Frontiers in bioscience : a journal and virtual library. 2008;13:4258-75.

104. Romeo Y, Zhang X, Roux PP. Regulation and function of the RSK family of protein kinases. The Biochemical journal. 2012;441(2):553-69.

105. Casalvieri KA, Matheson CJ, Backos DS, Reigan P. Selective Targeting of RSK Isoforms in Cancer. Trends in cancer. 2017;3(4):302-12.

106. Romeo Y, Roux PP. Paving the way for targeting RSK in cancer. Expert Opinion on Therapeutic Targets. 2011;15(1):5-9.

107. Poomakkoth N, Issa A, Abdulrahman N, Abdelaziz SG, Mraiche F. p90 ribosomal S6 kinase: a potential therapeutic target in lung cancer. Journal of translational medicine. 2016;14:14.

108. Houles T, Roux PP. Defining the role of the RSK isoforms in cancer. Seminars in cancer biology. 2018;48:53-61.

109. Roux PP, Blenis J. ERK and p38 MAPK-activated protein kinases: a family of protein kinases with diverse biological functions. Microbiology and molecular biology reviews : MMBR. 2004;68(2):320-44.

110. Roux PP, Ballif BA, Anjum R, Gygi SP, Blenis J. Tumor-promoting phorbol esters and activated Ras inactivate the tuberous sclerosis tumor suppressor complex via p90 ribosomal S6 kinase. Proc Natl Acad Sci U S A. 2004;101(37):13489-94.

111. Carriere A, Cargnello M, Julien LA, Gao H, Bonneil E, Thibault P, et al. Oncogenic MAPK signaling stimulates mTORC1 activity by promoting RSK-mediated raptor phosphorylation. Current biology : CB. 2008;18(17):1269-77.

112. Diehl JA, Cheng M, Roussel MF, Sherr CJ. Glycogen synthase kinase-3β regulates cyclin D1 proteolysis and subcellular localization. Genes & Development. 1998;12(22):3499-511.

113. Sears R, Nuckolls F, Haura E, Taya Y, Tamai K, Nevins JR. Multiple Ras-dependent phosphorylation pathways regulate Myc protein stability. Genes & Development. 2000;14(19):2501-14.

114. Shahbazian D, Roux PP, Mieulet V, Cohen MS, Raught B, Taunton J, et al. The mTOR/PI3K and MAPK pathways converge on eIF4B to control its phosphorylation and activity. The EMBO Journal. 2006;25(12):2781.

115. Anjum R, Roux PP, Ballif BA, Gygi SP, Blenis J. The tumor suppressor DAP kinase is a target of RSK-mediated survival signaling. Current biology : CB. 2005;15(19):1762-7.

116. Bonni A, Brunet A, West AE, Datta SR, Takasu MA, Greenberg ME. Cell Survival Promoted by the Ras-MAPK Signaling Pathway by Transcription-Dependent and -Independent Mechanisms. Science (New York, NY). 1999;286(5443):1358.

117. Fujita N, Sato S, Tsuruo T. Phosphorylation of p27Kip1 at threonine 198 by p90 ribosomal protein S6 kinases promotes its binding to 14-3-3 and cytoplasmic localization. The Journal of biological chemistry. 2003;278(49):49254-60.

118. David J-P, Mehic D, Bakiri L, Schilling AF, Mandic V, Priemel M, et al. Essential role of RSK2 in c-Fos–dependent osteosarcoma development. The Journal of clinical investigation. 2005;115(3):664-72.

119. Lawrence MC, Jivan A, Shao C, Duan L, Goad D, Zaganjor E, et al. The roles of MAPKs in disease. Cell Research. 2008;18:436.

120. Dehan E, Bassermann F, Guardavaccaro D, Vasiliver-Shamis G, Cohen M, Lowes KN, et al. betaTrCP- and Rsk1/2-mediated degradation of BimEL inhibits apoptosis. Mol Cell. 2009;33(1):109-16.

121. Lara R, Seckl MJ, Pardo OE. The p90 RSK family members: common functions and isoform specificity. Cancer research. 2013;73(17):5301-8.

122. Tanimura S, Hashizume J, Kurosaki Y, Sei K, Gotoh A, Ohtake R, et al. SH3P2 is a negative regulator of cell motility whose function is inhibited by ribosomal S6 kinase-mediated phosphorylation. Genes to Cells. 2011;16(5):514-26.

123. Doehn U, Hauge C, Frank SR, Jensen CJ, Duda K, Nielsen JV, et al. RSK Is a Principal Effector of the RAS-ERK Pathway for Eliciting a Coordinate Promotile/Invasive Gene Program and Phenotype in Epithelial Cells. Molecular Cell. 2009;35(4):511-22.

124. Sulzmaier FJ, Ramos JW. RSK isoforms in cancer cell invasion and metastasis. Cancer research. 2013;73(20):6099-105.

125. Woo MS, Ohta Y, Rabinovitz I, Stossel TP, Blenis J. Ribosomal S6 Kinase (RSK) Regulates Phosphorylation of Filamin A on an Important Regulatory Site. Molecular and Cellular Biology. 2004;24(7):3025.

126. Gawecka JE, Young-Robbins SS, Sulzmaier FJ, Caliva MJ, Heikkilä MM, Matter ML, et al. RSK2 Protein Suppresses Integrin Activation and Fibronectin Matrix Assembly and Promotes Cell Migration. Journal of Biological Chemistry. 2012;287(52):43424-37.

127. Sadoshima J, Qiu Z, Morgan JP, Izumo S. Angiotensin II and other hypertrophic stimuli mediated by G protein-coupled receptors activate tyrosine kinase, mitogen-activated protein kinase, and 90-kD S6 kinase in cardiac myocytes. The critical role of Ca(2+)-dependent signaling. Circ Res. 1995;76(1):1-15.

128. Takeishi Y, Huang Q, Abe J-i, Che W, Lee J-D, Kawakatsu H, et al. Activation of mitogen-activated protein kinases and p90 ribosomal S6 kinase in failing human hearts with dilated cardiomyopathy. Cardiovascular research. 2002;53(1):131-7.

129. Takeishi Y, Abe J, Lee JD, Kawakatsu H, Walsh RA, Berk BC. Differential regulation of p90 ribosomal S6 kinase and big mitogen-activated protein kinase 1 by ischemia/reperfusion and oxidative stress in perfused guinea pig hearts. Circ Res. 1999;85(12):1164-72.

130. Jaballah M, Mohamed IA, Alemrayat B, Al-Sulaiti F, Mlih M, Mraiche F. Na+/H+ Exchanger Isoform 1 Induced Cardiomyocyte Hypertrophy Involves Activation of p90 Ribosomal S6 Kinase. PloS one. 2015;10(4):e0122230.

131. Yamaguchi N, Chakraborty A, Pasek DA, Molkentin JD, Meissner G. Dysfunctional ryanodine receptor and cardiac hypertrophy: role of signaling

molecules. American journal of physiology Heart and circulatory physiology. 2011;300(6):H2187-95.

132. He Q, Harding P, LaPointe MC. PKA, Rap1, ERK1/2, and p90RSK mediate PGE2 and EP4 signaling in neonatal ventricular myocytes. American journal of physiology Heart and circulatory physiology. 2010;298(1):H136-43.

133. Lu Z, Abe J-i, Taunton J, Lu Y, Shishido T, McClain C, et al. Reactive Oxygen Species-Induced Activation of p90 Ribosomal S6 Kinase Prolongs Cardiac Repolarization Through Inhibiting Outward K+ Channel Activity. Circulation Research. 2008;103(3):269-78.

134. Abe J-I, Sandhu UG, Hoang NM, Thangam M, Quintana-Quezada RA, Fujiwara K, et al. Coordination of Cellular Localization-Dependent Effects of Sumoylation in Regulating Cardiovascular and Neurological Diseases. Advances in experimental medicine and biology. 2017;963:337-58.

135. Lin L, White AS, Hu K. Role of p90RSK in Kidney and Other Diseases. International journal of molecular sciences. 2019;20(4).

136. Le NT, Sandhu UG, Quintana-Quezada RA, Hoang NM, Fujiwara K, Abe JI. Flow signaling and atherosclerosis. Cellular and molecular life sciences : CMLS. 2017;74(10):1835-58.

137. Paez-Mayorga J, Chen AL, Kotla S, Tao Y, Abe RJ, He ED, et al. Ponatinib Activates an Inflammatory Response in Endothelial Cells via ERK5 SUMOylation. Frontiers in Cardiovascular Medicine. 2018;5(125).

138. Uitdehaag JC, de Roos JA, van Doornmalen AM, Prinsen MB, de Man J, Tanizawa Y, et al. Comparison of the cancer gene targeting and biochemical selectivities of all targeted kinase inhibitors approved for clinical use. PloS one. 2014;9(3):e92146.

139. Orsini M, Morceau F, Dicato M, Diederich M. Autophagy as a pharmacological target in hematopoiesis and hematological disorders. Biochemical pharmacology. 2018;152:347-61.

140. Bincoletto C, Bechara A, Pereira GJ, Santos CP, Antunes F, Peixoto da-Silva J, et al. Interplay between apoptosis and autophagy, a challenging puzzle: new perspectives on antitumor chemotherapies. Chemico-biological interactions. 2013;206(2):279-88.

141. Baquero P, Dawson A, Helgason GV. Autophagy and mitochondrial metabolism: insights into their role and therapeutic potential in chronic myeloid leukaemia. The FEBS journal. 2018.

142. Roy S, Debnath J. Autophagy and tumorigenesis. Seminars in immunopathology. 2010;32(4):383-96.

143. Zhu H, Tannous P, Johnstone JL, Kong Y, Shelton JM, Richardson JA, et al. Cardiac autophagy is a maladaptive response to hemodynamic stress. The Journal of clinical investigation. 2007;117(7):1782-93.

144. Feng Y, He D, Yao Z, Klionsky DJ. The machinery of macroautophagy. Cell Res. 2014;24(1):24-41.

145. Mizushima N, Klionsky DJ. Protein Turnover Via Autophagy: Implications for Metabolism. Annual Review of Nutrition. 2007;27(1):19-40.

146. Li DL, Hill JA. Cardiomyocyte autophagy and cancer chemotherapy. Journal of molecular and cellular cardiology. 2014;71:54-61.

147. Mizushima N, Yoshimori T, Levine B. Methods in Mammalian Autophagy Research. Cell. 2010;140(3):313-26.

148. Yoshii SR, Mizushima N. Monitoring and Measuring Autophagy. International journal of molecular sciences. 2017;18(9):1865.

149. Bellodi C, Lidonnici MR, Hamilton A, Helgason GV, Soliera AR, Ronchetti M, et al. Targeting autophagy potentiates tyrosine kinase inhibitor-induced cell death in Philadelphia chromosome-positive cells, including primary CML stem cells. The Journal of clinical investigation. 2009;119(5):1109-23.

150. Bjorkoy G, Lamark T, Pankiv S, Overvatn A, Brech A, Johansen T. Monitoring autophagic degradation of p62/SQSTM1. Methods in enzymology. 2009;452:181-97.

151. Mizushima N. Autophagy: process and function. Genes Dev. 2007;21(22):2861-73.

152. Levine B, Kroemer G. Autophagy in the pathogenesis of disease. Cell. 2008;132(1):27-42.

153. Rabinowitz JD, White E. Autophagy and metabolism. Science (New York, NY). 2010;330(6009):1344-8.

154. Ravanan P, Srikumar IF, Talwar P. Autophagy: The spotlight for cellular stress responses. Life sciences. 2017;188:53-67.

155. Boya P, González-Polo R-A, Casares N, Perfettini J-L, Dessen P, Larochette N, et al. Inhibition of Macroautophagy Triggers Apoptosis. Molecular and Cellular Biology. 2005;25(3):1025.

156. Glick D, Barth S, Macleod KF. Autophagy: cellular and molecular mechanisms. The Journal of pathology. 2010;221(1):3-12.

157. Liu EY, Ryan KM. Autophagy and cancer--issues we need to digest. Journal of cell science. 2012;125(Pt 10):2349-58.

158. Crighton D, Wilkinson S, O'Prey J, Syed N, Smith P, Harrison PR, et al. DRAM, a p53-induced modulator of autophagy, is critical for apoptosis. Cell. 2006;126(1):121-34.

159. Kimmelman AC, White E. Autophagy and Tumor Metabolism. Cell metabolism. 2017;25(5):1037-43.

160. Singh SS, Vats S, Chia AY, Tan TZ, Deng S, Ong MS, et al. Dual role of autophagy in hallmarks of cancer. Oncogene. 2018;37(9):1142-58.

161. Liang XH, Jackson S, Seaman M, Brown K, Kempkes B, Hibshoosh H, et al. Induction of autophagy and inhibition of tumorigenesis by beclin 1. Nature. 1999;402(6762):672-6.

162. Errafiy R, Aguado C, Ghislat G, Esteve JM, Gil A, Loutfi M, et al. PTEN increases autophagy and inhibits the ubiquitin-proteasome pathway in glioma cells independently of its lipid phosphatase activity. PloS one. 2013;8(12):e83318.

163. Arico S, Petiot A, Bauvy C, Dubbelhuis PF, Meijer AJ, Codogno P, et al. The tumor suppressor PTEN positively regulates macroautophagy by inhibiting the phosphatidylinositol 3-kinase/protein kinase B pathway. The Journal of biological chemistry. 2001;276(38):35243-6.

164. Bellot G, Garcia-Medina R, Gounon P, Chiche J, Roux D, Pouyssegur J, et al. Hypoxia-induced autophagy is mediated through hypoxia-inducible factor induction of BNIP3 and BNIP3L via their BH3 domains. Mol Cell Biol. 2009;29(10):2570-81.

165. Nakai A, Yamaguchi O, Takeda T, Higuchi Y, Hikoso S, Taniike M, et al. The role of autophagy in cardiomyocytes in the basal state and in response to hemodynamic stress. Nature medicine. 2007;13(5):619-24.

166. Matsui Y, Takagi H, Qu X, Abdellatif M, Sakoda H, Asano T, et al. Distinct roles of autophagy in the heart during ischemia and reperfusion: roles of AMP-activated protein kinase and Beclin 1 in mediating autophagy. Circ Res. 2007;100(6):914-22.

167. Yan L, Vatner DE, Kim SJ, Ge H, Masurekar M, Massover WH, et al. Autophagy in chronically ischemic myocardium. Proc Natl Acad Sci U S A. 2005;102(39):13807-12.

168. Yamaguchi O. Autophagy in the Heart. Circulation journal : official journal of the Japanese Circulation Society. 2019.

169. Ma X, Liu H, Foyil SR, Godar RJ, Weinheimer CJ, Hill JA, et al. Impaired autophagosome clearance contributes to cardiomyocyte death in ischemia/reperfusion injury. Circulation. 2012;125(25):3170-81.

170. Porrello ER, D'Amore A, Curl CL, Allen AM, Harrap SB, Thomas WG, et al. Angiotensin II type 2 receptor antagonizes angiotensin II type 1 receptor-mediated cardiomyocyte autophagy. Hypertension (Dallas, Tex : 1979). 2009;53(6):1032-40.

171. Taneike M, Yamaguchi O, Nakai A, Hikoso S, Takeda T, Mizote I, et al. Inhibition of autophagy in the heart induces age-related cardiomyopathy. Autophagy. 2010;6(5):600-6.

172. Nishino I, Fu J, Tanji K, Yamada T, Shimojo S, Koori T, et al. Primary LAMP-2 deficiency causes X-linked vacuolar cardiomyopathy and myopathy (Danon disease). Nature. 2000;406:906.

173. Ertmer A, Huber V, Gilch S, Yoshimori T, Erfle V, Duyster J, et al. The anticancer drug imatinib induces cellular autophagy. Leukemia. 2007;21:936.

174. Hu W, Lu S, McAlpine I, Jamieson JD, Lee DU, D. Marroquin L, et al. Mechanistic Investigation of Imatinib-Induced Cardiac Toxicity and the Involvement of c-Abl Kinase. Toxicological Sciences. 2012;129(1):188-99.

175. Kimura T, Uesugi M, Takase K, Miyamoto N, Sawada K. Hsp90 inhibitor geldanamycin attenuates the cytotoxicity of sunitinib in cardiomyocytes via inhibition of the autophagy pathway. Toxicology and applied pharmacology. 2017;329:282-92.

176. Hescheler J, Meyer R, Plant S, Krautwurst D, Rosenthal W, Schultz G. Morphological, biochemical, and electrophysiological characterization of a clonal cell (H9c2) line from rat heart. Circulation Research. 1991;69(6):1476-86.

177. Branco AF, Pereira SP, Gonzalez S, Gusev O, Rizvanov AA, Oliveira PJ. Gene Expression Profiling of H9c2 Myoblast Differentiation towards a Cardiac-Like Phenotype. PloS one. 2015;10(6):e0129303.

178. Korashy HM, Al-Suwayeh HA, Maayah ZH, Ansari MA, Ahmad SF, Bakheet SA. Mitogen-activated protein kinases pathways mediate the sunitinib-induced hypertrophy in rat cardiomyocyte H9c2 cells. Cardiovascular toxicology. 2015;15(1):41-51.

179. Will Y, Dykens JA, Nadanaciva S, Hirakawa B, Jamieson J, Marroquin LD, et al. Effect of the multitargeted tyrosine kinase inhibitors imatinib, dasatinib, sunitinib, and sorafenib on mitochondrial function in isolated rat heart mitochondria and H9c2 cells. Toxicological sciences : an official journal of the Society of Toxicology. 2008;106(1):153-61.

180. L'Ecuyer T, Horenstein MS, Thomas R, Vander Heide R. Anthracycline-induced cardiac injury using a cardiac cell line: potential for gene therapy studies. Molecular genetics and metabolism. 2001;74(3):370-9.

181. Sardao VA, Oliveira PJ, Holy J, Oliveira CR, Wallace KB. Morphological alterations induced by doxorubicin on H9c2 myoblasts: nuclear, mitochondrial, and cytoskeletal targets. Cell biology and toxicology. 2009;25(3):227-43.

182. Cui G, Chen H, Cui W, Guo X, Fang J, Liu A, et al. FGF2 Prevents Sunitinib-Induced Cardiotoxicity in Zebrafish and Cardiomyoblast H9c2 Cells. Cardiovascular toxicology. 2016;16(1):46-53.

183. Ye YE, Woodward CN, Narasimhan NI. Absorption, metabolism, and excretion of [(14)C]ponatinib after a single oral dose in humans. Cancer chemotherapy and pharmacology. 2017;79(3):507-18.

184. Zhang J, Salminen A, Yang X, Luo Y, Wu Q, White M, et al. Effects of 31 FDA approved small-molecule kinase inhibitors on isolated rat liver mitochondria. Archives of toxicology. 2017;91(8):2921-38.

185. Doherty KR, Wappel RL, Talbert DR, Trusk PB, Moran DM, Kramer JW, et al. Multi-parameter in vitro toxicity testing of crizotinib, sunitinib, erlotinib, and nilotinib in human cardiomyocytes. Toxicology and applied pharmacology. 2013;272(1):245-55.

186. French KJ, Coatney RW, Renninger JP, Hu CX, Gales TL, Zhao S, et al. Differences in Effects on Myocardium and Mitochondria by Angiogenic Inhibitors Suggest Separate Mechanisms of Cardiotoxicity. Toxicologic Pathology. 2010;38(5):691-702.

187. Mohamed IA, Gadeau AP, Fliegel L, Lopaschuk G, Mlih M, Abdulrahman N, et al. Na+/H+ exchanger isoform 1-induced osteopontin expression facilitates cardiomyocyte hypertrophy. PloS one. 2015;10(4):e0123318.

188. Sapkota GP, Cummings L, Newell FS, Armstrong C, Bain J, Frodin M, et al. BI-D1870 is a specific inhibitor of the p90 RSK (ribosomal S6 kinase) isoforms in vitro and in vivo. The Biochemical journal. 2007;401(1):29-38.

189. Wang X, Xia Y, Liu L, Liu M, Gu N, Guang H, et al. Comparison of MTT assay, flow cytometry, and RT-PCR in the evaluation of cytotoxicity of five prosthodontic materials. Journal of biomedical materials research Part B, Applied biomaterials. 2010;95(2):357-64.

190. Chen L, Zhao L, Samanta A, Mahmoudi SM, Buehler T, Cantilena A, et al. STAT3 balances myocyte hypertrophy vis-a-vis autophagy in response to Angiotensin II by modulating the AMPKalpha/mTOR axis. PloS one. 2017;12(7):e0179835.

191. Barry SP, Davidson SM, Townsend PA. Molecular regulation of cardiac hypertrophy. The International Journal of Biochemistry & Cell Biology. 2008;40(10):2023-39.

192. Lopez J, Tait SWG. Mitochondrial apoptosis: killing cancer using the enemy within. British Journal Of Cancer. 2015;112:957.

193. Prabhu KS, Siveen KS, Kuttikrishnan S, Iskandarani A, Tsakou M, Achkar IW, et al. Targeting of X-linked inhibitor of apoptosis protein and PI3-kinase/AKT signaling by embelin suppresses growth of leukemic cells. PloS one. 2017;12(7):e0180895.

194. Khan AQ, Siveen KS, Prabhu KS, Kuttikrishnan S, Akhtar S, Shaar A, et al. Curcumin-Mediated Degradation of S-Phase Kinase Protein 2 Induces Cytotoxic Effects in Human Papillomavirus-Positive and Negative Squamous Carcinoma Cells. Frontiers in Oncology. 2018;8(399).

195. Mlih M, Abdulrahman N, Gadeau AP, Mohamed IA, Jaballah M, Mraiche F. Na(+)/H (+) exchanger isoform 1 induced osteopontin expression in cardiomyocytes involves NFAT3/Gata4. Molecular and cellular biochemistry. 2015;404(1-2):211-20.

196. Homewood CA, Warhurst DC, Peters W, Baggaley VC. Lysosomes, pH and the Anti-malarial Action of Chloroquine. Nature. 1972;235(5332):50-2.

197. Kim H-Y. Analysis of variance (ANOVA) comparing means of more than two groups. Restorative dentistry & endodontics. 2014;39(1):74-7.

198. Le N-T, Heo K-S, Takei Y, Lee H, Woo C-H, Chang E, et al. A Crucial Role for p90RSK-Mediated Reduction of ERK5 Transcriptional Activity in Endothelial Dysfunction and Atherosclerosis. Circulation. 2013;127(4):486-99.

199. Méry B, Guy J-B, Vallard A, Espenel S, Ardail D, Rodriguez-Lafrasse C, et al. In Vitro Cell Death Determination for Drug Discovery: A Landscape Review of Real Issues. Journal of cell death. 2017;10:1179670717691251-.

200. Yussman MG, Toyokawa T, Odley A, Lynch RA, Wu G, Colbert MC, et al. Mitochondrial death protein Nix is induced in cardiac hypertrophy and triggers apoptotic cardiomyopathy. Nature medicine. 2002;8(7):725-30.

201. Kostin S, Pool L, Elsasser A, Hein S, Drexler HC, Arnon E, et al. Myocytes die by multiple mechanisms in failing human hearts. Circ Res. 2003;92(7):715-24.

202. Dorn GW, 2nd, Robbins J, Sugden PH. Phenotyping hypertrophy: eschew obfuscation. Circ Res. 2003;92(11):1171-5.

203. Tham YK, Bernardo BC, Ooi JYY, Weeks KL, McMullen JR. Pathophysiology of cardiac hypertrophy and heart failure: signaling pathways and novel therapeutic targets. Archives of toxicology. 2015;89(9):1401-38.

204. Yurinskaya V, Aksenov N, Moshkov A, Model M, Goryachaya T, Vereninov A. A comparative study of U937 cell size changes during apoptosis initiation by flow cytometry, light scattering, water assay and electronic sizing. Apoptosis : an international journal on programmed cell death. 2017;22(10):1287-95.

205. Maayah ZH, Ansari MA, El Gendy MA, Al-Arifi MN, Korashy HM. Development of cardiac hypertrophy by sunitinib in vivo and in vitro rat cardiomyocytes is influenced by the aryl hydrocarbon receptor signaling pathway. Archives of toxicology. 2014;88(3):725-38.

206. Bortner CD, Cidlowski JA. Chapter 3 Flow cytometric analysis of cell shrinkage and monovalent ions during apoptosis. Methods in Cell Biology. 66: Academic Press; 2001. p. 49-67.

207. Lizard G. Changes in light scatter properties are a general feature of cell death but are not characteristic of apoptotically dying cells. Cytometry. 2001;46(1):65-.

208. Kayabasi C, Okcanoglu TB, Yelken BO, Asik A, Susluer SY, Avci CB, et al. Comparative effect of imatinib and ponatinib on autophagy and miRNome in chronic myeloid leukemia. Gene. 2017;637:173-80.

209. Li M-L, Xu Y-Z, Lu W-J, Li Y-H, Tan S-S, Lin H-J, et al. Chloroquine potentiates the anticancer effect of sunitinib on renal cell carcinoma by inhibiting autophagy and inducing apoptosis. Oncology letters. 2018;15(3):2839-46.

210. Amith SR, Wilkinson JM, Fliegel L. Na+/H+ exchanger NHE1 regulation modulates metastatic potential and epithelial-mesenchymal transition of triple-negative breast cancer cells. Oncotarget. 2016;7(16):21091-113.

211. Abdel-Aziz AK, Shouman S, El-Demerdash E, Elgendy M, Abdel-Naim AB. Chloroquine synergizes sunitinib cytotoxicity via modulating autophagic, apoptotic and angiogenic machineries. Chemico-biological interactions. 2014;217:28-40.

212. Bain J, Plater L, Elliott M, Shpiro N, Hastie CJ, McLauchlan H, et al. The selectivity of protein kinase inhibitors: a further update. The Biochemical journal. 2007;408(3):297-315.

213. Yang Q, Zhang C, Wei H, Meng Z, Li G, Xu Y, et al. Caspase-Independent Pathway is Related to Nilotinib Cytotoxicity in Cultured Cardiomyocytes. Cellular Physiology and Biochemistry. 2017;42(6):2182-93.